

Sliced Rényi Pufferfish Privacy: Directional Additive Noise Mechanism and Private Learning with Gradient Clipping

Tao Zhang

Washington University in St. Louis

Yevgeniy Vorobeychik

Washington University in St. Louis

Abstract

We study privatization mechanism design and privacy accounting in the Pufferfish family, addressing two practical gaps of Rényi Pufferfish Privacy (RPP): high-dimensional optimal transport (OT) calibration and the absence of a general, mechanism-agnostic composition rule for iterative learning. We introduce Sliced Rényi Pufferfish Privacy (SRPP), which replaces high-dimensional comparisons by directional ones over a set of unit vectors, enabling geometry-aware and tractable guarantees. To calibrate noise without high-dimensional OT, we propose sliced Wasserstein mechanisms that compute per-direction (1-D) sensitivities, yielding closed-form, statistically stable, and anisotropic calibrations. We further define SRPP Envelope (SRPE) as computable upper bounds that are tightly implementable by these sliced Wasserstein mechanisms. For iterative deep learning algorithms, we develop a decompose-then-compose SRPP-SGD scheme with gradient clipping based on a History-Uniform Cap (HUC), a pathwise bound on one-step directional changes that is uniform over optimization history, and a mean-square variant (ms-HUC) that leverages subsampling randomness to obtain on-average SRPP guarantees with improved utility. The resulting HUC and ms-HUC accountants aggregate per-iteration, per-direction Rényi costs and integrate naturally with moments-accountant style analyses. Finally, when multiple mechanisms are trained and privatized independently under a common slicing geometry, our analysis yields graceful additive composition in both worst-case and mean-square regimes. Our experiments indicate that the proposed SRPP-based methods achieve favorable privacy–utility trade-offs in both static and iterative settings.

1 Introduction

Differential Privacy (DP) [9] is the de facto standard for measuring data privacy risk. It treats each individual record as a *secret* and requires that the output distribution of a randomized algorithm change only slightly when a single record is added

or removed. DP and its variants, such as Rényi DP (RDP) [20, 23] and zCDP [4], enjoy graceful composition properties that quantify cumulative privacy loss when the same (or related) datasets are used multiple times. These properties underpin DP-SGD [1], a canonical *decompose-then-compose* approach to private deep learning: each iteration applies a subsampled Gaussian mechanism with per-example gradient clipping and Gaussian noise, and a moments accountant aggregates per-iteration RDP into an overall (ϵ, δ) guarantee.

By adopting a similar worst-case probabilistic indistinguishability, Pufferfish Privacy (PP) [18] generalizes DP by allowing secrets beyond individual records and by modeling probabilistic relationships between secrets and datasets via priors on an adversary’s beliefs. Song et al. [29] provide the first general-purpose privatization mechanism for PP, the *Wasserstein mechanism*, which uses the ∞ -Wasserstein distance as an analogue of sensitivity and generalizes the Laplace mechanism. Ding [8] proposes a Kantorovich-based exponential (and Gaussian) additive-noise mechanism for PP calibrated to 1-Wasserstein sensitivity. However, computing ∞ -Wasserstein distances is statistically and computationally challenging in high dimensions, and tractable, general design principles for PP mechanisms remain largely open [15].

A second central limitation of PP is the lack of practical, general-purpose composition theorems for privacy accounting and iterative algorithms like SGD. Existing results require specific structural assumptions: universally composable evolution scenarios [18] assume deterministic secret-dataset relationships, while the Markov Quilt Mechanism [29] applies only to Bayesian networks. Recent work [35] explains this limitation fundamentally: the probabilistic secret-dataset relationship induces dependencies among mechanisms, breaking standard composition. Their proposed inverse composition requires solving an infinite-dimensional convex optimization problem, which is not straightforward to apply within iterative learning algorithms such as SGD.

Rényi Pufferfish Privacy (RPP) [25] partially addresses these issues by recasting PP in terms of Rényi divergences and introducing the General Wasserstein Mechanism (GWM),

which uses the shift-reduction lemma [2, 11] to calibrate additive noise via ∞ -Wasserstein distance. Extensions include an approximate version (GAWM) for improved utility and a distribution-aware variant (DAGWM) using p -Wasserstein distances to capture average-case data geometry. While these Wasserstein-based mechanisms significantly advance the PP framework, they inherit the curse of dimensionality from optimal transport: estimating Wasserstein distances and sensitivities remains statistically and computationally expensive in high dimensions, limiting practical applicability.

To address composition, RPP proves Privacy Amplification by Iteration (PABI) results for contractive noisy processes [25], enabling the first use of PP-style guarantees in private convex optimization. However, PABI requires contractivity of the update map, restricting applicability to non-convex objectives and non-contractive optimizers like momentum-based methods. Moreover, PABI still depends on Wasserstein distances between one-step updates, reintroducing high-dimensional optimal transport challenges. Consequently, PABI does not provide a universal, mechanism-agnostic composition theory for Pufferfish.

In this paper, we address these limitations by taking a directional, sliced view of RPP and by designing mechanisms and accountants that avoid high-dimensional optimal transport and contractivity assumptions. At a high level, we (i) introduce sliced RPP notions and sliced Wasserstein mechanisms that reduce high-dimensional calibration to one-dimensional problems, (ii) develop HUC- and ms-HUC-based SRPP-SGD schemes that support practical privacy accounting for subsampled gradient methods, and (iii) establish additive composition theorems for collections of SRPP/ms-SRPP mechanisms sharing a common slicing geometry. Our contributions are summarized as follows.

- We introduce two notions of *Sliced Rényi Pufferfish Privacy* (SRPP), average SRPP (Ave-SRPP) and joint SRPP (Joint-SRPP), as directional refinements of RPP that compare secrets along a fixed set of unit vectors. Ave-SRPP controls the *mean* Rényi distinguishability across slices, while Joint-SRPP controls the Rényi distinguishability of the *joint* pair of slice index and projection, penalizing rare high-risk directions that could be hidden by averaging. Having both notions lets us trade off utility and robustness to directional outliers while keeping the geometry-aware, tractable structure of SRPP.
- We propose *sliced Wasserstein mechanisms*, which replace d -dimensional Wasserstein sensitivities with per-direction (1D) sensitivities, and define *SRPP Envelope* (SRPE) as computable upper bounds that are tightly implementable by these mechanisms, yielding explicit privacy certificates for Ave-/Joint-SRPP.
- For iterative learning with gradient clipping, we develop SRPP-SGD based on a *History-Uniform Cap* (HUC), which provides additive per-iteration, per-direction

Rényi bounds and closed-form Gaussian calibration, and a mean-square variant (ms-HUC) together with ms-SRPP that leverage subsampling randomness to obtain on-average guarantees with improved utility. The resulting HUC and ms-HUC accountants integrate naturally with moments-accountant-style analyses and avoid both contraction assumptions and high-dimensional Wasserstein estimates, accommodating non-contractive optimizers such as SGD and Adam.

- When multiple mechanisms are trained independently and privatized via our SRPP/ms-SRPP schemes under a common slicing geometry, we prove graceful additive composition: the total Ave-/Joint- or ms-Ave/ms-Joint-SRPP cost is bounded by the sum of the per-mechanism costs, enabling modular, plug-and-play privacy accounting for pipelines and cascades.

1.1 Related Work

Privacy Beyond Individual Data Records. One-sided DP [19] protects the sensitive portion of a dataset (the “one side”), while non-sensitive records can be released with minimal or no protection. Fernandes et al [12] apply generalized DP using Earth Mover’s Distance on word embeddings to obfuscate authorship in text documents. Hardt and Roth [13] study differentially private singular vector computation under an entry-level privacy model, where the secret is each matrix entry. PAC Privacy [30, 31] and Residual PAC Privacy [36] bound the information-theoretic hardness of successful inference for general secrets beyond individual record presence, enabling automatic measurement and control via simulation. Pufferfish Privacy (PP) [18, 29] and Rényi Pufferfish Privacy (RPP) [25] are direct, full generalizations of DP and RDP, respectively, that consider general secrets beyond individual record presence while using the same probabilistic indistinguishability framework as their counterparts. Other distribution-based privacy notions, which protect distributions of data rather than individual records, include [5, 16].

Instantiations of Pufferfish Privacy. Several important instantiations of the Pufferfish Privacy framework have been developed to address specific privacy scenarios. Song et al [29] demonstrate PP’s application to correlated data, where dependencies between records violate the independence assumptions of standard DP. Zhang et al [37] instantiate PP for attribute privacy, protecting sensitive attributes rather than individual record presence. Zhang et al. [35] propose differential confounding privacy, which handles intrinsic probabilistic relationships between secrets and datasets, including dynamic and stochastic relationships where secrets must be derived from the data itself. Blowfish Privacy [14] extends differential privacy through policy specifications that allow data publishers to customize both the sensitive information requiring

protection and the publicly known constraints about the data, enabling more flexible privacy-utility trade-offs. Nuradha and Goldfeld [22] provide an information-theoretic formulation of PP in terms of conditional mutual information, termed MI PP, which satisfies improved composability properties compared to standard PP and enables mechanism analysis through information-theoretic tools. PP has also been instantiated in applied settings, including smart-meter time-series release and local energy markets [17] and time-series data trading under temporal correlations via the HORAE framework [21].

2 Preliminaries

We begin by providing background on Differential Privacy (DP), Pufferfish Privacy (PP), and Rényi Pufferfish Privacy (RPP).

2.1 Differential Privacy

Let X be the input dataset. Each data point x_i is defined over some measurable domain \mathcal{X}^\dagger , so that $x = (x_1, x_2, \dots, x_n) \in \mathcal{X} = (\mathcal{X}^\dagger)^n$. We say two datasets $x, x' \in \mathcal{X}$ are *adjacent* if they differ in exactly one data point.

Definition 2.1 ((ϵ, δ)-Differential Privacy [9]). *A randomized mechanism $\mathcal{M} : \mathcal{X} \rightarrow \mathcal{Y}$ is said to be (ϵ, δ)-differentially private (DP), with $\epsilon \geq 0$ and $\delta \in [0, 1]$, if for any pair of adjacent datasets x, x' , and for all $\mathcal{T} \subseteq \mathcal{Y}$, we have $\Pr[\mathcal{M}(x) \in \mathcal{T}] \leq e^\epsilon \Pr[\mathcal{M}(x') \in \mathcal{T}] + \delta$.*

The parameter ϵ is usually referred to as the *privacy budget*, and $\delta \in (0, 1]$ represents the failure probability. DP represents a worst-case, input-agnostic adversarial worst-case framework.

2.2 DP-SGD with Gradient Clipping

Differentially private stochastic gradient descent (DP-SGD) [1, 28] has become the standard approach for training neural networks with formal privacy guarantees.

Dataset. Let $x = (x_1, \dots, x_n) \in \mathcal{X} = \bar{\mathcal{X}}^n$ be the finite samples of data points, where each $x_i = (a_i, b_i) \in \bar{\mathcal{X}}$ consists of features a_i and label b_i . In this section, we take P_X^θ as the empirical (marginal) distribution of the data samples $x = (x_1, \dots, x_n) \in \mathcal{X} = \bar{\mathcal{X}}^n$ for all $\theta \in \Theta$. At iteration t , we draw a random mini-batch $I_t \subseteq [n]$ using a subsampling scheme $\{\eta, \rho\}$ characterized by a rate η and a scheme type ρ , where $\rho \in \{\text{WR}, \text{WOR}, \text{Poisson}\}$ denotes sampling with-replacement (WR), without-replacement (WOR), or via a Poisson process (Poisson), respectively. Let $X^t = (X_i)_{i \in I_t}$ denote the random mini-batch subsampled from x , with x' representing a particular realization.

Algorithm 1 Noise-perturbed SGD with gradient clipping

Require: Data x_1, \dots, x_n ; loss $\ell(\xi; x)$; stepsizes $(\eta_t)_{t=0}^{T-1}$; batch size B ; clip norm C ; noise covariances $(\Sigma_t)_{t=1}^T$.

- 1: Initialize parameters ξ_0
- 2: **for** $t = 0, \dots, T - 1$ **do**
- 3: Sample minibatch $I_t \subseteq [n]$ with $|I_t| = B$
- 4: For each $i \in I_t$:

$$g_t(x_i) \leftarrow \nabla_{\xi} \ell(\xi_t; x_i), \tilde{g}_t(x_i) \leftarrow g_t(x_i) \min \left\{ 1, \frac{C}{\|g_t(x_i)\|_2} \right\}$$
- 5: $\bar{g}_t \leftarrow \frac{1}{B} \sum_{i \in I_t} \tilde{g}_t(x_i)$
- 6: Draw $N_t \sim \mathcal{N}(0, \Sigma_t)$ and set $\hat{g}_t \leftarrow \bar{g}_t + N_t$
- 7: $\xi_{t+1} \leftarrow \theta_t - \eta_t \hat{g}_t$
- 8: **end for**
- 9: **return** θ_T ; compute privacy parameters from (Σ_t) according to DP guarantee.

Empirical Risk Minimization. In supervised learning, each example is $x_i = (a_i, b_i)$ with features a_i and label b_i . Let $\ell(\theta; x_i)$ denote the per-sample loss of a model with parameter ξ . The empirical risk minimization (ERM) problem is $\min_{\xi} F(\xi) := \frac{1}{n} \sum_{i=1}^n \ell(\theta; x_i)$.

Stochastic Gradient Descent. SGD approximately solves ERM by iteratively sampling minibatches and updating θ along noisy gradients. At iteration t , a subsampling scheme $\{\eta, \rho\}$ produces a random minibatch index set $I_t \subseteq [n]$ of size B and corresponding minibatch $x' = (x_i)_{i \in I_t}$. The (unclipped) stochastic gradient is

$$g_t(x_i) := \nabla_{\xi} \ell(\xi_t; x_i), \quad g_t := \frac{1}{B} \sum_{i \in I_t} g_t(x_i),$$

and the parameters are updated as $\xi_{t+1} = \xi_t - \eta_t g_t$, for step-size $\eta_t > 0$.

Gradient clipping and DP-SGD. DP-SGD [1, 28] modifies SGD in two ways: it clips per-example gradients to control sensitivity and adds noise to the averaged gradient for privacy. Each per-sample gradient is clipped at ℓ_2 radius C ,

$$\tilde{g}_t(x_i) := g_t(x_i) \min \left\{ 1, \frac{C}{\|g_t(x_i)\|_2} \right\},$$

and the averaged clipped gradient is

$$\bar{g}_t := \frac{1}{B} \sum_{i \in I_t} \tilde{g}_t(x_i). \quad (1)$$

Noise-perturbed SGD with gradient clipping (Algorithm 1) then draws Gaussian noise $N_t \sim \mathcal{N}(0, \Sigma_t)$, forms $\hat{g}_t = \bar{g}_t + N_t$, and updates $\xi_{t+1} = \xi_t - \eta_t \hat{g}_t$. In the classical DP setting, the

covariance sequence (Σ_t) is calibrated so that the resulting algorithm satisfies a target (ϵ, δ) -DP guarantee via an RDP or moments-accountant style analysis. Appendix C provides detailed discussion between group DP-SGD and our SRPP-SGD.

2.3 Pufferfish and Rényi Pufferfish Privacy

The Pufferfish Privacy (PP) framework [18] generalizes differential privacy (DP) by protecting arbitrary *secrets* linked to the data, rather than only individual records. Let S be the space of secrets and $Q \subseteq S \times S$ the set of secret pairs to be made indistinguishable. Unlike DP, which treats the dataset X as fixed, PP models X as a random variable drawn from a distribution $\theta \in \Theta$, where each θ represents a plausible adversarial prior or data-generating scenario. For each $\theta \in \Theta$, let $P_\theta(S, X)$ denote the joint law over secrets S and datasets X , with marginals P_θ^S and P_θ^X , and conditional $P_\theta(x | s) = P_\theta(s, x) / P_\theta^S(s)$. We write $\Pr_\theta[\cdot]$ and $\mathbb{E}_\theta[\cdot]$ for probability and expectation under $P_\theta(S, X)$, and refer to $\{S, Q, \Theta\}$ as the *Pufferfish scenario*.

Definition 2.2 (Pufferfish privacy (PP) [18, 37]). *Let $\epsilon \geq 0$ and $\delta \in (0, 1)$. A mechanism $\mathcal{M} : X \rightarrow \mathcal{Y}$ is (ϵ, δ) -Pufferfish private in (S, Q, Θ) if for all $\theta \in \Theta$, all $(s_i, s_j) \in Q$ with $P_\theta^S(s_i), P_\theta^S(s_j) \neq 0$, and all measurable $\mathcal{T} \subseteq \mathcal{Y}$,*

$$\Pr(\mathcal{M}(X) \in \mathcal{T} | S = s_i, \theta) \leq e^\epsilon \Pr(\mathcal{M}(X) \in \mathcal{T} | S = s_j, \theta) + \delta.$$

If $\delta = 0$, we say that \mathcal{M} satisfies ϵ -Pufferfish privacy.

Thus, PP replaces DP's notion of adjacent datasets with indistinguishability between *dataset distributions* induced by different secrets under the priors in Θ .

Recently, Pierquin et al. [25] extended PP using Rényi divergence, in the spirit of Rényi differential privacy (RDP) [20], yielding a more flexible and composition-friendly analysis of Pufferfish-type guarantees.

Definition 2.3 (Rényi Pufferfish privacy (RPP) [25]). *Let $\alpha > 1$ and $\epsilon \geq 0$. A mechanism \mathcal{M} is (α, ϵ) -RPP in (S, Q, Θ) if for all $\theta \in \Theta$ and $(s_i, s_j) \in Q$ with $P_\theta^S(s_i), P_\theta^S(s_j) > 0$,*

$$D_\alpha(\Pr(\mathcal{M}(X) | S = s_i, \theta) \| \Pr(\mathcal{M}(X) | S = s_j, \theta)) \leq \epsilon,$$

where $X \sim P_\theta^X$ and D_α is the Rényi divergence of order α ,

$$D_\alpha(P \| Q) := \frac{1}{\alpha - 1} \log \mathbb{E}_{Z \sim Q} \left[\left(\frac{P(Z)}{Q(Z)} \right)^\alpha \right], \quad (2)$$

for distributions P and Q on a common measurable space.

RPP reduces to PP in the limit $\alpha \rightarrow 1$ (analogous to RDP and DP) and will serve as the base notion for our sliced Rényi Pufferfish privacy framework.

2.4 Wasserstein Mechanisms

Wasserstein mechanisms are important for PP [29] and RPP [25] implementations.

Definition 2.4 (Coupling). *Let ν, μ be probability measures on $(\mathbb{R}^d, \mathcal{B}(\mathbb{R}^d))$. A coupling of (ν, μ) is any probability measure π on $(\mathbb{R}^d \times \mathbb{R}^d, \mathcal{B}(\mathbb{R}^d) \otimes \mathcal{B}(\mathbb{R}^d))$ whose marginals are ν and μ . We denote the set of all couplings by $\Pi(\nu, \mu)$.*

Definition 2.5 (∞ -Wasserstein distance). *Fix a norm $\|\cdot\|$ on \mathbb{R}^d . For probability measures ν, μ on \mathbb{R}^d , the ∞ -Wasserstein distance (∞ -WD) is*

$$W_\infty(\nu, \mu) = \inf_{\pi \in \Pi(\nu, \mu)} \sup_{(x, y) \in \text{supp}(\pi)} \|x - y\|.$$

The ∞ -Wasserstein Mechanism (∞ -WM) [29], based on the ∞ -Wasserstein distance, is the first general privatization mechanism that calibrates additive noise in PP framework by bounding the maximum shift between conditional query distributions. Pierquin et al. [25] extend the ∞ -WM to a *General Wasserstein Mechanism* (GWM) based on the *shift reduction lemma* [11]. We defer the introduction of the distribution-aware GWM [25] to Appendix A.

We first set up the necessary notations. Let $N \sim \zeta$ denote additive noise with distribution ζ on \mathbb{R}^d (e.g., Gaussian or Laplace). For $x \in \mathbb{R}^d$, the *shifted* distribution is $\zeta - x$ (i.e., the distribution of $U - x$ for $U \sim \zeta$). For probability measures ν, μ , their convolution is $\nu * \mu$ (i.e., the distribution of $U + V$ for independent $U \sim \nu, V \sim \mu$). Define the *Rényi envelop*,

$$R_\alpha(\zeta, z) = \sup_{\|a\| \leq z} D_\alpha(\zeta_{-a}, \zeta), \quad (3)$$

where $\|\cdot\|$ is some norm, and $\zeta_{-a} : w \rightarrow \zeta(w - a)$.

For any query function $f : \mathcal{X} \rightarrow \mathbb{R}^d$, define

$$\Delta_\infty = \max_{(s_i, s_j) \in Q, \theta \in \Theta} W_\infty(P(f(X) | s_i, \theta), P(f(X) | s_j, \theta)). \quad (4)$$

The GWM is formally defined as follows.

Theorem 2.6 (General Wasserstein mechanism (GWM) [25]). *Let $f : \mathcal{X} \rightarrow \mathbb{R}^d$ be a numerical query. Let $N = (N_1, \dots, N_d) \sim \zeta$ drawn independently of the dataset X . Then, $\mathcal{M}(X) = f(X) + N$ satisfies $(\alpha, R_\alpha(\zeta, \Delta_\infty))$ -RPP for all $\alpha \in (1, +\infty)$ and $R_\infty(\zeta, \Delta_\infty)$ -PP, where Δ_∞ is given by (4).*

GWM is a general framework for RPP and PP privatization. We can instantiate the Gaussian and Laplace mechanisms to recover familiar guarantees with Δ_∞ playing the role of sensitivity [25]. For example, $\mathcal{M}(X) = f(X) + N$ is (α, ϵ) -RPP if $N \sim \mathcal{N}(0, \frac{\alpha \Delta_\infty^2}{2\epsilon} I_d)$ with Δ_∞ computed using the L_2 norm. In addition, $\mathcal{M}(X) = f(X) + N$, where $N \sim \text{Lap}(0, \frac{\Delta_\infty}{\epsilon} I_d)$ with Δ_∞ computed using the L_1 norm is ϵ -PP.

The key limitation of Wasserstein mechanisms is due to the computational burden: in high dimensions, computing

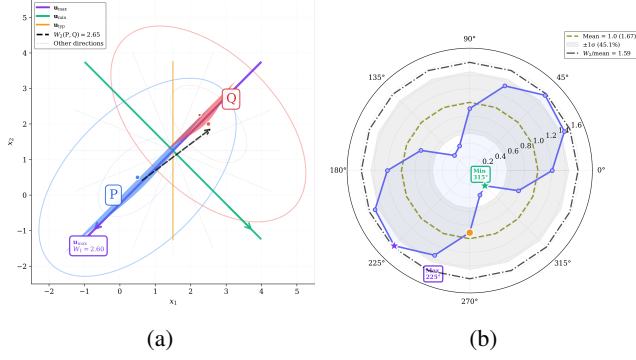


Figure 1: Geometry and sliced Wasserstein profile for two 2-D Gaussians P and Q. (a) Geometry of the distributions with selected projection directions: \mathbf{u}_{\max} (purple), \mathbf{u}_{\min} (green), and a typical direction \mathbf{u}_{typ} (orange), together with the global 2D Wasserstein shift. (b) Polar plot of the normalized 1-D Wasserstein distance as a function of projection angle; the polygon shows per-direction distances, the red dashed circle is their mean, the shaded band shows $\pm 1\text{std}$, and the black dash-dotted circle marks the global W_2 distance, with color-matched markers corresponding to the directions in (a).

both the sensitivity term Δ_∞ and the associated Rényi envelope $R_\alpha(\zeta, \Delta_\infty)$ is costly. Computing W_∞ or more generally W_p (Definition A.1 in Appendix A) between empirical distributions on \mathbb{R}^d requires solving large-scale optimal transport problems, whose complexity grows superlinearly in the sample size and suffers from the curse of dimensionality. Thus, the Wasserstein mechanism for RPP (and also PP) is difficult to scale beyond low or moderate-dimensional queries. This motivates us to propose *sliced Wasserstein mechanisms*, where we work with one-dimensional (1-D) projection of $f(X)$, leading to much more tractable computations in high dimensions, while preserving a meaningful Wasserstein-style geometry. The key component is *sliced Wasserstein sensitivity* introduced in the next section.

3 Sliced Wasserstein Sensitivity

In this section, we propose *sliced Wasserstein sensitivity*, obtained by applying slicing to the standard ∞ -Wasserstein distance, to address the computational challenges associated with Wasserstein mechanisms in high dimensions. We begin by introducing some notation. Let $f : \mathcal{X} \rightarrow \mathbb{R}^d$ be a query function, and for each $(s, \theta) \in \mathcal{S} \times \Theta$ let $F_s^\theta := \Pr(f(X) \in \cdot \mid s, \theta)$ denote the probability distribution of $f(X)$ under secret s and prior θ . For an additive noise $N \sim \zeta$ independent of X , we write $\mathcal{M}_s^\theta := \Pr(\mathcal{M}(X) \in \cdot \mid s, \theta)$ for the output distribution of a mechanism \mathcal{M} applied to X . For a measurable map $g : \mathcal{W} \rightarrow \mathcal{C}$ and a Borel measure μ on \mathcal{W} , the *pushforward*

$g_\# \mu$ on \mathcal{C} is defined by

$$g_\# \mu(A) = \mu(g^{-1}(A)), \quad \forall A \in \mathcal{B}(\mathcal{C}), \quad (5)$$

where $\mathcal{B}(\mathcal{C})$ denotes the Borel σ -algebra on \mathcal{C} . Let $\mathbb{S}^{d-1} = \{u \in \mathbb{R}^d : \|u\|_2 = 1\}$ be the unit sphere and let ω be a probability measure on \mathbb{S}^{d-1} . For each $u \in \mathbb{S}^{d-1}$, define the projection $\Psi^u : \mathbb{R}^d \rightarrow \mathbb{R}$ by $\Psi^u(a) = \langle a, u \rangle$. Then, for any Borel probability measure P on \mathbb{R}^d , the pushforward $\Psi^u_\# P$ is the one-dimensional (1-D) distribution of $\langle \hat{X}, u \rangle$ when $\hat{X} \sim P$.

Next, we define the *sliced Wasserstein distance*, which defines a metric for comparing probability measures on \mathbb{R}^d by integrating Wasserstein distances over all 1-D projections.

Definition 3.1 (Sliced Wasserstein Distance). *Let $\mathcal{P}_p(\mathbb{R}^d)$ denote the set of all Borel probability measures on \mathbb{R}^d with finite p -th moment, i.e., $\int_{\mathbb{R}^d} \|x\|^p d\mu(x) < \infty$ for all $\mu \in \mathcal{P}_p(\mathbb{R}^d)$. For $p \geq 1$ and $\mu, \nu \in \mathcal{P}_p(\mathbb{R}^d)$, the Sliced Wasserstein distance (SWD) is given by*

$$SW_p^p(\mu, \nu) := \int_{\mathbb{S}^{d-1}} W_p^p(\Psi^u_\# \mu, \Psi^u_\# \nu) d\lambda(u), \quad (6)$$

where λ is the uniform probability measure on \mathbb{S}^{d-1} .

The SWD is appealing because it reduces a high-dimensional optimal transport problem to an average of 1-D problems, for which W_p admits a closed form in terms of quantile functions. In practice, it can be estimated efficiently by sampling directions and sorting the projected samples. On \mathbb{R} (with the usual cost induced by the L_p norm), for 1-D measures $\hat{\mu}, \hat{\nu} \in \mathcal{P}_p(\mathbb{R})$ we have [24, Remark 2.30]:

$$W_p^p(\hat{\mu}, \hat{\nu}) = \int_0^1 |\hat{F}_\mu^{-1}(u) - \hat{F}_\nu^{-1}(u)|^p du, \quad (7)$$

where \hat{F}_μ^{-1} and \hat{F}_ν^{-1} denote the quantile functions of $\hat{\mu}$ and $\hat{\nu}$, respectively. Thus, the 1-D p -WD $W_p(\hat{\mu}, \hat{\nu})$ is equivalent to the L_p norm on a linear space (hence Hilbertian for $p = 2$), so its geometry is simple and linear, in sharp contrast to the much more complex geometry in higher dimensions. Figure 1 illustrates an example of slicing a W_2 for two 2-D Gaussian distributions.

In the standard OT sense, ∞ -SWD is the $p \rightarrow \infty$ endpoint of $SW_p^p(\mu, \nu)$. At the slice level, ∞ -SWD gives a natural analogue of the ∞ -WD (Definition 2.5) as the global sensitivity for RPP and PP: *the largest shift in the projected query output that can arise when the secret changes*. Then, given a Pufferfish scenario $\{\mathcal{S}, \mathcal{Q}, \Theta\}$, for each direction $u \in \mathbb{S}^{d-1}$, we define the *per-slice ∞ -Wasserstein sensitivity* as

$$\Delta_\infty^u := \max_{(s_i, s_j) \in \mathcal{Q}, \theta \in \Theta} W_\infty(\Psi^u_{\#} P_{s_i}^\theta \parallel \Psi^u_{\#} P_{s_j}^\theta). \quad (8)$$

Here, Δ_∞^u is the worst-case ∞ -WD, over all admissible pairs of secrets and priors, between the one-dimensional projections of the data distributions ($P_{s_i}^\theta$ and $P_{s_j}^\theta$) along direction u . It

therefore measures the maximal shift in the projected query output when the secret changes from s_i to s_j under any prior (of an potential adversary) in Θ , and will serve as the basic per-slice sensitivity parameter.

Conceptually, we might try to replace the per-slice Wasserstein sensitivity Δ_∞^u in (8) with a single scalar based on the SWD in Definition 3.1. However, SWD averages one-dimensional optimal-transport costs under a particular coupling and does not provide a uniform bound for all admissible couplings and all slices (or directions) that our 1-D per-slice Rényi envelope (11) in Section 4.4 requires.

However, any potential adversary observes the full dimensional query output, rather than the projected. Naively replacing the full-Wasserstein Δ_∞ with sliced-Wasserstein Δ_∞^u in the RPP noise calibration, while keeping the original (unsliced) RPP definition, creates a mismatch between the geometry of the mechanisms and the geometry of the divergence and can therefore yield unsound privacy bounds.

In particular, we recall that for any $u \in \mathbb{S}^{d-1}$, the projection $\Psi^u(x) = \langle x, u \rangle$ is 1-Lipschitz with respect to the Euclidean norm. Hence, for any pair of distributions μ, ν on \mathbb{R}^d ,

$$W_\infty(\Psi_\#^u \mu, \Psi_\#^u \nu) \leq W_\infty(\mu, \nu).$$

Indeed, for any coupling $\gamma \in \Pi(\mu, \nu)$ we have $|\Psi^u(x) - \Psi^u(y)| \leq \|x - y\|_2$ γ -almost surely (γ -a.s.), so taking the essential supremum and then the infimum over γ yields the inequality above. By applying this to $\mu = P_{s_i}^\theta$ and $\nu = P_{s_j}^\theta$, and then taking the supremum over $(s_i, s_j) \in Q$ and $\theta \in \Theta$, we have $\Delta_\infty^u \leq \Delta_\infty$, where Δ_∞ is given by (4). This motivates us to introduce *Sliced Rényi Pufferfish Privacy*, a sliced analogue of RPP tailored to SW mechanisms, formally presented in the next section.

4 Sliced Rényi Pufferfish Privacy

In this section, we introduce *Sliced Rényi Pufferfish Privacy* (SRPP), a directional refinement of RPP defined with respect to a *slice profile* (\mathcal{U}, ω) , where $\mathcal{U} \subseteq \mathbb{S}^{d-1}$ is a set of directions and ω is a probability measure on \mathbb{S}^{d-1} supported on \mathcal{U} . In the finite case, $\mathcal{U} = \{u_1, \dots, u_m\}$ and ω is the discrete distribution with weights $(\omega_1, \dots, \omega_m)$, so that $\int_{\mathbb{S}^{d-1}} f(u) d\omega(u)$ reduces to $\sum_{i=1}^m \omega_i f(u_i)$.

We define two variants: Average SRPP (Ave-SRPP, Section 4.1) and Joint SRPP (Joint-SRPP, Section 4.2). Ave-SRPP bounds the average per-slice Rényi divergence, while Joint-SRPP treats the slice index as part of the observation and aggregates per-slice divergences via a joint log-moment bound, making it more sensitive to rare high-risk directions and typically stronger. Section 4.3 gives their basic ordering and post-processing properties. Section 4.4 introduces SRPP envelopes (SRPE), which convert sliced Wasserstein sensitivities into computable bounds for both variants and are instantiated in

Section 4.5 as Gaussian sliced Wasserstein mechanisms under a chosen slice profile. Appendix B provides a detailed discussion of Ave-SRPP and Joint-SRPP.

4.1 Average SRPP

Our Ave-SRPP aggregates per-slice Rényi divergences by averaging.

Definition 4.1 (ω -Average Sliced Rényi Divergence (ω -Ave-SRD)). *For two probability distributions P and Q on \mathbb{R}^d , and a slice profile (\mathcal{U}, ω) , the Average Sliced Rényi Divergence (Ave-SRD) of order $\alpha > 1$ with respect to ω is*

$$\text{AveSD}_\alpha^\omega(P \| Q) := \int_{\mathbb{S}^{d-1}} D_\alpha(\Psi_\#^u P \| \Psi_\#^u Q) d\omega(u), \quad (9)$$

where D_α is the standard Rényi divergence.

Ave-SRD averages the 1-D Rényi divergences between the projected measures $\Psi_\#^u P$ and $\Psi_\#^u Q$ over directions $u \sim \omega$. When $d = 1$ and ω is a point mass, $\text{AveSD}_\alpha^\omega$ reduces to $D_\alpha(P \| Q)$.

Definition 4.2 ($(\alpha, \varepsilon, \omega)$ -Ave-SRPP). *Let $\alpha > 1$ and $\varepsilon \geq 0$. For a slice profile $\{\mathcal{U}, \omega\}$, a mechanism \mathcal{M} satisfies $(\alpha, \varepsilon, \omega)$ -Ave-SRPP in (S, Q, Θ) if for all $\theta \in \Theta$ and $(s_i, s_j) \in Q$ with $P_\theta^S(s_i), P_\theta^S(s_j) > 0$,*

$$\text{AveSD}_\alpha^\omega(\Pr(\mathcal{M}(X) | s_i, \theta) \| \Pr(\mathcal{M}(X) | s_j, \theta)) \leq \varepsilon.$$

Thus Ave-SRPP bounds the ω -average of the per-slice Rényi divergences between output distributions under any admissible pair of secrets.

4.2 Joint SRPP

Our Joint-SRPP aggregates them through a joint log-moment (Rényi) bound.

Definition 4.3 (Joint Sliced Rényi Divergence (Joint-SRD)). *For two probability distributions P and Q on \mathbb{R}^d , the joint sliced Rényi divergence (Joint-SRD) of order $\alpha > 1$ is*

$$\text{JSD}_\alpha^\omega(P \| Q) := \frac{1}{\alpha - 1} \log \mathbb{E}_{V \sim \omega} \left[\exp \left((\alpha - 1) D_\alpha(\Psi_\#^V P \| \Psi_\#^V Q) \right) \right]. \quad (10)$$

Joint-SRD aggregates the per-slice divergences multiplicatively via a log-moment transform, making it more sensitive than Ave-SRD to rare directions with large 1-D divergence (see Figure 2). When $d = 1$ and ω is a point mass, it reduces to the standard Rényi divergence $D_\alpha(P \| Q)$.

Definition 4.4 ($(\alpha, \varepsilon, \omega)$ -Joint-SRPP). *Let $\alpha > 1$ and $\varepsilon \geq 0$. A mechanism \mathcal{M} satisfies $(\alpha, \varepsilon, \omega)$ -Joint-SRPP in (S, Q, Θ) if for all $\theta \in \Theta$ and $(s_i, s_j) \in Q$ with $P_\theta^S(s_i), P_\theta^S(s_j) > 0$,*

$$\text{JSD}_\alpha^\omega(\Pr(\mathcal{M}(X) | s_i, \theta) \| \Pr(\mathcal{M}(X) | s_j, \theta)) \leq \varepsilon.$$

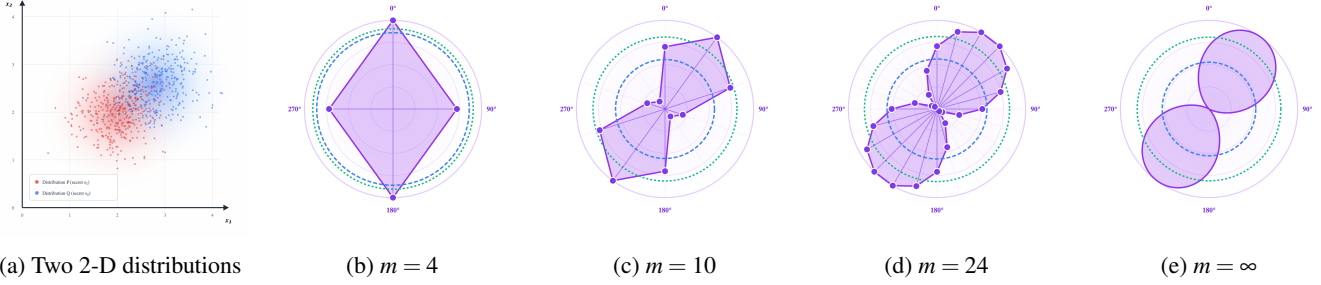


Figure 2: Sliced Rényi divergences for $\alpha = 4$ in 2-D, with uniform ω . (a) Two Gaussian distributions P (red) and Q (blue). (b)-(e) Polar plots showing divergence profile D_α for $m = 4, 10, 24$ slices and the continuous limit ($m = \infty$). The purple polygon shows per-slice divergences, blue dashed circle shows Ave-SRD (arithmetic mean across directions), and green dotted circle shows Joint-SRD (log-exponential mean emphasizing high-divergence directions). Joint-SRD \geq Ave-SRD in all cases, with both converging as m increases.

Joint-SRPP bounds the Joint-SRD divergence between secrets when an adversary can observe both the random slice index and the corresponding 1-D projection of the mechanism’s output.

4.3 Properties of SRPP

Ave-SRPP and Joint-SRPP use the same ingredients (per-slice Rényi divergences along 1-D projections) but aggregate them in different ways, leading to different strengths. Ave-SRPP averages the per-slice Rényi divergences over directions $u \sim \omega$, so it controls the mean distinguishability of secrets across slices (good for mean geometry across slices). Joint-SRPP instead can be interpreted as bounding the Rényi divergence of the joint observation of slice index $V \sim \omega$ and projection $\Psi_\#^V(\mathcal{M}(X))$, which captures and penalizes rare, high-risk directions that Ave-SRPP alone can hide in the average. Joint-SRPP is generally a stronger requirement than Ave-SRPP: satisfying Joint-SRPP implies the corresponding averaged bound, but not conversely. Appendix B provides a detailed discussion.

Ordering. Our two SRPP frameworks sit between each other and the standard RPP.

Proposition 4.1. Fix a slice profile $\{\mathcal{U}, \omega\}$. For $d \geq 1$, $\alpha > 1$, every secret pair $(s_i, s_j) \in \mathcal{Q}$ and every prior $\theta \in \Theta$,

$$\text{ASD}_\alpha^\omega(\mathcal{M}_{s_i}^\theta \| \mathcal{M}_{s_j}^\theta) \leq \text{JSD}_\alpha^\omega(\mathcal{M}_{s_i}^\theta \| \mathcal{M}_{s_j}^\theta) \leq D_\alpha(\mathcal{M}_{s_i}^\theta \| \mathcal{M}_{s_j}^\theta).$$

The ordering in Proposition 4.1 only compares the *numerical tightness of upper bounds* and does not induce a straightforward ranking of privacy strength between the three notions. For example, an (α, ϵ) -RPP guarantee implies the corresponding $(\alpha, \epsilon, \omega)$ -Joint/Ave-SRPP guarantees by Proposition 4.1, but the converse need not hold. Moreover, different choices of ω and different calibration strategies for the noise can lead to mechanisms with the same bound on ASD_α^ω or JSD_α^ω but

very different protections at the level of secrets and priors. For this reason, the inequalities in Proposition 4.1 should be interpreted as relations between divergence-based certificates, rather than as an absolute ranking of which framework is “more private”.

Post-processing immunity. One of the fundamental properties of RPP and DP is post-processing immunity (PPI): the privacy loss of a mechanism cannot be increased by arbitrary data-independent post-processing [10, 25]. Hence, the privacy parameters of the initial mechanism can be safely used as a (in general conservative) bound on the overall privacy cost of any post-processing pipeline. Because SRPP is built from 1-D RPP guarantees, both Ave-SRPP and Joint-SRPP inherit this PPI property. As in standard DP/RPP, obtaining a tighter certificate for the full pipeline by reanalyzing it as a single new mechanism can be challenging; in our case this is further complicated by the dimension- and geometry-aware structure (via the slice profile) of SRPP, so in practice, we typically reuse the SRPP parameters of the initial mechanism as a conservative bound.

4.4 Sliced Rényi Pufferfish Privacy Envelope

Having established SRPP as a family of dimension- and geometry-aware Rényi Pufferfish notions, along with its basic ordering and post-processing properties, we now turn to concrete privatization mechanisms. In this section, we introduce the *Sliced Rényi Pufferfish Privacy Envelope* (SRPE), an SRPP upper bound tightly calibrated via sliced Wasserstein sensitivity, thereby providing computable certificates for Ave-/Joint-SRPP. We refer to privatization mechanisms that realize this envelope as *sliced Wasserstein mechanisms*.

For any per-slice size function $\pi : \mathbb{S}^{d-1} \rightarrow \mathbb{R}_+$ and slice $u \in \mathbb{S}^{d-1}$, we can rewrite (3) to obtain the *per-slice Rényi*

envelope in as

$$R_\alpha(\zeta, \pi(u)) = \sup_{\|a\| < \pi(u)} D_\alpha(\zeta_{-a}, \zeta), \quad (11)$$

where ζ_{-a} denotes the distribution of $N - a$ when $N \sim \zeta$.

Lemma 4.1. *Fix a Pufferfish scenario (S, Q, Θ) and a slice profile $\{\mathcal{U}, \omega\}$. Let $\mathcal{M}(X) = f(X) + N$ with $N \sim \zeta$. For each prior $\theta \in \Theta$ and each $(s_i, s_j) \in Q$ with $P_\theta^S(s_i) > 0$ and $P_\theta^S(s_j) > 0$, we have, for all $\alpha > 1$,*

$$D_\alpha(\Psi_\#^\theta \mathcal{M}_{s_i}^\theta \parallel \Psi_\#^\theta \mathcal{M}_{s_j}^\theta) \leq R_\alpha(\zeta, z_\infty^\theta), \quad \forall u \in \mathcal{U},$$

where $\mathcal{M}_s^\theta = F_s^\theta * \zeta$ is the distribution of $f(X) + N$ given $(S = s, \theta)$, and

$$z_\infty^\theta := W_\infty(\Psi_\#^\theta F_{s_i}^\theta \parallel \Psi_\#^\theta F_{s_j}^\theta)$$

is the per-slice ∞ -Wasserstein distance between the projected pre-noise distributions $F_{s_i}^\theta$ and $F_{s_j}^\theta$.

Lemma 4.1 states that, along each direction u , the per-slice Rényi envelope evaluated at the shift radius z_∞^θ upper-bounds the actual Rényi divergence between the projected output distributions under secrets s_i and s_j .

We then define the *averaged Rényi envelope* as

$$\text{AR}_{\alpha, \omega}^\infty(\mathcal{M}_{s_i}^\theta \parallel \mathcal{M}_{s_j}^\theta) := \int_{\mathbb{S}^{d-1}} R_\alpha(\zeta, z_\infty^\theta) d\omega(u). \quad (12)$$

This quantity aggregates the per-slice Rényi envelope bounds over slice $u \sim \omega$ and will serve as our sliced Rényi envelope surrogate for the true averaged sliced Rényi divergence.

Definition 4.5 $((\alpha, \varepsilon, \omega)$ -Ave-SRPE). *Fix a slice profile $\{\mathcal{U}, \omega\}$. Let $\alpha > 1$ and $\varepsilon \geq 0$. A mechanism $\mathcal{M}(X) = f(X) + N$ with $N \sim \zeta$ satisfies $(\alpha, \varepsilon, \omega)$ -Averaged SRPP Envelope $((\alpha, \varepsilon, \omega)$ -Ave-SRPE) in (S, Q, Θ) if for all $\theta \in \Theta$ and $(s_i, s_j) \in Q$ with $P_\theta^S(s_i) > 0$ and $P_\theta^S(s_j) > 0$,*

$$\text{AR}_{\alpha, \omega}^\infty(\mathcal{M}_{s_i}^\theta \parallel \mathcal{M}_{s_j}^\theta) \leq \varepsilon. \quad (13)$$

The condition of Ave-SRPE requires that, for every prior θ and every admissible pair of secrets (s_i, s_j) , the averaged sliced Rényi envelope upper bound $\text{AR}_{\alpha, \omega}^\infty$ between the output distributions under s_i and s_j is at most ε . Equivalently, if we project the mechanism's outputs along all slices $u \sim \omega$ and bound the per-slice Rényi divergence via the envelope $R_\alpha(\zeta, z_\infty^\theta)$, then the ω -average of these bounds cannot exceed ε . Ave-SRPE thus provides a tractable, envelope-based surrogate for Ave-SRPP, obtained by replacing the true per-slice divergences with worst-case shift-based envelope bounds.

Similarly, we define the *joint sliced Rényi envelope* by

$$\text{JR}_{\alpha, \omega}^\infty(\mathcal{M}_{s_i}^\theta \parallel \mathcal{M}_{s_j}^\theta) := \frac{1}{\alpha - 1} \log \mathbb{E}_{V \sim \omega} [\exp((\alpha - 1) R_\alpha(\zeta, z_\infty^V))]. \quad (14)$$

Here, instead of averaging the per-slice envelope values linearly, we aggregate them via an exponential moment over $V \sim \omega$, followed by a log and $1/(\alpha - 1)$ rescaling. This construction mirrors the passage from an average of Rényi divergences to a joint Rényi divergence for the pair $(V, \Psi^V(\mathcal{M}(X)))$. As a result, $\text{JR}_{\alpha, \omega}^\infty$ is more sensitive to rare directions with large envelope values than its averaged counterpart $\text{AR}_{\alpha, \omega}^\infty$.

Definition 4.6 $((\alpha, \varepsilon, \omega)$ -Joint-SRPE). *Fix a slice profile $\{\mathcal{U}, \omega\}$. Let $\alpha > 1$ and $\varepsilon \geq 0$. A mechanism $\mathcal{M}(X) = f(X) + N$ with $N \sim \zeta$ satisfies $(\alpha, \varepsilon, \omega)$ -Joint SRPP Envelope $((\alpha, \varepsilon, \omega)$ -Joint-SRPE) in (S, Q, Θ) if for all $\theta \in \Theta$ and $(s_i, s_j) \in Q$ with $P_\theta^S(s_i) > 0$ and $P_\theta^S(s_j) > 0$,*

$$\text{JR}_{\alpha, \omega}^\infty(\mathcal{M}_{s_i}^\theta \parallel \mathcal{M}_{s_j}^\theta) \leq \varepsilon. \quad (15)$$

Joint-SRPE strengthens Ave-SRPE by requiring that the joint sliced Rényi envelope $\text{JR}_{\alpha, \omega}^\infty$ between the output distributions under s_i and s_j is bounded by ε for all priors and secret pairs. Intuitively, this means that even if a conceptualized adversary observes both the random slice V and its projected output, the envelope-based Rényi divergence between any two secrets remains bounded by ε . Thus, Joint-SRPE is the envelope-based analogue of Joint-SRPP and is generally stricter than its averaged counterpart.

4.5 Gaussian Sliced Wasserstein Mechanisms

In this section, we specialize to *Gaussian sliced Wasserstein mechanisms* of the form $\mathcal{M}(X) = f(X) + N$, where N is zero-mean Gaussian noise. Consider $N \sim \mathcal{N}(0, \sigma^2 I_d)$. For each slice $u \in \mathbb{S}^{d-1}$, the projected noise satisfies $\Psi_\#^\theta N \sim \mathcal{N}(0, \sigma^2)$, and the corresponding per-slice Rényi envelope is $R_\alpha(\zeta, z) = \frac{\alpha}{2\sigma^2} z^2$. Given $\{\mathcal{U}, \omega\}$ and Δ_∞^u in (8), define

$$\bar{\Delta}^2 := \int_{\mathbb{S}^{d-1}} (\Delta_\infty^u)^2 d\omega(u), \quad \Delta_*^2 := \sup_{u \in \mathcal{U}} (\Delta_\infty^u)^2.$$

Theorem 4.7. *Fix a slice profile $\{\mathcal{U}, \omega\}$. Let $\alpha > 1$ and $\varepsilon \geq 0$. A mechanism $\mathcal{M}(X) = f(X) + N$ with $N \sim \zeta$ satisfies $(\alpha, \varepsilon, \omega)$ -Ave-SRPE in (S, Q, Θ) if $\zeta = \mathcal{N}(0, \frac{\alpha \Delta_*^2}{2\varepsilon} I_d)$.*

Theorem 4.7 chooses σ^2 so that the averaged envelope $\text{AR}_{\alpha, \omega}^\infty$ across slices $u \sim \omega$ is exactly ε in the worst case over priors and secrets. In other words, calibrating the isotropic variance as $\sigma^2 = \alpha \bar{\Delta}^2 / (2\varepsilon)$ is sufficient (and tight at the envelope level) to guarantee $(\alpha, \varepsilon, \omega)$ -Ave-SRPE for \mathcal{M} .

Theorem 4.8. *Fix a slice profile $\{\mathcal{U}, \omega\}$. Let $\alpha > 1$ and $\varepsilon \geq 0$. A mechanism $\mathcal{M}(X) = f(X) + N$ with $N \sim \zeta$ satisfies $(\alpha, \varepsilon, \omega)$ -Joint-SRPE in (S, Q, Θ) if $\zeta = \mathcal{N}(0, \frac{\alpha \Delta_*^2}{2\varepsilon} I_d)$.*

From Theorem 4.8, taking $\sigma^2 = \alpha \Delta_*^2 / (2\varepsilon)$ ensures that this joint envelope is at most ε for all priors and secret pairs. Compared to Ave-SRPE, this calibration depends on the supremum over slices rather than the average, and thus generally yields a stronger privacy guarantee.

Algorithm 2 SRPP-SGD with gradient clipping (general form)

Require: Data x_1, \dots, x_n ; loss $\ell(\xi; x)$; subsampling scheme $\{\eta, \delta\}$; clip norm C ; update maps $(T_t)_{t=1}^T$; noise covariances $(\Sigma_t)_{t=1}^T$.

- 1: Initialize parameters ξ_0 ; set history $y_{<1} \leftarrow \xi_0$
 - 2: **for** $t = 1, \dots, T$ **do**
 - 3: Sample minibatch index set $l_t \subseteq [n]$ via scheme $\{\eta, \delta\}$;
 let $B_t \leftarrow |l_t|$
 - 4: For each $i \in l_t$:

$$g_t(x_i) \leftarrow \nabla_{\xi} \ell(\xi_{t-1}; x_i), \tilde{g}_t(x_i) \leftarrow g_t(x_i) \min \left\{ 1, \frac{C}{\|g_t(x_i)\|_2} \right\}$$
 - 5: $\bar{g}_t \leftarrow \frac{1}{B_t} \sum_{i \in l_t} \tilde{g}_t(x_i)$
 - 6: Draw $N_t \sim \mathcal{N}(0, \Sigma_t)$ and set $\hat{g}_t \leftarrow \bar{g}_t + N_t$
 - 7: $\xi_t \leftarrow T_t(\hat{g}_t; y_{<})$ {General update map}
 - 8: Update history $y_{<t+1}$ {e.g., $y_{<t+1} \leftarrow \xi_t$ for memoryless}
 - 9: **end for**
 - 10: **return** ξ_T ; compute SRPP parameters from (Σ_t) via HUC/ms-HUC accountant.
-

5 SRPP-Learning with Gradient Clipping

The global sensitivity of stochastic iterative algorithms such as SGD is notoriously hard to characterize directly under both DP and Pufferfish scenarios, making one-shot SRPP privatization using the sliced Wasserstein mechanisms insufficient for practical training. Following the decompose–then–compose philosophy of DP-SGD with gradient clipping (Section 2.2), we extend our static SRPP framework to stochastic learning by introducing *SRPP-SGD with gradient clipping*, the SRPP analogue of DP-SGD in the Pufferfish setting.

Sampling randomness. We first set up notation for the sampling randomness. Given a subsampling scheme $\{\eta, \rho\}$, let $(\mathcal{R}, \mathcal{B}, \mathbb{P}_{\eta, \rho})$ denote its probability space, with $\mathbb{P}_{\eta, \rho}$ the corresponding law. For a sampling draw $r \sim \mathbb{P}_{\eta, \rho}$, let $l_t(r) \subseteq [n]$ denote the (multi)set of selected indices at iteration t and $B_t(r) := |l_t(r)|$ its size. For $\rho \in \{\text{WR}, \text{WOR}\}$, we have $B_t(r) \equiv B$ (deterministic). For Poisson subsampling ($\rho = \text{Poisson}$), $B_t(r)$ is random. We write

$$\mathcal{B} : \bar{\mathcal{X}}^n \times \mathcal{R} \rightarrow \bar{\mathcal{X}}^{B_t(r)}, \quad x^t = \mathcal{B}(x; r) := (x_i)_{i \in l_t(r)},$$

for the (mini-batch) subsampling operator.

History and query. Let $y_{<t}$ denote the *history* at iteration t , with state space $\mathcal{Y}_{<t}$. For standard SGD, $y_{<t} = \xi_{t-1}$ is the current iterate. We make the dependence on the sampling draw explicit and write

$$f_t(x, y_{<t}; r) := f_t(\mathcal{B}(x; r), y_{<t}), \quad r \sim \mathbb{P}_{\eta, \rho}.$$

The clipped batch gradient in (1) can be written as $\bar{g}_t(r)$, and the gradient update as

$$\xi_t = f_t(x^t, y_{<t}; r) := \xi_{t-1} - \kappa \bar{g}_t(r),$$

where κ is the step size. When unambiguous, we suppress the dependence on r .

In DP-SGD, composition is key to the effectiveness of this approach [1, 6]. But PP/RPP generally lack graceful composition [18, 25, 29, 35], due to prior-induced dependencies between secrets and datasets [35]. The slicing process of SRPP does not circumvent such induced independence, and thus SRPP inherits the RPP’s lack of proper composition properties. To address this and make SRPP applicable to stochastic learning, we introduce the *History-Uniform Cap* (HUC) in the next section.

5.1 History-Uniform Cap

We define the HUC for a fixed Pufferfish scenario (\mathcal{S}, Q, Θ) and a slice profile $\{\mathcal{U}, \omega\}$. Let μ_s^θ denote the belief distribution of X given $(S = s, \theta)$. For any $(s_i, s_j) \in Q$ and $\theta \in \Theta$, let $\Pi(\mu_{s_i}^\theta, \mu_{s_j}^\theta)$ denote the set of couplings between $\mu_{s_i}^\theta$ and $\mu_{s_j}^\theta$ (Definition 2.4).

Definition 5.1 (History-Uniform Cap). A vector $h_t = (h_{t,i})_{i=1}^m \in \mathbb{R}_+^m$ is a *history-uniform cap (HUC)* for $\mathcal{U} = \{u_i\}_{i=1}^m$ at iteration t if, for all $\theta \in \Theta$, $(s_i, s_j) \in Q$, history $y_{<t}$ in the support, and every coupling $\gamma \in \Pi(\mu_{s_i}^\theta, \mu_{s_j}^\theta)$, we have $\gamma \times \mathbb{P}_{\eta, \rho}$ -a.s. in $((X, X'), R_t)$,

$$|\langle f_t(X, y_{<t}; R_t) - f_t(X', y_{<t}; R_t), u_i \rangle| \leq \sqrt{h_{t,i}}, \quad \forall i = 1, \dots, m. \quad (16)$$

Thus, a HUC $h_t = (h_{t,1}, \dots, h_{t,m})$ provides a *pathwise* bound that is uniform over histories: for every admissible coupling and every history $y_{<t}$ in support, the directional displacement along u_i is almost surely bounded by $\sqrt{h_{t,i}}$, and the constants $h_{t,i}$ do not depend on $y_{<t}$. Equivalently, there exists a PSD *HUC matrix* $H_t \succeq 0$ such that, $\gamma \times \mathbb{P}_{\eta, \rho}$ -a.s. in $((X, X'), R_t)$,

$$|\langle f_t(X, y_{<t}; R_t) - f_t(X', y_{<t}; R_t), u \rangle|^2 \leq u^\top H_t u, \quad \forall u \in \mathcal{U},$$

and we set $h_{t,i} = u_i^\top H_t u_i$ for $i = 1, \dots, m$. The HUC matrix H_t acts as a deterministic, history-uniform sensitivity ellipsoid for iteration t , while h_t records its directional values on \mathcal{U} .

We next show that a finite HUC always exists. We start by introducing necessary notions.

Discrepancy cap. A general (probabilistic) secret–dataset relation may alter attributes, individual data points, or global properties of datasets input to algorithms as the secret varies. Under minibatch subsampling from a fixed finite dataset $x = (x_1, \dots, x_n)$, its effect on the iteration- t update is fully captured

by how many sampled points differ between two coupled datasets. For a sampling draw $r \sim \mathbb{P}_{\eta, \rho}$ with index (multi)set $l_t(r)$ and size $B_t(r) = |l_t(r)|$, define the discrepancy

$$K_t(x, x'; r) := \sum_{j \in l_t(r)} \mathbf{1}\{x_j \neq x'_j\}. \quad (17)$$

Given a coupling $\gamma \in \Pi(\mu_{s_i}^\theta, \mu_{s_j}^\theta)$, the iteration- t discrepancy cap is the bound

$$K_t(\gamma) := \text{ess sup}_{((X, X'), R_t) \sim \gamma \times \mathbb{P}_{\eta, \rho}} K_t(X, X'; R_t).$$

If a pair $(s_i, s_j) \in Q$ guarantees that X and X' differ in at most \bar{K} coordinates γ -a.s., then $K_t(\gamma) \leq \min\{\bar{K}, B_t(r)\}$ at iteration t for the draw r . We say that a value K_t is a *feasible discrepancy cap* at iteration t (for the realized r) if $K_t \in [K_t(\gamma), B_t(r)]$ for all $\theta \in \Theta$ and $(s_i, s_j) \in Q$. Intuitively, a feasible discrepancy cap provides a uniform upper bound on the number of differing sampled points that can arise at round t across all priors and admissible secret pairs.

Update map and L_t -Lipschitz. At iteration t , we write the pre-perturbation update as a deterministic map $T_t : \mathbb{R}^d \times \mathcal{Y}_{< t} \rightarrow \mathbb{R}^d$:

$$f_t(x, y_{< t}; r) = T_t(\bar{g}_t(\mathcal{B}(x; r)); y_{< t}),$$

where $\bar{g}_t(\mathcal{B}(x; r)) \in \mathbb{R}^d$ is the clipped and averaged minibatch gradient. We say the iteration- t update map is L_t -Lipschitz (in its first argument) if there exists $L_t < \infty$ such that, for all $z, z' \in \mathbb{R}^d$ and all histories $y_{< t}$ in the support,

$$\|T_t(z; y_{< t}) - T_t(z'; y_{< t})\|_2 \leq L_t \|z - z'\|_2.$$

Here are two common cases.

(i) *Preconditioned SGD.* Suppose we use a preconditioner $A_t : \mathcal{Y}_{< t} \times \mathcal{R} \rightarrow \mathbb{R}^{d \times d}$, so that $T_t(z; y_{< t}) = \xi_{t-1} - A_t(y_{< t}, r)z$. Then T_t is L_t -Lipschitz with $L_t = \sup_{y_{< t}} \|A_t(y_{< t}, r)\|_{\text{op}}$ and $\|A\|_{\text{op}} := \sup_{\|v\|_2=1} \|Av\|_2$. In standard SGD, $A_t(y_{< t}, r) = \kappa I_d$, where κ is the step size.

(ii) *Proximal or projected updates.* Let

$$\text{prox}(v) := \arg \min_{w \in \mathbb{R}^d} \left\{ \frac{1}{2} \|w - v\|_2^2 + \bar{\lambda} \text{Reg}(w) \right\},$$

where $\bar{\lambda} > 0$ and $\text{Reg} : \mathbb{R}^d \rightarrow (-\infty, +\infty]$ is a proper, lower-semicontinuous, convex regularizer. Let $\bar{\Pi}_C$ be the Euclidean projection onto a closed convex set $C \subset \mathbb{R}^d$. Then, since both prox and $\bar{\Pi}_C$ are 1-Lipschitz, the same constant $L_t = \sup_{y_{< t}} \|A_t(y_{< t}, r)\|_{\text{op}}$ serves as a Lipschitz bound when $T_t(z; y_{< t}) = \text{prox}(\xi_{t-1} - A_t(y_{< t}, r)z)$ or $T_t(z; y_{< t}) = \bar{\Pi}_C(\xi_{t-1} - A_t(y_{< t}, r)z)$.

Assumption 5.2 (Slice-wise Lipschitz updates). *For each iteration t and each slice $u_i \in \mathcal{U}$, there exists a finite constant $L_{t,i} < \infty$ such that, for all $z, z' \in \mathbb{R}^d$ and all histories $y_{< t}$ in support,*

$$|u_i^\top (T_t(z; y_{< t}) - T_t(z'; y_{< t}))| \leq L_{t,i} |u_i^\top (z - z')|.$$

Assumption 5.2 requires that, along each slice direction u_i , the update map T_t does not amplify perturbations in the input gradient by more than a factor $L_{t,i}$ when projected onto the same slice direction. In other words, if we change the gradient in slice u_i , the component of the update along u_i can stretch at most $L_{t,i}$ times. Standard SGD and preconditioned SGD with bounded linear preconditioners satisfy this assumption.

Proposition 5.1. *Fix an iteration t and a slice profile $\{\mathcal{U}, \omega\}$. Suppose per-example gradients are clipped in ℓ_2 -norm at threshold $C > 0$. Let K_t be a feasible discrepancy cap at iteration t , and let $B_t \geq 1$ denote the (deterministic) minibatch size. Suppose Assumption 5.2 holds. Then for each $u_i \in \mathcal{U}$,*

$$h_{t,i} := \left(\frac{2K_t L_{t,i} C}{B_t} \right)^2 \quad (18)$$

is a valid HUC.

Proposition 5.1 says that, under slice-wise Lipschitz updates and ℓ_2 -clipping at level C , we can write down an explicit worst-case bound on how much the SGD update can move along each slice u_i when the secret changes. If at most K_t sampled examples differ in the minibatch of size B_t , then the change in the averaged (clipped) gradient along u_i is at most $\frac{2K_t C}{B_t}$, and the slice-wise Lipschitz constant $L_{t,i}$ can amplify this by at most a factor $L_{t,i}$ in the update. Thus the squared directional shift along u_i is bounded by $\left(\frac{2K_t L_{t,i} C}{B_t} \right)^2$, which is exactly the HUC cap $h_{t,i}$ in (18). Appendix D characterizes the minimality and attainability of HUC.

5.2 Mean-Square HUC

Any feasible discrepancy cap K_t used in $h_{t,i}$ is a uniform worst-case upper bound on the random discrepancy $K_t(X, X'; R_t)$ under $\gamma \times \mathbb{P}_{\eta, \rho}$. While this worst-case viewpoint is sound, it can be overly conservative in SGD, where the subsampling randomness η is independent of the prior and has a genuine averaging effect. To better reflect this structure and improve utility, we introduce a *mean-square HUC* (ms-HUC), which uniformly bounds the *expected* squared directional shifts over subsampling, while retaining worst-case uniformity over priors, secrets, and couplings.

Definition 5.3 (Mean-square history-uniform cap (ms-HUC)). *Fix t and a slicing set $\mathcal{U} = \{u_i\}_{i=1}^m \subset \mathbb{S}^{d-1}$. A vector $h_t^{\text{ms}} = (h_{t,i}^{\text{ms}})_{i=1}^m \in \mathbb{R}_+^m$ is a mean-square history-uniform cap (ms-HUC) for \mathcal{U} at iteration t if, for all $\theta \in \Theta$, all $(s_i, s_j) \in Q$, all histories $y_{< t}$ in the support, and every coupling $\gamma \in \Pi(\mu_{s_i}^\theta, \mu_{s_j}^\theta)$, we have, for γ -almost every (X, X') ,*

$$\mathbb{E}_{\eta_t} [|\langle f_t(X, y_{< t}; \eta_t) - f_t(X', y_{< t}; \eta_t), u_i \rangle|^2] \leq h_{t,i}^{\text{ms}}, \quad \forall i = 1, \dots, m,$$

where the expectation is taken only over the subsampling randomness $\eta_t \sim \mathbb{P}_\eta$.

Let \bar{K}_t^2 be any scalar such that, for all $\theta \in \Theta$, $(s_i, s_j) \in Q$, all histories $y_{<t}$ in the support, and all couplings $\gamma \in \Pi(\mu_{s_i}^\theta, \mu_{s_j}^\theta)$, we have, for γ -almost every (X, X') ,

$$\mathbb{E}_{\eta_t} [K_t(X, X'; \eta_t)^2] \leq \bar{K}_t^2. \quad (19)$$

Proposition 5.2. Fix an iteration t and a slicing set $\mathcal{U} = \{u_i\}_{i=1}^m \subset \mathbb{S}^{d-1}$. Assume:

1. Per-example gradients are ℓ_2 -clipped at radius $C > 0$.
2. The minibatch size $B_t \geq 1$ is deterministic.
3. Assumption 5.2 holds with constants $\{L_{t,i}\}_{i=1}^m$.

For each $\theta \in \Theta$, $(s_i, s_j) \in Q$, history $y_{<t}$ in the support, and $\gamma \in \Pi(\mu_{s_i}^\theta, \mu_{s_j}^\theta)$, let \bar{K}_t^2 satisfy (19). Then the vector $h_t^{\text{ms}} = (h_{t,i}^{\text{ms}})_{i=1}^m$ with

$$h_{t,i}^{\text{ms}} := \left(\frac{2L_{t,i}C}{B_t} \right)^2 \bar{K}_t^2, \quad i = 1, \dots, m, \quad (20)$$

is a valid ms-HUC.

Proposition 5.2 shows that, under slice-wise Lipschitz updates and ℓ_2 -clipping, the mean-square discrepancy \bar{K}_t^2 directly yields a closed-form ms-HUC. In particular, if \bar{K}_t^2 uniformly bounds the expected squared discrepancy K_t^2 over subsampling, then the mean-square directional shift along each slice u_i is controlled by $h_{t,i}^{\text{ms}} = \left(\frac{2L_{t,i}C}{B_t} \right)^2 \bar{K}_t^2$. Thus h_t^{ms} is a valid ms-HUC.

To calibrate privacy using $\mathbb{E}_{\eta_t} [K_t^2]$ instead of a worst-case K_t , we now introduce mean-square variants of Ave- and Joint-SRPP that match the ms-HUC notion. Let η denote all subsampling randomness used in SRPP-SGD, and for each fixed η , let $\mathcal{M}_s^{\theta, \eta}$ be the distribution of the mechanism's output under prior θ and secret s , conditional on η .

Definition 5.4 (Mean-square Average SRPP (ms-Ave-SRPP)). Fix $\alpha > 1$ and a slice profile (\mathcal{U}, ω) . A mechanism \mathcal{M} with subsampling randomness η satisfies $(\alpha, \epsilon, \omega)$ -ms-Ave-SRPP if, for all $\theta \in \Theta$ and all $(s_i, s_j) \in Q$,

$$\mathbb{E}_{\eta} \left[\text{ASD}_{\alpha}^{\omega}(\mathcal{M}_{s_i}^{\theta, \eta} \parallel \mathcal{M}_{s_j}^{\theta, \eta}) \right] \leq \epsilon.$$

Here the expectation is taken only over η .

Compared to standard Ave-SRPP, ms-Ave-SRPP keeps the same sliced Rényi divergence and the same uniformity over priors and secrets, but relaxes the guarantee from a worst-case bound for each subsampling pattern η to an *on-average* bound over the subsampling randomness. The geometry is unchanged; only the quantifier over η moves inside an expectation.

Definition 5.5 (Mean-square Joint SRPP (ms-Joint-SRPP)). Under the same setup as Definition 5.4, a mechanism \mathcal{M} satisfies $(\alpha, \epsilon, \omega)$ -ms-Joint-SRPP if, for all $\theta \in \Theta$ and all $(s_i, s_j) \in Q$,

$$\mathbb{E}_{\eta} \left[\text{JSD}_{\alpha}^{\omega}(\mathcal{M}_{s_i}^{\theta, \eta} \parallel \mathcal{M}_{s_j}^{\theta, \eta}) \right] \leq \epsilon.$$

Here, ms-Joint-SRPP is the mean-square analogue of Joint-SRPP: it still treats the slice index and projection jointly, but now requires that the joint sliced Rényi divergence be small *on average over subsampling* rather than for every fixed realization of η . As with ms-Ave-SRPP, the only change from the standard notion is replacing a worst-case guarantee in η by an expectation over η .

5.3 HUC Accountant for Gaussian Noise

Similar to DP-SGD, an important issue of SRPP-SGD is computing the aggregated privacy cost of the entire training process, i.e., the *composition* part of SRPP-SGD as a decompose-then-compose privatization scheme. In this section, we set out to show how HUC can circumvent the RPP/SRPP's lack of graceful composition properties and enable a privacy *accountant* process to compute the privacy costs along the SGD-based training process. We refer to it as *HUC accountant*.

We start by introducing the Gaussian slice Rényi Envelope, which gives a per-iteration, per-slice RPP cost after noise perturbation.

Lemma 5.1. Fix t and a slicing direction $u_i \in \mathbb{S}^{d-1}$. Let $N_t \sim \mathcal{N}(0, \Sigma_t)$ be independent of $((X, X'), R_t)$ and set $Y_t = f_t(X, y_{<t}; R_t) + N_t$. Define $v_{t,i} := u_i^\top \Sigma_t u_i$, and let $h_t = (h_{t,1}, \dots, h_{t,m})$ be any HUC vector. Then, for any $\alpha > 1$, we have

$$\text{D}_{\alpha} \left(\Pr(\langle Y_t, u_i \rangle \mid s_i, \theta) \parallel \Pr(\langle Y_t, u_i \rangle \mid s_j, \theta) \right) \leq \frac{\alpha}{2} \frac{h_{t,i}}{v_{t,i}}. \quad (21)$$

For ease of exposition, we absorb any step-size κ and pre-conditioning into the covariance Σ_t of the Gaussian noise. Lemma 5.1 gives a per-slice Rényi cost at iteration t directly in terms of the HUC component $h_{t,i}$ and the variance $v_{t,i}$ of the projected noise.

Theorem 5.6. Fix a slicing profile $\{\mathcal{U}, \omega\}$. Let $h = \{h_1, \dots, h_T\}$ with each $h_t = (h_{t,1}, \dots, h_{t,m})$ as a valid HUC vector. Let $N_t \stackrel{i.i.d.}{\sim} \mathcal{N}(0, \sigma^2 I_d)$. Then, for any $\alpha > 1$, we have:

- (i) **Ave-SRPP:** For any $\sigma^2 \geq \frac{\alpha}{2\epsilon} \sum_{t=1}^T \sum_{\ell=1}^m \omega_{\ell} h_{t,\ell}$, Algorithm 2 is $(\alpha, \epsilon, \omega)$ -Ave-SRPP.
- (ii) **Joint-SRPP:** For any $\sigma^2 \geq \frac{\alpha}{2\epsilon} \sum_{t=1}^T \max_{\ell} h_{t,\ell}$, Algorithm 2 is $(\alpha, \epsilon, \omega)$ -Joint-SRPP.

Theorem 5.6 shows that once a valid sequence of $h_t = 1^T$ has been constructed for a fixed slicing set \mathcal{U} , the overall SRPP guarantee for the entire SGD trajectory reduces to explicit, closed-form calibration conditions on the Gaussian noise. Both Ave-SRPP and Joint-SRPP are ensured by choosing a single variance parameter σ^2 large enough to offset the cumulative per-step HUC contributions, either in the ω -weighted average form (part (i)) or under the worst-slice aggregation (part (ii)).

Theorem 5.7. Fix a slicing profile $\{\mathcal{U}, \omega\}$ with $\mathcal{U} = \{u_\ell\}_{\ell=1}^m$ and $\omega \in \Delta(\mathcal{U})$. Let $h^{\text{ms}} = \{h_1^{\text{ms}}, \dots, h_T^{\text{ms}}\}$ with each $h_t^{\text{ms}} = (h_{t,1}^{\text{ms}}, \dots, h_{t,m}^{\text{ms}})$ a valid ms-HUC vector. Let $N_t \stackrel{\text{i.i.d.}}{\sim} \mathcal{N}(0, \sigma^2 I_d)$. Then, for any $\alpha > 1$, we have:

- (i) **ms-Ave-SRPP:** If $\sigma^2 \geq \frac{\alpha}{2\varepsilon} \sum_{t=1}^T \sum_{\ell=1}^m \omega_\ell h_{t,\ell}^{\text{ms}}$, then Algorithm 2 satisfies $(\alpha, \varepsilon, \omega)$ -ms-Ave-SRPP.
- (ii) **ms-Joint-SRPP:** If $\sigma^2 \geq \frac{\alpha}{2\varepsilon} \sum_{t=1}^T \max_\ell h_{t,\ell}^{\text{ms}}$, then Algorithm 2 satisfies $(\alpha, \varepsilon, \omega)$ -ms-Joint-SRPP.

Theorem 5.7 is the mean-square analogue of Theorem 5.6. Once we have a sequence of ms-HUC caps h_t^{ms} that bound the average (over subsampling) squared directional shifts at each iteration, the overall ms-SRPP guarantee for the full SGD trajectory reduces to the same kind of closed-form calibration on a single noise level σ^2 . Part (i) ensures an $(\alpha, \varepsilon, \omega)$ ms-Ave-SRPP bound by matching the ω -weighted sum of ms-HUCs, while part (ii) does the same for ms-Joint-SRPP using the worst-slice aggregation. Compared to the standard HUC case, the structure of the accountant is unchanged; the only difference is that the guarantee is now on-average over subsampling randomness.

5.4 Composition of SRPP-SGD Mechanisms

In this section, we show that HUC- and ms-HUC-based SRPP/ms-SRPP-SGD mechanisms also enjoy additive composition. For clarity, we present the setup and results in terms of HUC and SRPP; the same arguments apply verbatim to ms-HUC and ms-SRPP by replacing the corresponding notions.

We consider J SRPP-SGD mechanisms $\mathcal{M}_1, \dots, \mathcal{M}_J$ acting on the same dataset X . Without loss of generality, we take the primitive output of each mechanism to be a vector in a common parameter space \mathbb{R}^d (e.g., a final clipped update or parameter vector), and we fix a shared slice profile (\mathcal{U}, ω) with $\mathcal{U} = \{u_\ell\}_{\ell=1}^m \subset \mathbb{S}^{d-1}$ and $\omega \in \Delta(\mathcal{U})$. For each $j \in \{1, \dots, J\}$, the run $\mathcal{M}_j : X \rightarrow \mathbb{R}^d$ is an SRPP-SGD mechanism with iterates $\theta_t^{(j)} \in \mathbb{R}^d$ ($t = 0, \dots, T_j$), additive Gaussian noises $N_t^{(j)} \sim \mathcal{N}(0, \Sigma_t^{(j)})$, and an associated HUC (or ms-HUC) sequence $h^{(j)} = \{h_t^{(j)}\}_{t=1}^{T_j}$ that satisfies the conditions of Theorem 5.6 (resp. Theorem 5.7). The composed mechanism is

$$\vec{\mathcal{M}}(X) := (\mathcal{M}_1(X), \dots, \mathcal{M}_J(X)) \in (\mathbb{R}^d)^J. \quad (22)$$

Theorem 5.8. Fix a slice profile $\{\mathcal{U}, \omega\}$ and a Pufferfish scenario $\{\mathcal{S}, Q, \Theta\}$. Let $\vec{\mathcal{M}}$ be the composition mechanism defined in (22). Fix any $\Xi \in \{\text{Ave}, \text{Joint}, \text{ms-Ave}, \text{ms-Joint}\}$. Suppose that, for each $j \in \{1, \dots, J\}$, the mechanism \mathcal{M}_j is $(\alpha, \varepsilon_j, \omega)$ - Ξ -SRPP. Then the composed mechanism $\vec{\mathcal{M}}$ is $(\alpha, \sum_{j=1}^J \varepsilon_j, \omega)$ - Ξ -SRPP.

In other words, for any fixed SRPP notion (Ave, Joint, or their mean-square counterparts), the privacy costs of J SRPP-SGD mechanisms acting on the same data and slice profile add up linearly: the composed mechanism has the same α and ω , with total privacy cost $\sum_j \varepsilon_j$.

6 Experiments

We empirically evaluate our Gaussian sliced Wasserstein mechanisms in both the static and stochastic-learning settings. For static queries, we instantiate SRPP guarantees (Section 4), and for iterative training we use SRPP/ms-SRPP together with gradient clipping to privatize SGD (Section 5). Full experimental details and additional plots are deferred to Appendix O.

6.1 Gaussian Sliced Wasserstein Mechanisms

Dataset and Pufferfish scenario. We evaluate our sliced Wasserstein mechanisms on three standard tabular benchmarks in an attribute-privacy setting [37]: Adult Census [3] (race as secret, $k = 5$), Cleveland Heart Disease [7], and Student Performance [27], with Pufferfish query set $Q = \{(s_i, s_j) : s_i \neq s_j\}$. We present results for Adult and Appendix O shows results for the other datasets. For Adult, we consider both the natural imbalanced race prior (majority race probability 0.86) and a balanced, stratified subsample with a uniform 0.20 prior over the five race categories. We study two query families: (i) low-dimensional summary statistics (means, standard deviations, and rates of selected features) conditioned on each secret value; and (ii) machine learning (logistic regression, random forest, and SVM) queries on Adult, trained separately per secret group. In all experiments, we use Gaussian mechanisms $Y = \mathcal{M}(X) + N$, where $N \sim \mathcal{N}(0, I_d \sigma)$ with σ calibrated via our sliced SRPP. Utility is measured by mean squared error and related norms between $\mathcal{M}(X)$ and Y . We also use a prior-aware Gaussian MAP attack on the secret attribute to perform empirical privacy auditing, reporting accuracy and advantage over the prior baseline (i.e., 0.86 for imbalanced Adult, 0.20 for balanced Adult); an advantage near zero indicates that the mechanism prevents meaningful secret inference beyond the prior.

Figures 3a-3d and 3e-3h show utility-privacy trade-off as a function of the SRPP budget ε on balanced and imbalanced Adult datasets for four query types. Across all four queries, the behavior is consistent for both balanced and imbalanced

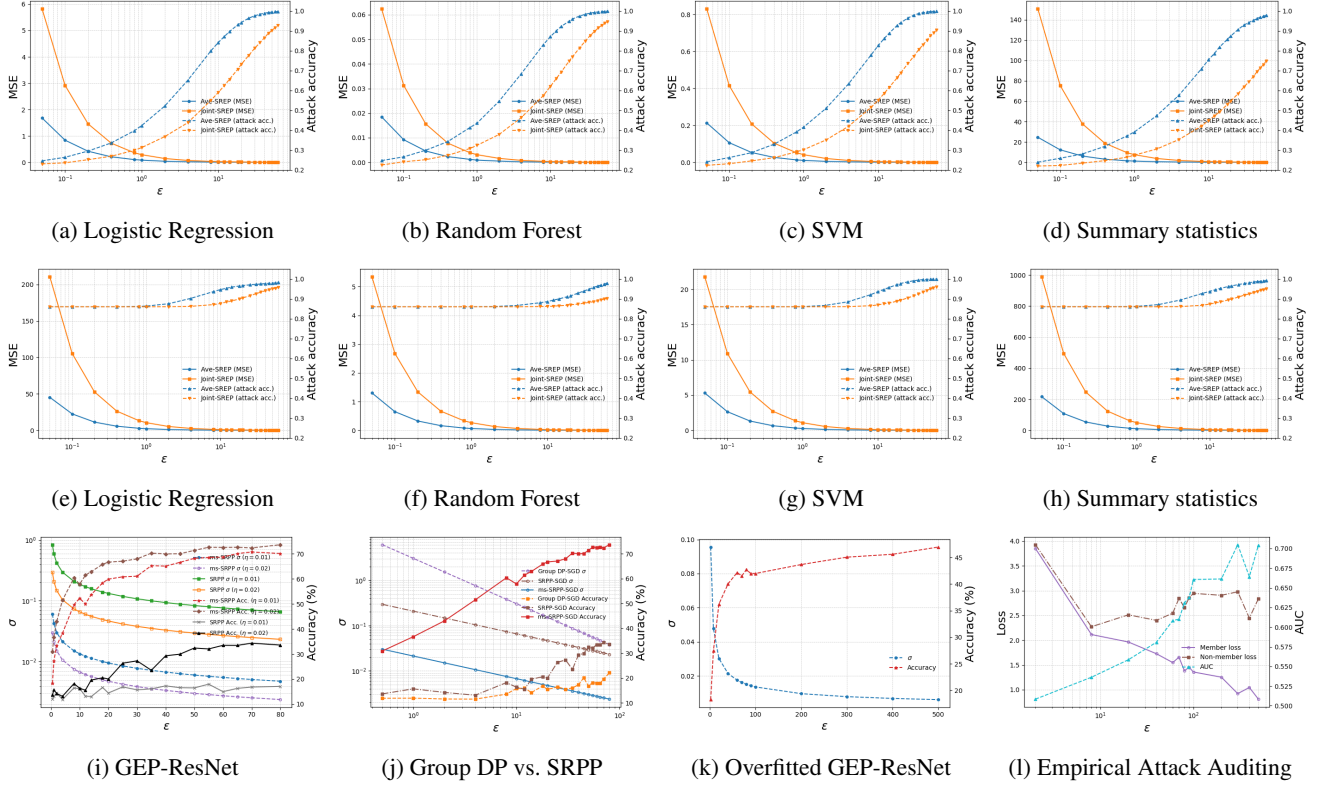


Figure 3: (a)-(d) with $\alpha = 4$ compares Ave-/Joint-SRPE on the balanced Adult dataset (uniform 0.2 prior over races), for four query families: logistic regression, linear SVM, random forest feature importances, and summary statistics. Each panel plots the utility–privacy tradeoff as a function of the SRPP budget ϵ . (e)-(h) with $\alpha = 4$ performs the same tasks on the imbalanced Adult dataset (uniform 0.86 prior over races). (i) compares SRPP-SGD and ms-SRPP-SGD on CIFAR-10 for two sampling rates ($\eta = 0.01$ and $\eta = 0.02$), showing the calibrated per-iteration noise scale σ (left axis, log-scale) and test accuracy (right axis) as a function of the privacy budget ϵ . (j) shows per-step Gaussian noise scale σ , and CIFAR-10 test accuracy for group-DP-SGD, SRPP-SGD, and ms-SRPP-SGD under the same clipping, subsampling ($\eta = 0.01$ and $\eta = 0.02$), and model setup. (k) presents overfitted SRPP-SGD on CIFAR-10 for $\eta = 0.02$. (l) illustrates member/non-member losses and attack AUC of the empirical MIA as a function of the ms-SRPP budget ϵ . All (i)-(l) use $\alpha = 16$. Appendix O provides detailed numerical values.

settings. For very strong privacy (small ϵ), both Ave- and Joint-SRPP force high noise and the MAP attack accuracy stays close to the prior baselines (i.e., 0.2 and 0.86), indicating that the mechanism reveals little additional information about the race. As ϵ increases, MSE decreases toward zero while attack accuracy rises monotonically, reflecting the expected utility-privacy trade-off. In addition, at any fixed ϵ , Joint-SRPP is more conservative than Ave-SRPP: it induces larger MSE but yields uniformly lower attacker accuracy. This gap is most visible in the moderate privacy regime, where the Ave-SRPP curves already allow the attacker to reach substantially higher accuracy, while Joint-SRPP keeps the attack much closer to the prior baseline.

6.2 SRPP-SGD Using Gaussian Noise

We evaluate our HUC-based SRPP-SGD and ms-SRPP-SGD mechanisms on image classification with Gaussian

noise added to clipped gradients in a DP-SGD-style training pipeline. In our implementation, the HUC envelope is instantiated using a *global* ℓ_2 -Lipschitz bound on the (clipped, averaged) gradient update map. Specifically, for each iteration t we bound the change in the update under neighboring worlds by a scalar constant L_t , so the global sensitivity of the update in Euclidean norm is at most L_t . This global envelope automatically upper-bounds all one-dimensional projections and therefore induces valid SRPP guarantees for any slicing profile (\mathcal{U}, ω) via the linear-update setting. Hence, Ave- and Joint-SRPP-SGD would have the same HUC. Appendix O.2 provides more details.

Dataset and Pufferfish scenario. We use CIFAR-10 (50,000 training and 10,000 test images). We create a two-world Pufferfish scenario, where *textttcat* is designated as the secret class, and construct two worlds s_0 and s_1 that differ only in the prevalence of this class: in the prior, the *cat* frequency shifts from $p_{\text{low}} = 0.10000$ to $p_{\text{high}} = 0.10004$. The

realized world s_0 is then fixed and encoded by overwriting the CIFAR-10 training labels with the realized label vector; all training procedures (private and non-private) operate only on this realized world.

Models. Our main model is a ResNet-22 similar to [32], implemented with ELU activations, GroupNorm-based layers, a 3×3 adaptive average pooling, and a linear classifier on a standardized $64 \times 3 \times 3$ feature vector. The architecture is made differentially private-compatible (ready for Opacus [34]) by replacing non-DP-friendly components (such as non-picklable shortcuts) with equivalent modules.

SRPP-SGD and ms-SRPP-SGD training. Training follows the standard DP-SGD template: at each iteration, per-sample gradients are clipped to an ℓ_2 bound C and then perturbed by isotropic Gaussian noise. We use a worst-case discrepancy cap K_{cap} for SRPP-SGD and use $\mathbb{E}_\eta[K_t^2]$ for ms-SRPP-SGD. We pre-compute, for each target SRPP and ms-SRPP budget ϵ at a fixed Rényi order $\alpha = 16$, a per-step noise scale $\sigma(\epsilon)$ that ensures the resulting Gaussian mechanisms satisfies the SRPP- and ms-SRPP-SGD under the given Pufferfish scenario. In addition, we also involve group-DP-SGD, under the same setup except the noise calibration: for group-DP-SGD, we following the standard DP-SGD [1], and apply convert it to group DP using $\mathbb{E}_\eta[K_t^2]$ ($\mathbb{E}_\eta[K_t^2] \leq K_{\text{cap}}$) as the group size. As a baseline, we also include group-DP-SGD under the same training setup but with noise calibrated via the standard DP-SGD accountant [1], and then converted to group DP by using $\mathbb{E}_\eta[K_t^2]$ (with $\mathbb{E}_\eta[K_t^2] \leq K_{\text{cap}}$) as the effective group size.

Overfitted regime and empirical privacy attacker. In addition to the above accuracy-focused experiments on the full training set, we run a separate overfitted regime tailored to empirical privacy evaluation. We restrict the training data to a small random subset of CIFAR-10 (on the order of 10^3 images), substantially increase the number of epochs, and remove or reduce weight decay, so that the resulting private SRPP-SGD models exhibit markedly higher training accuracy than test accuracy. On these overfitted models, we apply the loss-threshold membership inference attack of Yeom et al. [33]: for each trained model, we draw disjoint sets of member and non-member points, compute per-example cross-entropy losses, and use the negative loss as a scalar membership score (lower loss \Rightarrow more likely member). We report the ROC AUC of this score as a function of the privacy budget ϵ and compare against a non-private overfitted baseline trained on the same subset.

As shown in Figure 3i, across all ϵ and for both step sizes, ms-SRPP consistently requires much smaller Gaussian noise than worst-case SRPP: the ms-SRPP σ curves lie well below their SRPP counterparts, often by a factor of several and approaching an order of magnitude around $\epsilon \approx 20$ –40. This tighter calibration directly translates into higher utility. For small budgets both methods yield low accuracy, but as ϵ increases the ms-SRPP models continue to improve, reach-

ing roughly 60%–70% test accuracy at the largest budgets, whereas SRPP saturates around 20%–35%. The same pattern holds for both $\eta = 0.01$ and $\eta = 0.02$: ms-SRPP dominates SRPP in terms of the accuracy–privacy tradeoff, demonstrating that replacing a worst-case discrepancy cap K_{cap} by the mean-square cap $\mathbb{E}_\eta[K_t^2]$ yields substantially milder noise for the same ϵ .

Although DP, SRPP, and ms-SRPP are different privacy notions (see Appendix C), Figure 3j illustrates what happens if we try to protect the same Pufferfish secret using a group-DP framework (see Appendix C for more details). When group-DP-SGD is calibrated for an effective group size equal to $\mathbb{E}_\eta[K_t^2]$, the required Gaussian noise scale σ is substantially larger than for SRPP-SGD, and especially ms-SRPP-SGD, across the entire range of ϵ . At tight budgets (small ϵ), group-DP-SGD operates at the largest σ values on the plot and its test accuracy stays close to chance, while SRPP-SGD and ms-SRPP-SGD achieve visibly higher accuracies with much smaller noise. Even at moderate and large ϵ , group-DP-SGD remains dominated in utility by both SRPP variants. This suggests that, in our Pufferfish setting, simply converting DP-SGD to group-DP using $\mathbb{E}_\eta[K_t^2]$ leads to overly conservative noise calibration and cannot practically substitute for SRPP/ms-SRPP when the goal is to protect the secret-level prevalence.

In the overfitted setting (Figure 3k), empirical behavior of ms-SRPP-SGD matches the privacy–utility trade-off seen in Figure 3i. Figure 3l shows the stress-test performance of the empirical membership-inference attacks (at inference time of the model). Here, tighter ms-SRPP budgets (smaller ϵ) correspond to larger calibrated noise, lower test accuracy, and weaker membership inference, while looser budgets reduce the noise and improve accuracy at the cost of stronger membership-inference signals.

7 Conclusion

We introduced Sliced Rényi Pufferfish Privacy (SRPP), a directional refinement of RPP that replaces high-dimensional Wasserstein mechanism with a tractable 1-D sliced version. Our sliced Wasserstein mechanisms achieve closed-form Gaussian calibration, while Average and Joint variants provide flexible geometry-aware guarantees. For iterative learning, we developed SRPP-SGD based on the History-Uniform Cap (HUC), enabling decompose-then-compose privatization. The mean-square variant (ms-HUC) leverages subsampling randomness for improved utility, with both accountants supporting graceful additive composition across mechanisms. Experiments demonstrate favorable privacy-utility tradeoffs, with ms-SRPP-SGD requiring substantially less noise than worst-case variants. SRPP provides a practical path toward protecting distributional secrets in machine learning pipelines.

References

- [1] Martin Abadi, Andy Chu, Ian Goodfellow, H. Brendan McMahan, Ilya Mironov, Kunal Talwar, and Li Zhang. Deep learning with differential privacy. In *Proceedings of the 2016 ACM SIGSAC Conference on Computer and Communications Security, CCS '16*, page 308–318, 2016.
- [2] Jason Altschuler and Kunal Talwar. Privacy of noisy stochastic gradient descent: More iterations without more privacy loss. *Advances in Neural Information Processing Systems*, 35:3788–3800, 2022.
- [3] Barry Becker and Ronny Kohavi. Adult. *UCI Machine Learning Repository*, 10:C5XW20, 1996.
- [4] Mark Bun and Thomas Steinke. Concentrated differential privacy: Simplifications, extensions, and lower bounds. In *Theory of cryptography conference*, pages 635–658. Springer, 2016.
- [5] Michelle Chen and Olga Ohrimenko. Protecting global properties of datasets with distribution privacy mechanisms. In *International Conference on Artificial Intelligence and Statistics*, pages 7472–7491. PMLR, 2023.
- [6] Xiangyi Chen, Steven Z Wu, and Mingyi Hong. Understanding gradient clipping in private sgd: A geometric perspective. *Advances in Neural Information Processing Systems*, 33:13773–13782, 2020.
- [7] Robert Detrano, Andras Janosi, Walter Steinbrunn, Matthias Pfisterer, Johann-Jakob Schmid, Sarbjit Sandhu, Kern H Guppy, Stella Lee, and Victor Froelicher. International application of a new probability algorithm for the diagnosis of coronary artery disease. *The American journal of cardiology*, 64(5):304–310, 1989.
- [8] Ni Ding. Kantorovich mechanism for pufferfish privacy. In *International Conference on Artificial Intelligence and Statistics*, pages 5084–5103. PMLR, 2022.
- [9] Cynthia Dwork, Frank McSherry, Kobbi Nissim, and Adam Smith. Calibrating noise to sensitivity in private data analysis. In *Theory of cryptography conference*, pages 265–284. Springer, 2006.
- [10] Cynthia Dwork and Aaron Roth. The algorithmic foundations of differential privacy. *Foundations and Trends in Theoretical Computer Science*, 9(3–4):211–407, 2014.
- [11] Vitaly Feldman, Ilya Mironov, Kunal Talwar, and Abhradeep Thakurta. Privacy amplification by iteration. In *2018 IEEE 59th Annual Symposium on Foundations of Computer Science (FOCS)*, pages 521–532. IEEE, 2018.
- [12] Natasha Fernandes, Mark Dras, and Annabelle McIver. Generalised differential privacy for text document processing. In *International Conference on Principles of Security and Trust*, pages 123–148. Springer International Publishing Cham, 2019.
- [13] Moritz Hardt and Aaron Roth. Beyond worst-case analysis in private singular vector computation. In *Proceedings of the forty-fifth annual ACM symposium on Theory of computing*, pages 331–340, 2013.
- [14] Xi He, Ashwin Machanavajjhala, and Bolin Ding. Blowfish privacy: Tuning privacy-utility trade-offs using policies. In *Proceedings of the 2014 ACM SIGMOD International Conference on Management of Data, SIGMOD '14*, page 1447–1458. Association for Computing Machinery, 2014.
- [15] Sushil Jajodia, Pierangela Samarati, and Moti Yung. *Encyclopedia of Cryptography, Security and Privacy*. Springer, 2025.
- [16] Yusuke Kawamoto and Takao Murakami. Local obfuscation mechanisms for hiding probability distributions. In *European Symposium on Research in Computer Security*, pages 128–148. Springer, 2019.
- [17] Stephan Kessler, Erik Buchmann, and Klemens Böhm. Deploying and evaluating pufferfish privacy for smart meter data. In *2015 IEEE 12th Intl Conf on Ubiquitous Intelligence and Computing and 2015 IEEE 12th Intl Conf on Autonomic and Trusted Computing and 2015 IEEE 15th Intl Conf on Scalable Computing and Communications and Its Associated Workshops (UIC-ATC-ScalCom)*, pages 229–238. IEEE, 2015.
- [18] Daniel Kifer and Ashwin Machanavajjhala. Pufferfish: A framework for mathematical privacy definitions. *ACM Transactions on Database Systems (TODS)*, 39(1):1–36, 2014.
- [19] Ios Kotsogiannis, Stelios Doudalis, Sam Haney, Ashwin Machanavajjhala, and Sharad Mehrotra. One-sided differential privacy. In *2020 IEEE 36th International Conference on Data Engineering (ICDE)*, pages 493–504. IEEE, 2020.
- [20] Ilya Mironov. Rényi differential privacy. In *2017 IEEE 30th Computer Security Foundations Symposium (CSF)*, pages 263–275, 2017.
- [21] Chaoyue Niu, Zhenzhe Zheng, Shaojie Tang, Xiaofeng Gao, and Fan Wu. Making big money from small sensors: Trading time-series data under pufferfish privacy. In *IEEE INFOCOM 2019-IEEE Conference on Computer Communications*, pages 568–576. IEEE, 2019.

- [22] Theshani Nuradha and Ziv Goldfeld. Pufferfish privacy: An information-theoretic study. *IEEE Transactions on Information Theory*, 69(11):7336–7356, 2023.
- [23] Nicolas Papernot and Thomas Steinke. Hyperparameter tuning with renyi differential privacy. *arXiv preprint arXiv:2110.03620*, 2021.
- [24] Gabriel Peyré, Marco Cuturi, et al. Computational optimal transport: With applications to data science. *Foundations and Trends® in Machine Learning*, 11(5-6):355–607, 2019.
- [25] Clément Pierquin, Aurélien Bellet, Marc Tommasi, and Matthieu Boussard. Rényi pufferfish privacy: General additive noise mechanisms and privacy amplification by iteration via shift reduction lemmas. In *International Conference on Machine Learning (ICML 2024)*, 2024.
- [26] Paul R. Rider. Generalized cauchy distributions. *Annals of the Institute of Statistical Mathematics*, 9:215–223, 1957.
- [27] Alice Silva. Using data mining to predict secondary school student performance. 2008.
- [28] Shuang Song, Kamalika Chaudhuri, and Anand D Sarwate. Stochastic gradient descent with differentially private updates. In *2013 IEEE global conference on signal and information processing*, pages 245–248. IEEE, 2013.
- [29] Shuang Song, Yizhen Wang, and Kamalika Chaudhuri. Pufferfish privacy mechanisms for correlated data. In *Proceedings of the 2017 ACM International Conference on Management of Data*, SIGMOD ’17, page 1291–1306, 2017.
- [30] Mayuri Sridhar, Hanshen Xiao, and Srinivas Devadas. Pac-private algorithms. In *2025 IEEE Symposium on Security and Privacy (SP)*, pages 3839–3857. IEEE, 2025.
- [31] Hanshen Xiao and Srinivas Devadas. Pac privacy: Automatic privacy measurement and control of data processing. In *Annual International Cryptology Conference*, pages 611–644. Springer, 2023.
- [32] Hanshen Xiao, Jun Wan, and Srinivas Devadas. Geometry of sensitivity: Twice sampling and hybrid clipping in differential privacy with optimal gaussian noise and application to deep learning. In *Proceedings of the 2023 ACM SIGSAC Conference on Computer and Communications Security*, pages 2636–2650, 2023.
- [33] Samuel Yeom, Irene Giacomelli, Matt Fredrikson, and Somesh Jha. Privacy risk in machine learning: Analyzing the connection to overfitting. In *2018 IEEE 31st computer security foundations symposium (CSF)*, pages 268–282. IEEE, 2018.
- [34] Ashkan Yousefpour, Igor Shilov, Alexandre Sablayrolles, Davide Testuggine, Karthik Prasad, Mani Malek, John Nguyen, Sayan Ghosh, Akash Bharadwaj, Jessica Zhao, et al. Opacus: User-friendly differential privacy library in pytorch. *arXiv preprint arXiv:2109.12298*, 2021.
- [35] Tao Zhang, Bradley A Malin, Netanel Raviv, and Yevgeniy Vorobeychik. Differential confounding privacy and inverse composition. *arXiv preprint arXiv:2408.12010*, 2024.
- [36] Tao Zhang and Yevgeniy Vorobeychik. Breaking the gaussian barrier: Residual-pac privacy for automatic privatization. *arXiv preprint arXiv:2506.06530*, 2025.
- [37] Wanrong Zhang, Olga Ohrimenko, and Rachel Cummings. Attribute privacy: Framework and mechanisms. In *Proceedings of the 2022 ACM Conference on Fairness, Accountability, and Transparency, FAccT ’22*, page 757–766, New York, NY, USA, 2022. Association for Computing Machinery.

A Background: Distribution Aware General Wasserstein Mechanism

In this appendix we recall the Distribution Aware General Wasserstein Mechanism (DAGWM) of [25], which refines the General Wasserstein Mechanism (GWM) for Rényi Pufferfish Privacy (RPP) by replacing worst-case ∞ -Wasserstein sensitivities with p -Wasserstein quantities that better capture average-case geometry.

Definition A.1 (p -Wasserstein distance). *Fix a norm $\|\cdot\|$ on \mathbb{R}^d and let $1 \leq p < \infty$. For probability measures ν, μ on \mathbb{R}^d with finite p -th moments, the p -Wasserstein distance is*

$$W_p(\nu, \mu) := \inf_{\pi \in \Pi(\nu, \mu)} \left(\int_{\mathbb{R}^d \times \mathbb{R}^d} \|x - y\|^p d\pi(x, y) \right)^{1/p}$$

If either ν or μ lacks a finite p -th moment, set $W_p(\nu, \mu) = +\infty$.

For $1 \leq p \leq s \leq \infty$, $W_p(\nu, \mu) \leq W_s(\nu, \mu)$; moreover $W_r(\nu, \mu)$ converges to $W_\infty(\nu, \mu)$ as $p \rightarrow \infty$ when the probability measure has compact support.

To improve the utility of the GWM, Pierquin et al. [25] leverage p -Wasserstein distance to constrain the sensitivity instead of ∞ -Wasserstein distances. This replaces the worst-case transportation cost between $\Pr(f(X) | s_i, \theta)$ and $\Pr(f(X) | s_j, \theta)$ by moments of the transportation cost. Let ζ be a noise distribution and, for $(s_i, s_j) \in Q$ and $\theta \in \Theta$, write $\mu_i^\theta = P(f(X) | s_i, \theta)$. For $q \geq 1$ and $\alpha > 1$, define

$$\Delta_G^{\zeta, q, \alpha} := \max_{(s_i, s_j), \theta} \inf_{(X, Y) \sim \Pi(\mu_i^\theta, \mu_j^\theta)} \mathbb{E} \left[\exp(q(\alpha - 1) D_{q(\alpha-1)+1}(\zeta, \zeta * (X - Y))) \right]. \quad (23)$$

Theorem A.2 (Distribution Aware General Wasserstein Mechanism (DAGWM) [25]). *Let $f : X \rightarrow \mathbb{R}^d$ be a query function and ζ noise distribution of \mathbb{R}^d . Let $q \geq 1$. For $(s_i, s_j) \in Q, \theta \in \Theta$, let $\mu_i^\theta = \Pr(f(X) | s_i, \theta)$. Let $N = (N_1, \dots, N_d) \sim \zeta$ drawn independently of the dataset X . Then, $\mathcal{M}(X) = f(X) + N$ satisfies $\left(\alpha, \frac{\log(\Delta_G^{\zeta, q, \alpha})}{q(\alpha-1)} \right)$ -RPP for all $\alpha \in (1, +\infty)$*

and $\lim_{\alpha \rightarrow +\infty} \frac{\log(\Delta_G^{\zeta, q, \alpha})}{q(\alpha-1)}$ -PP, where $\Delta_G^{\zeta, q, \alpha}$ is given by (23).

The DAGWM supports privatization using noises from the generalized Cauchy distribution.

Definition A.3 (Generalized Cauchy Distributions [26]). *Let $k \geq 2, \lambda > 0$. We say that the real random variable $V \sim \text{GCauchy}(\lambda, k)$ if it has the following density:*

$$\zeta_{k, \lambda}(x) = \frac{\beta_{k, \lambda}}{((1 + (\lambda x)^2)^{k/2}), x \in \mathbb{R} \text{ and } \int \zeta_{k, \lambda}(x) dx = 1.$$

When $k = 2$, it reduces to the standard Cauchy distribution.

For any query function $f : X \rightarrow \mathbb{R}^d$, define

$$\Delta_G^{dkq(\alpha-1)} = \max_{\substack{(s_i, s_j) \in S \\ \theta \in \Theta}} W_{dkq(\alpha-1)}(P(f(X) | s_i, \theta), P(f(X) | s_j, \theta)), \quad (24)$$

where $W_{dkq(\alpha-1)}$ is p -Wasserstein distance with $p = dkq(\alpha - 1)$, computed with the ℓ_2 norm.

Corollary A.1 (DAGWM-Cauchy Mechanism [25]). *Let $f : X \rightarrow \mathbb{R}^d$ be a query function. Let Q_α denote the Legendre polynomial of integer index $\alpha > 1$ and \bar{Q}_α as the polynomial derived from Q_α by only its non-negative coefficients. Let $k \geq 2$ and $q \geq 1$ such that $kq(\alpha - 1)/2$ is an integer. Then, $\mathcal{M}(X) = f(X) + N$ with $N = (N_1, \dots, N_d) \stackrel{iid}{\sim} \text{GCauchy}(\lambda, k)$ is $(\alpha, \hat{\epsilon})$ -RPP, where*

$$\hat{\epsilon} = \frac{d \log \frac{\beta_{k, \lambda} \pi}{\lambda} \bar{Q}_{kq(\alpha-1)/2} \left(1 + \left(\frac{\Delta_G^{dkq(\alpha-1)}}{d\lambda} \right)^2 \right)}{q(\alpha - 1)}$$

with $\Delta_G^{dkq(\alpha-1)}$ given by (24).

The DAGWM is proved to offer more utility than the GWM at no additional privacy cost [25].

Curse of dimensionality for DAGWM. Although DAGWM replaces ∞ -Wasserstein sensitivities by p -Wasserstein distances in (23), it does not eliminate the curse of dimensionality inherent to optimal transport. For a query $f : X \rightarrow \mathbb{R}^d$, the calibration term $\Delta_G^{\zeta, q, \alpha}$ in (23) and $\Delta_G^{dkq(\alpha-1)}$ in (24) depend on high-dimensional W_p -distances, $W_p(P(f(X) | s_i, \theta), P(f(X) | s_j, \theta))$ in \mathbb{R}^d . In practice, these quantities must be estimated from empirical distributions based on n samples. Classical results on empirical Wasserstein distances imply that, for probability measures on \mathbb{R}^d with bounded support and finite p -th moments, the expected estimation error obeys

$$\mathbb{E}[|W_p(\hat{\mu}_n, \mu) - W_p(\mu, \nu)|] \gtrsim c_d n^{-1/d},$$

for some dimension-dependent constant $c_d > 0$. Thus, to achieve a target accuracy ϵ in the Wasserstein sensitivity (and hence in the DAGWM calibration), the required sample size scales at least as $n = \Omega(\epsilon^{-d})$. Moreover, computing W_p (or a sufficiently accurate approximation) between two n -point empirical measures in \mathbb{R}^d entails solving a high-dimensional optimal transport problem, whose complexity also grows rapidly with both n and d . Consequently, while DAGWM improves the distribution-awareness of RPP, it still inherits the statistical and computational curse of dimensionality of high-dimensional Wasserstein distances, and may become impractical when $f(X)$ is moderately or highly dimensional.

B Average vs. Joint SRPP

Average SRPP (Ave-SRPP) and Joint SRPP (Joint-SRPP) are built from the same ingredients, Rényi divergences of one-dimensional projections, but aggregate these per-direction costs in different ways, leading to distinct strengths and use cases.

Recall that for any pair of probability measures P, Q on \mathbb{R}^d and a slice profile $\{\mathcal{U}, \omega\}$, the average sliced Rényi divergence of order $\alpha > 1$ is

$$\text{AveSD}_\alpha^\omega(P\|Q) := \int_{\mathbb{S}^{d-1}} D_\alpha(\pi_{u\#}P \parallel \pi_{u\#}Q) d\omega(u),$$

while the joint sliced Rényi divergence is

$$\text{JSD}_\alpha^\omega(P\|Q) := \frac{1}{\alpha-1} \log \mathbb{E}_{U \sim \omega} \left[\exp((\alpha-1) D_\alpha(\pi_{U\#}P \parallel \pi_{U\#}Q)) \right].$$

Ave-SRPP requires that, for every prior $\theta \in \Theta$ and every secret pair $(s_0, s_1) \in Q$, the *average* sliced Rényi divergence between the corresponding output probability distribution is bounded by ϵ . Joint-SRPP instead bounds the log-moment aggregation of per-slice divergences, which can be interpreted as the Rényi divergence between the joint distributions $(\tilde{P}(\cdot, \cdot))$ of the *slice (index) and the projected output*. In particular, if we define the sliced channel

$$\text{Slice}(M) : x \rightarrow (U, \pi_U(\mathcal{M}(x))), \quad U \sim \omega,$$

then the Joint-SRD coincides with the standard Rényi divergence

$$\text{JSD}_\alpha^V(P\|Q) = D_\alpha(\tilde{P}(U, \pi_U(Z_P)) \parallel \tilde{P}(U, \pi_U(Z_Q))),$$

where $Z_P \sim P$ and $Z_Q \sim Q$. In this sense, Joint-SRPP is exactly RPP applied to the augmented, “sliced” observation $(U, \pi_U(\mathcal{M}(X)))$, whereas Ave-SRPP only controls the *mean* per-direction divergence.

These two aggregation schemes are ordered between each other and the full Rényi divergence. For any P, Q on \mathbb{R}^d and any slice distribution ω ,

$$\text{AveSD}_\alpha^\omega(P\|Q) \leq \text{JSD}_\alpha^\omega(P\|Q) \leq D_\alpha(P\|Q),$$

and the same inequalities hold for the corresponding output laws under any fixed Pufferfish model (\mathcal{S}, Q, Θ) (Proposition 4.1). Thus, at the level of numerical certificates, Joint-SRPP is always at least as “conservative” as Ave-SRPP for the same $(\alpha, \epsilon, \omega)$, and both are upper-bounded by the unsliced RPP divergence.

Why do we introduce both notions? Although Ave-SRPP and Joint-SRPP are closely related, they serve complementary purposes:

- **Ave-SRPP for geometry-aware *average* protection.**

Ave-SRPP directly reflects the geometry induced by the slicing distribution ω and is naturally aligned with sliced Wasserstein mechanism privatization, where one averages per-direction sensitivities. Formally, it controls the *expected* sliced Rényi divergence when the projection direction is drawn from ω . Equivalently, it quantifies privacy risk as if one only observed a single one-dimensional view sampled from ω , with average Rényi cost at most ϵ . This “single-slice observer” is purely an analytic device: the actual mechanism always outputs the full d -dimensional vector, and the sliced view is used only to define a geometry-aware privacy budget. In practice, this makes Ave-SRPP a natural *calibration target*, often yielding tighter, more utility-friendly noise levels than enforcing a worst-case bound simultaneously in every direction.

- **Joint-SRPP for robust, slice-aware guarantees.**

Joint-SRPP instead can be interpreted as if it treats the slice index as part of the observation channel and bounds the Rényi divergence of the joint pair $(U, \pi_U(\mathcal{M}(X)))$. In terms of risk quantification, this corresponds to accounting for an observer that can exploit knowledge of *which* direction was used, not just the projected value. Thus Joint-SRPP protects against worst-case sliced distinguishability over the randomized slicing procedure, rather than its average, and provides a more conservative, slice-aware notion of privacy than Ave-SRPP.

C Relationship to Group DP-SGD

The dependence on the discrepancy cap K_t (worst-case) and its mean-square analogue $\mathbb{E}_\eta[K_t^2]$ in our SRPP/ms-SRPP privatization of SGD naturally raises the question: *can group DP-SGD, with an appropriate group size, serve as a reliable proxy for SRPP-SGD when the protected information is a specific Pufferfish secret?* In this appendix, we clarify the relationship between SRPP-/ms-SRPP-SGD and group DP-SGD, and explain why the latter cannot generally substitute for the former when one cares about secret-level Pufferfish guarantees.

Our SRPP- and ms-SRPP-SGD mechanisms are calibrated directly from the HUC and ms-HUC envelopes developed in Section ???. For a fixed Rényi order $\alpha > 1$ and a target sliced privacy budget ϵ , the corresponding theorems give an upper bound on the per-run SRPP or ms-SRPP cost in terms of the HUC/ms-HUC sequence $\{h_t\}$ and the per-step noise covariances $\{\Sigma_t\}$. In our experiments we specialize to isotropic Gaussian noise $\Sigma_t = \sigma^2 I$ and, for each desired ϵ , solve the resulting bound for a noise scale $\sigma(\epsilon)$ that guarantees the prescribed SRPP or ms-SRPP budget. This calibration is explicitly secret-aware: H_{total} depends on the Pufferfish scenario (\mathcal{S}, Q, Θ) through the discrepancy caps K_t and mean-square

discrepancy caps $\mathbb{E}_\eta[K_t^2]$, which, for each iteration t , bound the ℓ_2 -distance between the clipped, averaged gradient updates under any admissible secret pair $(s_i, s_j) \in Q$ and any coupling of their corresponding data-generating distributions.

In contrast, standard group DP-SGD is calibrated with respect to a *dataset-level* adjacency relation

$$X \sim_k X' \iff d_H(X, X') \leq k,$$

where d_H is Hamming distance and $k \in \mathbb{N}$ is a chosen group size. A mechanism M is (ϵ_g, δ_g) -group-DP for group size k if

$$\Pr[M(X) \in E] \leq e^{\epsilon_g} \Pr[M(X') \in E] + \delta_g, \quad \forall E \subseteq \mathcal{Y}, \forall X \sim_k X'. \quad (25)$$

In DP-SGD, one typically fixes k and uses a moments accountant to obtain (ϵ_g, δ_g) as a function of k , the sampling probability $q = L/N$, the number of steps T , and the per-step noise scale σ_{DP} .

A natural question is whether group DP-SGD can be used as a proxy for SRPP/ms-SRPP-SGD by setting the group size to $k = \mathbb{E}_\eta[K_t^2]$. In what follows, we focus on this mean-square quantity because using the worst-case cap K_t as an effective group size would only further increase the required noise and make group DP even more conservative.

In this section, we clarify two points:

- There is no general result that, given a group-DP guarantee (25) for some group size k , produces an (α, ϵ) -SRPP or ms-SRPP guarantee for an arbitrary Pufferfish scenario (S, Q, Θ) . In particular, even if we set $k = \mathbb{E}_\eta[K_t^2]$ based on our HUC/ms-HUC analysis, there is no closed-form or universal mapping from $(\epsilon_g, \delta_g, k)$ to an SRPP/ms-SRPP budget ϵ .
- Even when we fix a specific Pufferfish scenario (S, Q, Θ) and choose the group size $k = \mathbb{E}_\eta[K_t^2]$, the resulting (ϵ_g, δ_g) group-DP-SGD guarantee is in general not a certified conservative bound for our (α, ϵ) SRPP/ms-SRPP guarantees, and there is no theorem ensuring that this group-DP guarantee upper-bounds the leakage measured in the SRPP/ms-SRPP sense.

C.1 No Universal Mapping

We first formalize the absence of a universal conversion from group-DP guarantees to SRPP/ms-SRPP guarantees.

Definition C.1 (Hypothetical DP \rightarrow SRPP conversion). *A DP-to-SRPP conversion map is a function*

$$F : (0, \infty) \times [0, 1] \times \mathbb{N} \rightarrow (0, \infty]$$

that, for given group-DP parameters (ϵ_g, δ_g) and group size k , assigns an SRPP budget $F(\epsilon_g, \delta_g, k)$ with the following property: for every mechanism \mathcal{M} and every Pufferfish scenario (S, Q, Θ) , if \mathcal{M} is (ϵ_g, δ_g) -group-DP with group size k , then

for all $\theta \in \Theta$ and all $(s_i, s_j) \in Q$ the SRPP/ms-SRPP divergence between the laws of \mathcal{M} under $(S = s_i, \theta)$ and $(S = s_j, \theta)$ is bounded by $F(\epsilon_g, \delta_g, k)$.

Our first result is that such a universal conversion map cannot exist.

Proposition C.1. *There is no function F satisfying Definition C.1, even if we restrict to pure group-DP ($\delta_g = 0$) and to finite secret sets S .*

Proof of Proposition C.1. Fix any candidate function F . We construct a counterexample.

Let the dataset space be $X = \{X_0, X_1\}$, and choose $k \in \mathbb{N}$ so that $d_H(X_0, X_1) > k$, where d_H is the Hamming distance. Under the group adjacency relation $X \sim_k X'$ (defined by $d_H(X, X') \leq k$), there are no *distinct* adjacent pairs: the only pairs with $d_H(X, X') \leq k$ are (X_0, X_0) and (X_1, X_1) . Hence, for any mechanism \mathcal{M} and any (ϵ_g, δ_g) , the group-DP inequality (25) is trivially satisfied, so \mathcal{M} is (ϵ_g, δ_g) -group-DP for all choices of (ϵ_g, δ_g) and k .

Now define a Pufferfish scenario with two secrets $S = \{0, 1\}$, a single prior $\Theta = \{\theta\}$, and a deterministic data-generating process

$$P_\theta(X = X_0 \mid S = 0) = 1, \quad P_\theta(X = X_1 \mid S = 1) = 1.$$

In other words, the secret value deterministically selects which of the two datasets is realized.

Consider the mechanism \mathcal{M} that simply reveals the secret:

$$\mathcal{M}(X_0) = 0, \quad \mathcal{M}(X_1) = 1.$$

As argued above, \mathcal{M} is (ϵ_g, δ_g) -group-DP for *all* (ϵ_g, δ_g) and all k , because there are no nontrivial adjacent dataset pairs.

However, the SRPP (and RPP/PP) divergence between the output distributions under $S = 0$ and $S = 1$ is infinite: for any measurable set E containing 0 but not 1 we have

$$\Pr[\mathcal{M}(X) \in E \mid S = 0] = 1, \quad \Pr[\mathcal{M}(X) \in E \mid S = 1] = 0.$$

In particular, the Rényi divergence of any order $\alpha > 1$ between the laws of $\mathcal{M}(X)$ given $S = 0$ and $S = 1$ is $+\infty$, so no finite SRPP budget can hold.

This contradicts the existence of a finite-valued $F(\epsilon_g, \delta_g, k)$ that would upper-bound SRPP leakage whenever \mathcal{M} is (ϵ_g, δ_g) -group-DP with group size k . Since $(\epsilon_g, \delta_g, k)$ were arbitrary, no such universal conversion function F can exist. \square

Proposition C.1 remains true if, instead of allowing arbitrary mechanisms, we restrict attention to mechanisms obtained by running DP-SGD and calibrating noise for a fixed group size k (including the specific choices $k = K_{\text{cap}}$ or $k \approx \mathbb{E}_\eta[K_t^2]$ from our HUC/ms-HUC analysis). We can always construct a Pufferfish scenario whose secrets are encoded in dataset differences at Hamming distance strictly

greater than k and hence outside the scope of the group-DP guarantee. Therefore, even when the group-DP parameters $(\epsilon_g, \delta_g, k)$ are known from a moments-accountant analysis of DP-SGD, there is no closed-form or universal transformation that converts them into the SRPP/ms-SRPP budget used in our HUC/ms-HUC-based SRPP-SGD calibration.

C.2 No Safe Bounds

We now specialize to the Pufferfish scenarios used in our experiments of SGD privatization, where the secret encodes the prevalence of a protected class (e.g. the `cat` label in CIFAR-10). Concretely, we consider two secret values s_0, s_1 which correspond to two label configurations on the same feature set, with different prevalences p_{low} and p_{high} of the protected class. Let $X^{(0)}$ and $X^{(1)}$ denote the realized datasets under $S = s_0$ and $S = s_1$, respectively, and let

$$\tilde{\Delta} := d_H(X^{(0)}, X^{(1)})$$

be the number of points whose labels differ between the two secrets.

In our HUC/sm-HUC analysis, $\tilde{\Delta}$ enters explicitly through the random variable K_t (the number of “differing” examples in a mini-batch at step t) and its cap K_{cap} (the worst-case throughout) or second moment $\mathbb{E}_\eta[K_t^2]$, which yield a scalar $\hat{\gamma}^2$ and hence H_{total} for SRPP/ms-SRPP accounting. One might ask whether it is sufficient, instead, to treat such quantities as an *effective group size* and calibrate a standard group DP-SGD with $k = \mathbb{E}_\eta[K_t^2]$. The following proposition shows that, even in prevalence-based scenarios, such a group-DP guarantee does not induce a general conservative (i.e., “safe”) bound for the secret.

Proposition C.2. *Fix any group size $k \in \mathbb{N}$ and any group-DP parameters (ϵ_g, δ_g) . There exist:*

- (i) *a prevalence-based Pufferfish scenario (S, Q, Θ) with two secrets $s_0, s_1 \in S$ whose realized datasets $X^{(0)}, X^{(1)}$ satisfy $d_H(X^{(0)}, X^{(1)}) > k$, and*
- (ii) *a mechanism \mathcal{M} that is (ϵ_g, δ_g) -group-DP with group size k*

such that the SRPP/ms-SRPP leakage between $(S = s_0, \theta)$ and $(S = s_1, \theta)$ under \mathcal{M} is infinite (in particular, not bounded by any finite function of $(\epsilon_g, \delta_g, k)$).

Proof. Fix $k \in \mathbb{N}$ and (ϵ_g, δ_g) . Choose a dataset size $N > k$ and an integer $\tilde{\Delta} \in \{k+1, \dots, N\}$. We construct a prevalence-based Pufferfish scenario and a mechanism \mathcal{M} .

Prevalence-based Pufferfish scenario. Let the data domain be $\tilde{X} = X \times \{0, 1\}$, where the second coordinate is a binary label indicating membership in the protected class (e.g. `cat` vs. “not-cat”). Let \mathcal{X} be the space of datasets of size N over \tilde{X} : $\mathcal{X} := \tilde{X}^N$. Fix two label configurations (datasets) $X^{(0)}, X^{(1)} \in \mathcal{X}$ on the same feature vectors such that:

- (i) the empirical prevalence of the protected class in $X^{(0)}$ is p_{low} , and in $X^{(1)}$ is p_{high} , with $p_{\text{high}} \neq p_{\text{low}}$, and
- (ii) exactly Δ labels differ between $X^{(0)}$ and $X^{(1)}$, so that

$$d_H(X^{(0)}, X^{(1)}) = \Delta > k$$

For example, we may take $X^{(0)}$ to have $\lfloor p_{\text{low}}N \rfloor$ protected labels and $X^{(1)}$ to have $\lfloor p_{\text{high}}N \rfloor$ protected labels, obtained by flipping exactly Δ labels.

Define a Pufferfish scenario with:

$$S = \{s_0, s_1\}, \quad \Theta = \{\theta\}, \quad Q = \{(s_0, s_1), (s_1, s_0)\}.$$

The data-generating mechanism is deterministic:

$$P_\theta(X = X^{(0)} \mid S = s_0) = 1, \quad P_\theta(X = X^{(1)} \mid S = s_1) = 1.$$

Thus, the secret S selects which prevalence configuration (dataset) is realized.

Group-DP adjacency and mechanism. Consider the group-DP adjacency relation on \mathcal{X} defined by Hamming distance at most k :

$$X \sim_k X' \iff d_H(X, X') \leq k.$$

Since $d_H(X^{(0)}, X^{(1)}) = \Delta > k$, the pair $(X^{(0)}, X^{(1)})$ is *not* adjacent. In particular, the group-DP constraint (25) never compares the joint law of $(\mathcal{M}(X^{(0)}), \mathcal{M}(X^{(1)}))$.

We now construct a mechanism \mathcal{M} . First, pick any mechanism $\mathcal{M}_0 : \mathcal{X} \rightarrow \mathcal{Y}$ that is (ϵ_g, δ_g) -group-DP with group size k (for example, the constant mechanism $\mathcal{M}_0(X) \equiv y_*$ for some $y_* \in \mathcal{Y}$). Such a mechanism exists for all $(\epsilon_g, \delta_g, k)$.

Define a new mechanism \mathcal{M} by modifying \mathcal{M}_0 only on the two special datasets $X^{(0)}$ and $X^{(1)}$:

$$\mathcal{M}(X) := \begin{cases} y_0, & \text{if } X = X^{(0)}, \\ y_1, & \text{if } X = X^{(1)}, \\ \mathcal{M}_0(X), & \text{otherwise,} \end{cases}$$

where $y_0, y_1 \in \mathcal{Y}$ are two distinct outputs such that $\mathcal{M}(X^{(0)})$ and $\mathcal{M}(X^{(1)})$ are almost surely separated (for example, take deterministic outputs $y_0 \neq y_1$).

We claim that \mathcal{M} is still (ϵ_g, δ_g) -group-DP with group size k . To see this, note that the definition of group-DP requires (25) to hold for all adjacent pairs $X \sim_k X'$, i.e. all pairs with $d_H(X, X') \leq k$. We distinguish two cases:

- (i) If $X \sim_k X'$ and $\{X, X'\} \cap \{X^{(0)}, X^{(1)}\} = \emptyset$, then $\mathcal{M}(X) = \mathcal{M}_0(X)$ and $\mathcal{M}(X') = \mathcal{M}_0(X')$, so the inequality (25) holds for \mathcal{M} because it holds for \mathcal{M}_0 .
- (ii) If $X \sim_k X'$ and, say, $X = X^{(0)}$, then $d_H(X^{(0)}, X') \leq k$ and $X' \neq X^{(1)}$ (since $d_H(X^{(0)}, X^{(1)}) = \Delta > k$). By construction, \mathcal{M} agrees with \mathcal{M}_0 on X' , and we can choose the distribution of $\mathcal{M}(X^{(0)})$ so that (25) holds for all such adjacent pairs; for example, we can set $\mathcal{M}(X^{(0)}) \stackrel{d}{=} \mathcal{M}_0(X^{(0)})$

and then only encode the secret in the choice of labels $(X^{(0)}, X^{(1)})$ in the Pufferfish scenario, rather than in the law of $\mathcal{M}(X^{(0)})$ itself. An entirely analogous argument applies if $X = X^{(1)}$.

Thus \mathcal{M} can be constructed so that it remains (ϵ_g, δ_g) -group-DP with group size k and yet its behavior on the two realized datasets $X^{(0)}$ and $X^{(1)}$ is separated as much as we like.

SRPP/ms-SRPP leakage. Under the Pufferfish scenario above, the distribution of $\mathcal{M}(X)$ given $S = s_0$ is the law of $\mathcal{M}(X^{(0)})$, and the distribution of $\mathcal{M}(X)$ given $S = s_1$ is the law of $\mathcal{M}(X^{(1)})$. By choosing \mathcal{M} so that these two laws are mutually singular (e.g. deterministic, distinct outputs), we obtain

$$\Pr[\mathcal{M}(X) \in E \mid S = s_0] = 1, \quad \Pr[\mathcal{M}(X) \in E \mid S = s_1] = 0$$

for some measurable set $E \subseteq \mathcal{Y}$. Hence the Rényi divergence of any order $\alpha > 1$ between the laws of $\mathcal{M}(X)$ under $S = s_0$ and $S = s_1$ is $+\infty$, so the SRPP (and ms-SRPP) leakage between these two secrets is infinite. In particular, it cannot be bounded by any finite function of $(\epsilon_g, \delta_g, k)$.

Since $(\epsilon_g, \delta_g, k)$ were arbitrary, this establishes the claim. \square

Proposition C.2 shows that, even when we work with prevalence-based Pufferfish secrets as in our CIFAR-10 experiments, simply calibrating DP-SGD with a group size chosen from our HUC/ms-HUC analysis (for example $k = K_{\text{cap}}$ or $k \approx \mathbb{E}_\eta[K_t^2]$) does *not* yield a certified bound in the SRPP/ms-SRPP sense. Group-DP is a guarantee indexed by Hamming-adjacent dataset pairs, whereas SRPP/ms-SRPP explicitly quantify the divergence between output distributions induced by different secrets (and different priors) in a given Pufferfish scenario. Our HUC/sm-HUC-based SRPP-SGD calibration is therefore not a reparameterization of group DP-SGD; it is a distinct analysis that targets secret-level leakage for the specified Pufferfish scenario.

D Minimality and Attainability of HUC

Proposition D.1. Fix t , a slicing set $\mathcal{U} = \{u_i\}_{i=1}^m \subset \mathbb{S}^{d-1}$, a history $y_{<t} \in \mathcal{Y}_{<t}$, and an admissible coupling γ . Define the shift

$$\Delta_t(X, X'; R_t) := f_t(X, y_{<t}; R_t) - f_t(X', y_{<t}; R_t). \quad (26)$$

Let $P := \gamma \times \mathbb{P}_{\eta, P}$ and $\mu_t := (\Delta_t)_\# P$ be the pushforward measure of Δ_t , and define

$$\text{ELS}_t := \text{supp}(\mu_t) = \{z \in \mathbb{R}^d : \mu_t(\mathcal{B}_{\bar{\epsilon}}(z)) > 0 \text{ for all } \bar{\epsilon} > 0\},$$

where $\mathcal{B}_{\bar{\epsilon}}(z)$ is a ball of radius $\bar{\epsilon}$ centered at z . For each slice u_i , define

$$\phi_t(u_i) := \sup_{\Delta \in \text{ELS}_t} |\langle \Delta, u_i \rangle| \quad \text{and} \quad h_{t,i}^* := \phi_t(u_i)^2.$$

Then, the following holds.

- (i) **Minimality.** Any HUC $h_t = (h_{t,1}, \dots, h_{t,m})$ for $(y_{<t}, \gamma)$ satisfies $h_{t,i} \geq h_{t,i}^*$ for all $i \in [m]$.
- (ii) **Attainability.** If ELS_t is compact, then for each $i \in [m]$ there exists $\Delta_i^* \in \text{ELS}_t$ with $|\langle \Delta_i^*, u_i \rangle| = \phi_t(u_i)$; hence $h_{t,i}^*$ is attained.

However, the HUC constructed in Proposition 5.1 is generally not tight; it is a computable conservative bound. Proposition D.1 characterizes the *minimal* HUC and specifies when it is attained. In particular, any valid HUC h_t must satisfy $h_{t,i} \geq h_{t,i}^*$ for all $i \in [m]$, and the minimal cap h_t^* is attained whenever the essential shift set ELS_t is compact.

In our setting, compactness of ELS_t follows from three ingredients: (i) per-example clipping, which uniformly bounds each individual gradient contribution; (ii) a finite discrepancy cap together with a deterministic (or bounded) batch size; and (iii) an L_t -Lipschitz post-update map. These yield a uniform almost-sure bound $\|\Delta_t\|_2 \leq C_t$ for some finite C_t , and hence $\text{ELS}_t \subset \bar{B}(0, C_t)$, which is closed and bounded in \mathbb{R}^d and therefore compact.

The following corollary follows Proposition D.1.

Corollary D.1. Consider the linear, blockwise-clipped case where

$$f_t(x, y_{<t}; R_t) = \xi_{t-1} - A_t \bar{g}_t(x; R_t),$$

with A_t independent of $((X, X'), R_t)$, and per-block clipping thresholds $\{C_b\}_{b=1}^{B_{\text{blk}}}$ over an orthogonal block decomposition with projectors $\{P_b\}_{b=1}^{B_{\text{blk}}}$. Assume that, for each block b , the blockwise gradient differences can attain the clipping radius in directions aligned with the vectors $P_b A_t^\top u_i$ (for the slices of interest). Then the minimal per-slice HUC is

$$h_{t,i}^* = \left(\frac{2K_t}{B_t}\right)^2 \left(\sum_{b=1}^{B_{\text{blk}}} C_b \|P_b A_t^\top u_i\|_2\right)^2, \quad i \in [m]. \quad (27)$$

D.1 Proof of Proposition D.1

We begin with a simple measure-theoretic observation. Let μ be a Borel probability measure on \mathbb{R}^d with support $\text{U} = \text{supp}(\mu)$, and let $g : \mathbb{R}^d \rightarrow \mathbb{R}$ be continuous. If $g(\Delta) \leq c$ holds μ -a.s., then necessarily

$$\sup_{\Delta \in \text{U}} g(\Delta) \leq c.$$

Indeed, suppose for contradiction that there exists $\Delta^* \in \text{U}$ with $g(\Delta^*) > c$. By continuity of g , there exists $\bar{\epsilon} > 0$ such that $g(\Delta) > c$ for all Δ in the open Euclidean ball $B_{\bar{\epsilon}}(\Delta^*)$. Since $\Delta^* \in \text{U} = \text{supp}(\mu)$, we have $\mu(B_{\bar{\epsilon}}(\Delta^*)) > 0$, which contradicts the assumption $g(\Delta) \leq c$ μ -a.s.

(i) Minimality. In our setting, for any slice $u_i \in \mathbb{S}^{d-1}$ define the continuous map

$$g_{u_i}(\Delta) := |\langle \Delta, u_i \rangle|, \quad \Delta \in \mathbb{R}^d.$$

The HUC inequality for a given h_t asserts that

$$g_{u_i}(\Delta_t(X, X'; R_t)) = |\langle \Delta_t(X, X'; R_t), u_i \rangle| \leq \sqrt{h_{t,i}} \quad \mu_t\text{-a.s.},$$

where μ_t is the pushforward measure of Δ_t and $\text{ELS}_t = \text{supp}(\mu_t)$. Applying the auxiliary observation with $\mu = \mu_t$, $g = g_{u_i}$, and $c = \sqrt{h_{t,i}}$ yields

$$\sup_{\Delta \in \text{ELS}_t} |\langle \Delta, u_i \rangle| \leq \sqrt{h_{t,i}}.$$

Hence $\phi_t(u_i) \leq \sqrt{h_{t,i}}$ and therefore

$$h_{t,i}^* = \phi_t(u_i)^2 \leq h_{t,i}.$$

This holds for each $i \in [m]$, proving minimality.

(ii) Attainability. Assume ELS_t is compact. The map $g_{u_i}(\Delta) = |\langle \Delta, u_i \rangle|$ is continuous, so by the Weierstrass Extreme Value Theorem it attains its maximum on ELS_t . Thus there exists $\Delta_i^* \in \text{ELS}_t$ such that

$$g_{u_i}(\Delta_i^*) = \max_{\Delta \in \text{ELS}_t} g_{u_i}(\Delta) = \phi_t(u_i).$$

Consequently, $h_{t,i}^* = \phi_t(u_i)^2$ is attained for each $i \in [m]$.

D.2 Proof of Corollary D.1

We work at a fixed iteration t and suppress the t -index when the meaning is clear.

Step 1: Characterizing the feasible shifts. In the linear case,

$$f_t(x, y_{<}; R_t) = \xi_{t-1} - A_t \bar{g}_t(x; R_t),$$

so for any coupled pair (X, X') and sampling draw R_t ,

$$\begin{aligned} \Delta_t(X, X'; R_t) &:= f_t(X, y_{<}; R_t) - f_t(X', y_{<}; R_t) \\ &= -A_t (\bar{g}_t(X; R_t) - \bar{g}_t(X'; R_t)). \end{aligned}$$

Let

$$v := \bar{g}_t(X; R_t) - \bar{g}_t(X'; R_t).$$

Under blockwise clipping with thresholds $\{C_b\}_{b=1}^{B_{\text{blk}}}$ and discrepancy cap K_t (i.e., at most K_t indices differ in the mini-batch), we have, for each block b ,

$$\|P_b v\|_2 \leq \frac{2C_b}{B_t} K_t \quad \gamma \times \mathbb{P}_{\eta, \rho}\text{-a.s.}$$

since at most K_t per-example contributions in that block can change, and each change is clipped to radius C_b in that block.

Thus any realized v lies in the (blockwise) product of Euclidean balls

$$\mathcal{V} := \left\{ v \in \mathbb{R}^d : \|P_b v\|_2 \leq \alpha_b := \frac{2C_b K_t}{B_t}, \quad b = 1, \dots, B_{\text{blk}} \right\}.$$

Consequently, any realized shift has the form

$$\Delta = -A_t v \quad \text{with } v \in \mathcal{V}.$$

By Proposition D.1, the minimal per-slice cap is

$$h_{t,i}^* = \sup_{\Delta \in \text{ELS}_t} |\langle \Delta, u_i \rangle|^2,$$

where ELS_t is the essential shift set. Under the assumption that the blockwise gradient differences *can attain* the clipping radius in directions aligned with $P_b A_t^\top u_i$, the essential shift set ELS_t coincides with the set

$$\{-A_t v : v \in \mathcal{V}\},$$

so

$$h_{t,i}^* = \sup_{v \in \mathcal{V}} |\langle -A_t v, u_i \rangle|^2 = \sup_{v \in \mathcal{V}} |\langle v, A_t^\top u_i \rangle|^2.$$

Step 2: Optimizing over the blockwise constraints. Fix a slice index i and write

$$w := A_t^\top u_i.$$

Decompose both v and w into blocks:

$$v = \sum_{b=1}^{B_{\text{blk}}} v_b, \quad v_b := P_b v, \quad w = \sum_{b=1}^{B_{\text{blk}}} w_b, \quad w_b := P_b w.$$

The constraints on v are

$$\|v_b\|_2 \leq \alpha_b := \frac{2C_b K_t}{B_t}, \quad b = 1, \dots, B_{\text{blk}}.$$

Then

$$\langle v, w \rangle = \sum_{b=1}^{B_{\text{blk}}} \langle v_b, w_b \rangle.$$

To maximize $|\langle v, w \rangle|$ subject to the blockwise constraints, we may choose each block v_b independently. The optimal choice in block b aligns v_b with w_b (or its negative), i.e.,

$$v_b^* = \alpha_b \frac{w_b}{\|w_b\|_2} \quad \text{whenever } w_b \neq 0,$$

and $v_b^* = 0$ if $w_b = 0$. This gives

$$\langle v_b^*, w_b \rangle = \alpha_b \|w_b\|_2,$$

and the summed inner product becomes

$$\sup_{v \in \mathcal{V}} |\langle v, w \rangle| = \sum_{b=1}^{B_{\text{blk}}} \alpha_b \|w_b\|_2 = \frac{2K_t}{B_t} \sum_{b=1}^{B_{\text{blk}}} C_b \|P_b A_t^\top u_i\|_2.$$

Therefore,

$$h_{t,i}^* = \sup_{v \in \mathcal{V}} |\langle v, w \rangle|^2 = \left(\frac{2K_t}{B_t} \right)^2 \left(\sum_{b=1}^{B_{\text{blk}}} C_b \|P_b A_t^\top u_i\|_2 \right)^2.$$

Step 3: Attainability. By assumption, for each block b we can realize gradient differences whose clipped contributions saturate the radius C_b in directions aligned with $P_b A_t^\top u_i$, and there exists a sampling outcome R_t that selects exactly those K_t indices. This makes the blockwise equalities $\|v_b\|_2 = \alpha_b$ attainable and yields an update shift Δ_t^* such that

$$|\langle \Delta_t^*, u_i \rangle|^2 = h_{t,i}^*.$$

Hence the supremum is attained, and $h_{t,i}^*$ is indeed the minimal HUC for slice u_i in this linear, blockwise-clipped setting.

E Proof of Proposition 4.1

Fix a slice profile $\{\mathcal{U}, \omega\}$, a prior $\theta \in \Theta$, and a secret pair $(s_i, s_j) \in \mathcal{Q}$ with $P_\theta^S(s_i), P_\theta^S(s_j) > 0$. Write

$$P := \mathcal{M}_{s_i}^\theta, \text{ and } Q := \mathcal{M}_{s_j}^\theta$$

for the output probability measures of the mechanism under s_i and s_j , respectively. Let $\{\mathcal{U}, \omega\}$ with $\mathcal{U} = \{u_\ell\}_{\ell=1}^m$ and $\omega = \{\omega_\ell\}_{\ell=1}^m$ be the discrete slicing profile, and denote

$$D_\ell := D_\alpha(u_{\ell\#}P \| u_{\ell\#}Q), \quad \ell = 1, \dots, m.$$

By Definition 4.1, the average sliced Rényi divergence is

$$\text{ASD}_\alpha^\omega(P \| Q) = \sum_{\ell=1}^m \omega_\ell D_\ell.$$

By Definition 4.3, the joint sliced Rényi divergence is

$$\text{JSD}_\alpha^\omega(P \| Q) = \frac{1}{\alpha-1} \log \left(\sum_{\ell=1}^m \omega_\ell \exp((\alpha-1)D_\ell) \right).$$

Part 1: $\text{ASD}_\alpha^\omega(P \| Q) \leq \text{JSD}_\alpha^\omega(P \| Q)$.

Let Z be the random variable $Z = D_\ell$ when $u_\ell \sim \omega$. Then,

$$\mathbb{E}[Z] = \sum_{\ell=1}^m \omega_\ell D_\ell = \text{ASD}_\alpha^\omega(P \| Q),$$

and

$$\text{JSD}_\alpha^\omega(P \| Q) = \frac{1}{\alpha-1} \log \mathbb{E}[\exp((\alpha-1)Z)]$$

For $\alpha > 1$, $\exp((\alpha-1)z)$ is convex. Then, Jensen's inequality gives

$$\mathbb{E}[\exp((\alpha-1)Z)] \geq \exp((\alpha-1)\mathbb{E}[Z]).$$

Thus, by taking log and dividing by $(\alpha-1)$, we get

$$\text{JSD}_\alpha^\omega(P \| Q) \geq \mathbb{E}[Z] = \text{ASD}_\alpha^\omega(P \| Q).$$

Part 2: $\text{JSD}_\alpha^\omega(P \| Q) \leq D_\alpha(P \| Q)$.

Define a *sliced observation channel* Slice as follows. Given $Y \in \mathbb{R}^d$, first draw $U \sim \omega$ independently of Y , then set $\hat{Z} := \langle Y, U \rangle$ (inner product) and output the pair

$$\text{Slice}(Y) := (U, \hat{Z}).$$

Let P^{Slice} (resp. Q^{Slice}) denote the probability measure of $\text{Slice}(Y)$ when $Y \sim P$ (resp. $Y \sim Q$):

$$P^{\text{Slice}}(u_\ell, \cdot) = \omega_\ell u_{\ell\#}P, \quad Q^{\text{Slice}}(u_\ell, \cdot) = \omega_\ell u_{\ell\#}Q.$$

Assume that $u_{\ell\#}P$ and $u_{\ell\#}Q$ admit densities, and denote them by p_ℓ and q_ℓ , respectively. Then the joint distribution P^{Slice} on $\{1, \dots, m\} \times \mathbb{R}$ has density

$$f(\ell, \hat{z}) = \omega_\ell p_\ell(\hat{z}),$$

and similarly the joint distribution Q^{Slice} has

$$g(\ell, \hat{z}) = \omega_\ell q_\ell(\hat{z}).$$

The Rényi divergence of order $\alpha > 1$ between these joint probability measures is

$$\begin{aligned} D_\alpha(P^{\text{Slice}} \| Q^{\text{Slice}}) &= \frac{1}{\alpha-1} \log \sum_{\ell=1}^m \int f(\ell, \hat{z})^\alpha g(\ell, \hat{z})^{1-\alpha} d\hat{z} \\ &= \frac{1}{\alpha-1} \log \sum_{\ell=1}^m \omega_\ell \int p_\ell(z)^\alpha q_\ell(z)^{1-\alpha} dz \\ &= \frac{1}{\alpha-1} \log \sum_{\ell=1}^m \omega_\ell \exp((\alpha-1)D_\ell) \\ &= \text{JSD}_\alpha^\omega(P \| Q), \end{aligned}$$

since

$$D_\ell = D_\alpha(u_{\ell\#}P \| u_{\ell\#}Q) = \frac{1}{\alpha-1} \log \int p_\ell(z)^\alpha q_\ell(z)^{1-\alpha} dz.$$

Thus, we have

$$\text{JSD}_\alpha^\omega(P \| Q) = D_\alpha(P^{\text{Slice}} \| Q^{\text{Slice}}).$$

Now, we know that (U, \hat{Z}) is obtained from Y by a (randomized) post-processing that does not depend on the secret or prior. That is, we first draw $U \sim \omega$, then apply the measurable map $(Y, U) \mapsto (U, \langle Y, U \rangle)$. The Rényi divergence is an f -divergence with $f(t) = t^\alpha$, hence satisfies the data-processing inequality: for any Markov kernel K ,

$$D_\alpha(PK \| QK) \leq D_\alpha(P \| Q).$$

When the kernel K is the sliced channel Slice, we obtain

$$D_\alpha(P^{\text{Slice}} \| Q^{\text{Slice}}) \leq D_\alpha(P \| Q).$$

That is,

$$\text{JSD}_\alpha^\omega(P\|Q) \leq D_\alpha(P\|Q).$$

By combining **Part 1** and **Part 2**, we can claim

$$\text{ASD}_\alpha^\omega(\mathcal{M}_{s_i}^\theta\|\mathcal{M}_{s_j}^\theta) \leq \text{JSD}_\alpha^\omega(\mathcal{M}_{s_i}^\theta\|\mathcal{M}_{s_j}^\theta) \leq D_\alpha(\mathcal{M}_{s_i}^\theta\|\mathcal{M}_{s_j}^\theta),$$

□

F Proof of Lemma 4.1

Fix a prior $\theta \in \Theta$, a secret pair $(s_i, s_j) \in \mathcal{Q}$ with $P_\theta^S(s_i), P_\theta^S(s_j) > 0$, a slice direction $u \in \mathcal{U}$, and an order $\alpha > 1$. Define the 1-D projected pre-noise probability measures as

$$P_u := P_{\#}^u F_{s_i}^\theta \quad \text{and} \quad Q_u := \Psi_{\#}^u F_{s_j}^\theta.$$

By definition of the per-slice ∞ -Wasserstein distance,

$$z_\infty^u := W_\infty(P_u, Q_u) = \inf_{\pi \in \Pi(P_u, Q_u)} \text{ess sup}_{(z, z') \sim \pi} |z - z'|.$$

Therefore, for every $\varepsilon > 0$ there exists a coupling $\pi_\varepsilon \in \Pi(P_u, Q_u)$ such that

$$|Z - Z'| \leq z_\infty^u + \varepsilon \quad \text{for } \pi_\varepsilon\text{-almost every } (Z, Z'). \quad (28)$$

Step 1. We first represent the sliced mechanism as a mixture of shifts. Let $\tilde{N} := \Psi_{\#}^u(N)$ be the projected noise with distribution $\Psi_{\#}^u \zeta$. With abuse of notation, we denote this 1-D noise distribution again by ζ .

Conditioned on a pre-noise scalar $z \in \mathbb{R}$, the sliced mechanism output is $z + \tilde{N}$, whose probability measure is the shifted noise distribution:

$$\zeta_z(A) := \Pr(z + \tilde{N} \in A) = \zeta(A - z), \quad \text{for } A \subseteq \mathbb{R}.$$

Under secret s_i , the sliced output distribution is therefore

$$\Psi_{\#}^u \mathcal{M}_{s_i}^\theta = \int \zeta_z P_u(dz).$$

Similarly, under s_j ,

$$\Psi_{\#}^u \mathcal{M}_{s_j}^\theta = \int \zeta_{z'} Q_u(dz').$$

Using the coupling π_ε between P_u and Q_u , we can represent $\Psi_{\#}^u \mathcal{M}_{s_i}^\theta$ and $\Psi_{\#}^u \mathcal{M}_{s_j}^\theta$ as mixtures over pairs (z, z') :

$$\Psi_{\#}^u \mathcal{M}_{s_i}^\theta = \int \zeta_z \pi_\varepsilon(dz, dz') \quad \text{and} \quad \Psi_{\#}^u \mathcal{M}_{s_j}^\theta = \int \zeta_{z'} \pi_\varepsilon(dz, dz').$$

Step 2. Next, we obtain a pointwise Rényi divergence between shifted noises. Let ζ_z denote the distribution of $\tilde{N} + z$ for $z \in \mathbb{R}$. Fix a pair (z, z') with $z \in \mathbb{R}$ and $z' \in \mathbb{R}$. Since Rényi

divergence is invariant under common bijective transformations, the corresponding shifted noise probability measures ζ_z and $\zeta_{z'}$ satisfy

$$D_\alpha(\zeta_z\|\zeta_{z'}) = D_\alpha(\zeta_{z-z'}\|\zeta).$$

By the definition of the shift-Rényi envelope

$$R_\alpha(\zeta, r) := \sup_{|a| \leq r} D_\alpha(\zeta_a\|\zeta),$$

we have, for every $z \in \mathbb{R}$ and $z' \in \mathbb{R}$,

$$D_\alpha(\zeta_z\|\zeta_{z'}) \leq R_\alpha(\zeta, |z - z'|).$$

Combining with the coupling bound (28), we obtain the uniform pointwise bound

$$D_\alpha(\zeta_z\|\zeta_{z'}) \leq R_\alpha(\zeta, z_\infty^u), \quad (29)$$

for π_ε -a.e. (z, z') .

Step 3. We proceed with the full mixtures $\Psi_{\#}^u \mathcal{M}_{s_i}^\theta$ and $\Psi_{\#}^u \mathcal{M}_{s_j}^\theta$. Rényi divergence of order $\alpha > 1$ is jointly quasi-convex in its arguments. That is, for any probability measure μ over an index set and any family $\{P_\beta, Q_\beta\}$,

$$D_\alpha\left(\int P_\beta \mu(d\beta) \parallel \int Q_\beta \mu(d\beta)\right) \leq \text{ess sup}_\beta D_\alpha(P_\beta\|Q_\beta).$$

For finite mixtures, this follows from the standard inequality

$$D_\alpha\left(\sum_k \lambda_k P_k \parallel \sum_k \lambda_k Q_k\right) \leq \max_k D_\alpha(P_k\|Q_k),$$

and the general case can be obtained by approximating μ by finite-support measures (a standard argument for f -divergences).

In our setting we take $\beta = (z, z')$, $\mu = \pi$ (the coupling from Step 1), and $P_\beta = \zeta_z$ and $Q_\beta = \zeta_{z'}$. Then

$$\Psi_{\#}^u \mathcal{M}_{s_i}^\theta = \int P_\beta \pi(dz, dz'), \quad \Psi_{\#}^u \mathcal{M}_{s_j}^\theta = \int Q_\beta \pi(dz, dz').$$

Hence

$$D_\alpha(\Psi_{\#}^u \mathcal{M}_{s_i}^\theta\|\Psi_{\#}^u \mathcal{M}_{s_j}^\theta) \leq \text{ess sup}_{(z, z') \sim \pi} D_\alpha(\zeta_z\|\zeta_{z'}).$$

Combining this with the pointwise bound from Step 2,

$$D_\alpha(\zeta_z\|\zeta_{z'}) \leq R_\alpha(\zeta, z_\infty^u)$$

for π -a.e. (z, z') , yields

$$D_\alpha(\Psi_{\#}^u \mathcal{M}_{s_i}^\theta\|\Psi_{\#}^u \mathcal{M}_{s_j}^\theta) \leq R_\alpha(\zeta, z_\infty^u),$$

which is the desired per-slice envelope bound. □

G Proof of Theorem 4.7

Fix $\theta \in \Theta$ and $(s_i, s_j) \in Q$ with $P_\theta^S(s_i), P_\theta^S(s_j) > 0$, and fix a slice profile $\{\mathcal{U}, \omega\}$. Let F_s^θ be the distribution of the pre-noise output $f(X)$ given $(S = s, \theta)$, and let

$$P := \mathcal{M}_{s_i}^\theta = F_{s_i}^\theta * \zeta \quad \text{and} \quad Q := \mathcal{M}_{s_j}^\theta = F_{s_j}^\theta * \zeta.$$

Step 1. We start by establishing a per-slice envelop bound using Lemma 4.1. For any direction $u \in \mathcal{U}$, applying Lemma 4.1 to the 1-D projection $\Psi^u(y) = \langle y, u \rangle$ gives, for all $\alpha > 1$,

$$D_\alpha(\Psi_\#^u P \parallel \Psi_\#^u Q) \leq R_\alpha(\zeta, z_\infty^u(\theta, s_i, s_j)),$$

where $z_\infty^u(\theta, s_i, s_j)$ is any upper bound on the 1-D shift between the pre-noise probability measures $\Psi_\#^u F_{s_i}^\theta$ and $\Psi_\#^u F_{s_j}^\theta$. By definition,

$$z_\infty^u(\theta, s_i, s_j) \leq \tilde{\Delta}_\infty^u(\theta, s_i, s_j) := W_\infty(\Psi_\#^u F_{s_i}^\theta \parallel \Psi_\#^u F_{s_j}^\theta),$$

and $R_\alpha(\zeta, \cdot)$ is non-decreasing in its second argument. Thus, we have

$$D_\alpha(\Psi_\#^u P \parallel \Psi_\#^u Q) \leq R_\alpha(\zeta, \tilde{\Delta}_\infty^u(\theta, s_i, s_j)) \quad (30)$$

for all $u \in \mathcal{U}$.

Step 2. Next, we consider Gaussian noise $\zeta = \mathcal{N}(0, \sigma^2 I_d)$. For any slice $u \in \mathcal{U}$, the projected noise $\Psi^u(N)$ is one-dimensional Gaussian $\mathcal{N}(0, \sigma^2)$. For any shift $a \in \mathbb{R}$, the shifted probability measure is $\mathcal{N}(a, \sigma^2)$, and the Rényi divergence of order $\alpha > 1$ between $\mathcal{N}(a, \sigma^2)$ and $\mathcal{N}(0, \sigma^2)$ is

$$D_\alpha(\mathcal{N}(a, \sigma^2) \parallel \mathcal{N}(0, \sigma^2)) = \frac{\alpha a^2}{2\sigma^2}.$$

Therefore, the 1-D Gaussian shift envelope is

$$R_\alpha(\zeta, z) := \sup_{|a| \leq z} D_\alpha(\zeta - a \parallel \zeta) = \sup_{|a| \leq z} \frac{\alpha a^2}{2\sigma^2} = \frac{\alpha}{2\sigma^2} z^2.$$

Substituting $z = \tilde{\Delta}_\infty^u(\theta, s_i, s_j)$ into (30) yields

$$D_\alpha(\Psi_\#^u P \parallel \Psi_\#^u Q) \leq \frac{\alpha}{2\sigma^2} (\tilde{\Delta}_\infty^u(\theta, s_i, s_j))^2. \quad (31)$$

By Definition 4.1, the ω -average sliced Rényi divergence is

$$\text{ASD}_\alpha^\omega(P \parallel Q) = \int_{\mathbb{S}^{d-1}} D_\alpha(\Psi_\#^u P \parallel \Psi_\#^u Q) d\omega(u).$$

Using the bound (31) and the linearity of the integral, we have

$$\begin{aligned} \text{ASD}_\alpha^\omega(P \parallel Q) &\leq \int_{\mathbb{S}^{d-1}} \frac{\alpha}{2\sigma^2} (\Delta_u^\infty(\theta, s_i, s_j))^2 d\omega(u) \\ &= \frac{\alpha}{2\sigma^2} \int_{\mathcal{U}} (\Delta_u^\infty(\theta, s_i, s_j))^2 d\omega(u) \\ &= \frac{\alpha}{2\sigma^2} \Delta^2(\theta, s_i, s_j). \end{aligned}$$

Step 3. By definition of $\bar{\Delta}^2$,

$$\Delta^2(\theta, s_i, s_j) \leq \bar{\Delta}^2$$

for all $\theta, (s_i, s_j)$. Therefore

$$\text{ASD}_\alpha^\omega(P \parallel Q) \leq \frac{\alpha}{2\sigma^2} \bar{\Delta}^2.$$

With the choice

$$\sigma^2 = \frac{\alpha \bar{\Delta}^2}{2\varepsilon},$$

we obtain, for every $\theta, (s_i, s_j)$,

$$\text{ASD}_\alpha^\omega(\mathcal{M}_{s_i}^\theta \parallel \mathcal{M}_{s_j}^\theta) \leq \varepsilon.$$

Since θ and (s_i, s_j) were arbitrary, this is exactly the $(\alpha, \varepsilon, \omega)$ -Ave-SRPE guarantee in (S, Q, Θ) . \square

H Proof of Theorem 4.8

Fix $\theta \in \Theta$ and $(s_i, s_j) \in Q$ with $P_\theta^S(s_i), P_\theta^S(s_j) > 0$, and fix a slice profile $\{\mathcal{U}, \omega\}$. Let F_s^θ denote the pre-noise distribution of $f(X)$ given $(S = s, \theta)$, and let

$$P := \mathcal{M}_{s_i}^\theta = F_{s_i}^\theta * \zeta, \quad \text{and} \quad Q := \mathcal{M}_{s_j}^\theta = F_{s_j}^\theta * \zeta.$$

Step 1. Fix a slice $u \in \mathcal{U}$. Lemma 4.1 applied to the 1-D projection $\Psi^u(y) = \langle y, u \rangle$ states that, for all $\alpha > 1$,

$$D_\alpha(\Psi_\#^u P \parallel \Psi_\#^u Q) \leq R_\alpha(\zeta, z_\infty^u(\theta, s_i, s_j)),$$

where $z_\infty^u(\theta, s_i, s_j)$ upper-bounds the 1-D shift (in W_∞) between the pre-noise probability measures $\Psi_\#^u F_{s_i}^\theta$ and $\Psi_\#^u F_{s_j}^\theta$. By definition,

$$z_\infty^u(\theta, s_i, s_j) \leq \tilde{\Delta}_\infty^u(\theta, s_i, s_j) := W_\infty(\Psi_\#^u F_{s_i}^\theta \parallel \Psi_\#^u F_{s_j}^\theta),$$

and the envelope $R_\alpha(\zeta, \cdot)$ is non-decreasing in its second argument. Hence

$$D_\alpha(\Psi_\#^u P \parallel \Psi_\#^u Q) \leq R_\alpha(\zeta, \tilde{\Delta}_\infty^u(\theta, s_i, s_j)) \quad (32)$$

for all $u \in \mathcal{U}$.

Step 2. Now, we specialize to Gaussian noise $\zeta = \mathcal{N}(0, \sigma^2 I_d)$. For any fixed slice $u \in \mathcal{U}$, the projected noise $\Psi^u(N)$ is 1-D Gaussian $\mathcal{N}(0, \sigma^2)$. If we shift by $a \in \mathbb{R}$, the noise becomes $\mathcal{N}(a, \sigma^2)$, and the order- α Rényi divergence between $\mathcal{N}(a, \sigma^2)$ and $\mathcal{N}(0, \sigma^2)$ is

$$D_\alpha(\mathcal{N}(a, \sigma^2) \parallel \mathcal{N}(0, \sigma^2)) = \frac{\alpha a^2}{2\sigma^2}.$$

Therefore the 1-D Gaussian shift envelope is

$$R_\alpha(\zeta, z) := \sup_{|a| \leq z} D_\alpha(\zeta - a \parallel \zeta) = \sup_{|a| \leq z} \frac{\alpha a^2}{2\sigma^2} = \frac{\alpha}{2\sigma^2} z^2.$$

Substituting $z = \tilde{\Delta}_\infty^u(\theta, s_i, s_j)$ into (32), we obtain

$$D_\alpha(\Psi_\#^u P \parallel \Psi_\#^u Q) \leq \frac{\alpha}{2\sigma^2} (\tilde{\Delta}_\infty^u(\theta, s_i, s_j))^2. \quad (33)$$

By Definition 4.2, the joint sliced Rényi divergence of order $\alpha > 1$ with slicing distribution ω is

$$\text{JSD}_\alpha^\omega(P \parallel Q) := \frac{1}{\alpha - 1} \log \int_{\mathbb{S}^{d-1}} \exp\left((\alpha - 1) D_\alpha(\Psi_\#^u P \parallel \Psi_\#^u Q)\right) d\omega(u)$$

Using the bound (33), we get for each u

$$D_\alpha(\Psi_\#^u P \parallel \Psi_\#^u Q) \leq \frac{\alpha}{2\sigma^2} (\tilde{\Delta}_\infty^u(\theta, s_i, s_j))^2 \leq \frac{\alpha}{2\sigma^2} \Delta_\star^2(\theta, s_i, s_j),$$

where

$$\Delta_\star^2(\theta, s_i, s_j) := \sup_{u \in \mathcal{U}} (\tilde{\Delta}_\infty^u(\theta, s_i, s_j))^2.$$

Therefore, we have

$$\begin{aligned} \text{JSD}_\alpha^\omega(P \parallel Q) &= \frac{1}{\alpha - 1} \log \int_{\mathbb{S}^{d-1}} \exp\left((\alpha - 1) D_\alpha(\Psi_\#^u P \parallel \Psi_\#^u Q)\right) d\omega(u) \\ &\leq \frac{1}{\alpha - 1} \log \int_{\mathbb{S}^{d-1}} \exp\left((\alpha - 1) \frac{\alpha}{2\sigma^2} \Delta_\star^2(\theta, s_i, s_j)\right) d\omega(u). \end{aligned}$$

Here, the integrand is independent of u , so the integral is just the constant itself:

$$\begin{aligned} &\int_{\mathbb{S}^{d-1}} \exp\left((\alpha - 1) \frac{\alpha}{2\sigma^2} \Delta_\star^2(\theta, s_i, s_j)\right) d\omega(u) \\ &= \exp\left((\alpha - 1) \frac{\alpha}{2\sigma^2} \Delta_\star^2(\theta, s_i, s_j)\right). \end{aligned}$$

Hence

$$\begin{aligned} \text{JSD}_\alpha^\omega(P \parallel Q) &\leq \frac{1}{\alpha - 1} \log \exp\left((\alpha - 1) \frac{\alpha}{2\sigma^2} \Delta_\star^2(\theta, s_i, s_j)\right) \\ &= \frac{\alpha}{2\sigma^2} \Delta_\star^2(\theta, s_i, s_j). \end{aligned}$$

Step 3. By definition of the global constant Δ_\star^2 , we have

$$\Delta_\star^2(\theta, s_i, s_j) \leq \Delta_\star^2$$

for all $\theta \in \Theta$, $(s_i, s_j) \in Q$. Thus

$$\text{JSD}_\alpha^\omega(\mathcal{M}_{s_i}^\theta \parallel \mathcal{M}_{s_j}^\theta) \leq \frac{\alpha}{2\sigma^2} \Delta_\star^2.$$

With the choice

$$\sigma^2 = \frac{\alpha \Delta_\star^2}{2\varepsilon},$$

we obtain

$$\text{JSD}_\alpha^\omega(\mathcal{M}_{s_i}^\theta \parallel \mathcal{M}_{s_j}^\theta) \leq \varepsilon$$

for every $\theta \in \Theta$ and $(s_i, s_j) \in Q$ with positive prior mass. This is exactly the $(\alpha, \varepsilon, \omega)$ -Joint-SRPE guarantee in (\mathcal{S}, Q, Θ) .

I Proof of Proposition 5.1

Fix an iteration t and a slice profile $\{\mathcal{U}, \omega\}$ with $\mathcal{U} = \{u_i\}_{i=1}^m$. Fix arbitrarily a prior $\theta \in \Theta$, a secret pair $(s_i, s_j) \in Q$ with $P_\theta^S(s_i), P_\theta^S(s_j) > 0$, a history $y_{<t}$ in the support, and a coupling $\gamma \in \Pi(\mu_{s_i}^\theta, \mu_{s_j}^\theta)$. Let $(X, X') \sim \gamma$ and $R_t \sim \mathbb{P}_{\eta, \rho}$ denote the minibatch sampling randomness at iteration t . For a draw r of R_t , let $\mathbf{l}_t(r) \subseteq [n]$ be the minibatch index (multi)set and $B_t(r) := |\mathbf{l}_t(r)|$ its size.

Step 1. By assumption, the minibatch size is deterministic, so we write $B_t := B_t(r) \geq 1$. For a dataset $x = (x_1, \dots, x_n)$, let $g_j(x)$ be the per-example gradient on x_j , and define the ℓ_2 -clipped gradient

$$\tilde{g}_j(x) := g_j(x) \min\left\{1, \frac{C}{\|g_j(x)\|_2}\right\}.$$

Then $\|\tilde{g}_j(x)\|_2 \leq C$ for all j and all x . The averaged clipped minibatch gradient at iteration t is

$$\bar{g}_t(\mathcal{B}(x; r)) := \frac{1}{B_t} \sum_{j \in \mathbf{l}_t(r)} \tilde{g}_j(x),$$

and similarly for x' . The discrepancy cap at iteration t (see (17)) is

$$K_t(x, x'; r) := \sum_{j \in \mathbf{l}_t(r)} \mathbf{1}\{x_j \neq x'_j\}.$$

By definition, at most $K_t(x, x'; r)$ indices in $\mathbf{l}_t(r)$ differ between x and x' , so only those terms can change their contribution to the average of gradients.

Whenever $x_j \neq x'_j$, we have

$$\|\tilde{g}_j(x) - \tilde{g}_j(x')\|_2 \leq \|\tilde{g}_j(x)\|_2 + \|\tilde{g}_j(x')\|_2 \leq 2C.$$

Therefore,

$$\begin{aligned} \|\bar{g}_t(\mathcal{B}(x; r)) - \bar{g}_t(\mathcal{B}(x'; r))\|_2 &\leq \frac{1}{B_t} K_t(x, x'; r) (2C) \\ &= \frac{2C}{B_t} K_t(x, x'; r). \end{aligned}$$

For any slice $u_i \in \mathcal{U}$, this implies

$$|\langle \bar{g}_t(\mathcal{B}(x; r)) - \bar{g}_t(\mathcal{B}(x'; r)), u_i \rangle| \leq \frac{2C}{B_t} K_t(x, x'; r). \quad (34)$$

Step 2. At iteration t , the pre-perturbation update is

$$f_t(x, y_{<t}; r) = T_t(\bar{g}_t(\mathcal{B}(x; r)); y_{<t}),$$

and similarly $f_t(x', y_{<t}; r) = T_t(\bar{g}_t(\mathcal{B}(x'; r)); y_{<t})$. Let

$$z := \bar{g}_t(\mathcal{B}(x; r)), \quad z' := \bar{g}_t(\mathcal{B}(x'; r)).$$

By Assumption 5.2, for each $u_i \in \mathcal{U}$ there exists $L_{t,i} < \infty$ such that, for all $z, z' \in \mathbb{R}^d$ and all histories $y_{<t}$,

$$|u_i^\top (T_t(z; y_{<t}) - T_t(z'; y_{<t}))| \leq L_{t,i} |u_i^\top (z - z')|.$$

Applying this with the z, z' defined above and using (34), we obtain

$$\begin{aligned} |\langle f_t(x, y_{<t}; r) - f_t(x', y_{<t}; r), u_i \rangle| &\leq L_{t,i} \frac{2C}{B_t} K_t(x, x'; r) \\ &= \frac{2CL_{t,i}}{B_t} K_t(x, x'; r). \end{aligned}$$

Squaring both sides yields

$$|\langle f_t(x, y_{<t}; r) - f_t(x', y_{<t}; r), u_i \rangle|^2 \leq \left(\frac{2CL_{t,i}}{B_t} K_t(x, x'; r) \right)^2.$$

Step 3. By definition of a feasible discrepancy cap at iteration t , K_t satisfies

$$K_t(x, x'; r) \leq K_t$$

for $\gamma \times \mathbb{P}_{\eta, \rho}$ -almost every $((X, X'), R_t)$, uniformly over all $\theta \in \Theta$, $(s_i, s_j) \in Q$, histories $y_{<t}$ in support, and couplings γ . Thus, for $\gamma \times \mathbb{P}_{\eta, \rho}$ -a.e. $((X, X'), R_t)$,

$$|\langle f_t(X, y_{<t}; R_t) - f_t(X', y_{<t}; R_t), u_i \rangle|^2 \leq \left(\frac{2K_t L_{t,i} C}{B_t} \right)^2 =: h_{t,i}.$$

Since the bound holds for all $i = 1, \dots, m$ and is uniform over $\theta, (s_i, s_j), y_{<t}$, and γ , the vector $h_t = (h_{t,1}, \dots, h_{t,m})$ with

$$h_{t,i} := \left(\frac{2K_t L_{t,i} C}{B_t} \right)^2$$

satisfies the HUC condition (16). Therefore h_t is a valid history-uniform cap at iteration t , as claimed. \square

J Proof of Proposition 5.2

Fix an iteration t and a slice profile $\{\mathcal{U}, \omega\}$ with $\mathcal{U} = \{u_i\}_{i=1}^m \subset \mathbb{S}^{d-1}$. Let $\theta \in \Theta$, $(s_i, s_j) \in Q$, a history $y_{<t}$ in the support, and a coupling $\gamma \in \Pi(\mu_{s_i}^\theta, \mu_{s_j}^\theta)$ be arbitrary. Let $(X, X') \sim \gamma$. In addition, let $\eta_t \sim \mathbb{P}_\eta$ denote the subsampling randomness at iteration t . We write $\bar{g}_t(X; \eta_t)$ and $\bar{g}_t(X'; \eta_t)$ for the clipped, averaged minibatch gradients, and $f_t(X, y_{<t}; \eta_t)$, $f_t(X', y_{<t}; \eta_t)$ for the corresponding pre-perturbation updates.

Step 1. By per-example ℓ_2 -clipping at threshold C and the definition of the discrepancy $K_t(X, X'; \eta_t)$, the argument in the proof of Proposition 5.1 gives, for every realization of η_t ,

$$\|\bar{g}_t(X; \eta_t) - \bar{g}_t(X'; \eta_t)\|_2 \leq \frac{2C}{B_t} K_t(X, X'; \eta_t).$$

Hence, for any slice $u_i \in \mathcal{U}$,

$$|\langle \bar{g}_t(X; \eta_t) - \bar{g}_t(X'; \eta_t), u_i \rangle| \leq \frac{2C}{B_t} K_t(X, X'; \eta_t). \quad (35)$$

Define the pre-update difference

$$\Delta_t^{\text{pre}}(X, X'; \eta_t) := \bar{g}_t(X; \eta_t) - \bar{g}_t(X'; \eta_t),$$

and the update difference

$$\Delta_t(X, X'; \eta_t) := f_t(X, y_{<t}; \eta_t) - f_t(X', y_{<t}; \eta_t).$$

By Assumption 5.2, for each slice $u_i \in \mathcal{U}$ and every realization of η_t ,

$$|\langle \Delta_t(X, X'; \eta_t), u_i \rangle| \leq L_{t,i} |\langle \Delta_t^{\text{pre}}(X, X'; \eta_t), u_i \rangle|.$$

Combining this with (35) yields the pathwise bound

$$|\langle \Delta_t(X, X'; \eta_t), u_i \rangle| \leq \frac{2L_{t,i}C}{B_t} K_t(X, X'; \eta_t) \quad (36)$$

for all $i = 1, \dots, m$ and all η_t .

Step 2. Fix (X, X') in the support. Squaring both sides of (36) and taking expectations with respect to $\eta_t \sim \mathbb{P}_\eta$, we obtain, for each $i = 1, \dots, m$,

$$\mathbb{E}_{\eta_t} [|\langle \Delta_t(X, X'; \eta_t), u_i \rangle|^2] \leq \left(\frac{2L_{t,i}C}{B_t} \right)^2 \mathbb{E}_{\eta_t} [K_t(X, X'; \eta_t)^2].$$

By the definition of the mean-square discrepancy cap \bar{K}_t^2 in (19), we have, for γ -almost every (X, X') ,

$$\mathbb{E}_{\eta_t} [K_t(X, X'; \eta_t)^2] \leq \bar{K}_t^2.$$

Therefore, for γ -almost every (X, X') ,

$$\mathbb{E}_{\eta_t} [|\langle \Delta_t(X, X'; \eta_t), u_i \rangle|^2] \leq \left(\frac{2L_{t,i}C}{B_t} \right)^2 \bar{K}_t^2 = h_{t,i}^{\text{ms}}, \quad i = 1, \dots, m.$$

Step 3. Since $\theta \in \Theta$, $(s_i, s_j) \in Q$, $y_{<t}$, and $\gamma \in \Pi(\mu_{s_i}^\theta, \mu_{s_j}^\theta)$ were arbitrary, the above bound holds for all admissible priors, secret pairs, histories, and couplings, and for γ -almost every (X, X') . By Definition 5.3 of a mean-square history-uniform cap, this exactly means that

$$h_t^{\text{ms}} = (h_{t,i}^{\text{ms}})_{i=1}^m \quad \text{and} \quad h_{t,i}^{\text{ms}} = \left(\frac{2L_{t,i}C}{B_t} \right)^2 \bar{K}_t^2,$$

is a valid ms-HUC at iteration t . \square

K Proof of Lemma 5.1

Fix t , a slice $u_i \in \mathbb{S}^{d-1}$, a prior $\theta \in \Theta$, and a secret pair $(s_i, s_j) \in Q$ with $P_\theta^S(s_i), P_\theta^S(s_j) > 0$. Let $\gamma \in \Pi(\mu_{s_i}^\theta, \mu_{s_j}^\theta)$ be any admissible coupling of the dataset beliefs, and draw

$$((X, X'), R_t) \sim \gamma \times \mathbb{P}_{\eta, \rho}.$$

Define the update difference

$$\tilde{\Delta}_t(X, X'; R_t) := f_t(X, y_{<t}; R_t) - f_t(X', y_{<t}; R_t). \quad (37)$$

By the HUC condition for h_t , we have

$$|\langle \Delta_t(X, X'; R_t), u_i \rangle| \leq \sqrt{h_{t,i}} \quad \text{for } \gamma \times \mathbb{P}_{\eta, \rho}\text{-a.e. } ((X, X'), R_t). \quad (38)$$

Step 1. Project onto the slice u_i and write

$$\tilde{Y}_t := \langle Y_t, u_i \rangle = \langle f_t(X, y_{<t}; R_t), u_i \rangle + \langle N_t, u_i \rangle.$$

Because $N_t \sim \mathcal{N}(0, \Sigma_t)$ is independent of $((X, X'), R_t)$, the projected noise is one-dimensional Gaussian

$$\langle N_t, u_i \rangle \sim \mathcal{N}(0, v_{t,i}), \quad v_{t,i} = u_i^\top \Sigma_t u_i > 0,$$

and the two conditionals under s_i and s_j differ only by a mean shift along u_i . Define

$$\begin{aligned} a(X, X'; R_t) &:= \langle \Delta_t(X, X'; R_t), u_i \rangle \\ &= \langle f_t(X, y_{<t}; R_t) - f_t(X', y_{<t}; R_t), u_i \rangle. \end{aligned}$$

Then, conditioned on a realization $((X, X'), R_t)$, we can write

$$\begin{aligned} \tilde{Y}_t \mid (s_i, \theta, X, X', R_t) &\sim \mathcal{N}(\mu + a, v_{t,i}), \\ \tilde{Y}_t \mid (s_j, \theta, X, X', R_t) &\sim \mathcal{N}(\mu, v_{t,i}), \end{aligned}$$

for some baseline mean μ that cancels in the divergence.

For two 1-D Gaussians with the same variance $v_{t,i}$ and mean difference a , the Rényi divergence of order $\alpha > 1$ is

$$D_\alpha(\mathcal{N}(\mu + a, v_{t,i}) \parallel \mathcal{N}(\mu, v_{t,i})) = \frac{\alpha a^2}{2v_{t,i}}. \quad (39)$$

By the HUC bound (38), we have $|a(X, X'; R_t)| \leq \sqrt{h_{t,i}}$ for $\gamma \times \mathbb{P}_{\eta, \rho}$ -almost every $((X, X'), R_t)$, so

$$D_\alpha(\mathcal{N}(\mu + a, v_{t,i}) \parallel \mathcal{N}(\mu, v_{t,i})) \leq \frac{\alpha}{2v_{t,i}} h_{t,i}. \quad (40)$$

Step 2. Let $S := (X, X', R_t)$ denote the joint randomness with probability measure $\mathbf{v} := \gamma \times \mathbb{P}_{\eta, \rho}$. For each realization $s \in \text{supp}(\mathbf{v})$, define

$$P_s := \mathcal{N}(\mu + a(s), v_{t,i}), \quad Q_s := \mathcal{N}(\mu, v_{t,i}).$$

Then the 1-D marginals under secrets s_i and s_j can be written as mixtures with the same mixing measure \mathbf{v} :

$$P := \Pr(\langle Y_t, u_i \rangle \mid s_i, \theta) = \int P_s \mathbf{v}(ds),$$

$$Q := \Pr(\langle Y_t, u_i \rangle \mid s_j, \theta) = \int Q_s \mathbf{v}(ds).$$

We now use the following standard inequality for Rényi divergence under mixtures with common weights: for $\alpha > 1$ and any probability measure \mathbf{v} ,

$$D_\alpha\left(\int P_s \mathbf{v}(ds) \parallel \int Q_s \mathbf{v}(ds)\right) \leq \text{ess sup}_s D_\alpha(P_s \parallel Q_s). \quad (41)$$

One way to see (41) is to consider the joint distributions on (S, Z) under two secrets:

$$R(ds, dz) := \mathbf{v}(ds)P_s(dz) \quad \text{and} \quad \tilde{R}(ds, dz) := \mathbf{v}(ds)Q_s(dz).$$

By the data-processing inequality for Rényi divergence (applied to the channel $(S, Z) \mapsto Z$),

$$D_\alpha(P \parallel Q) \leq D_\alpha(R \parallel \tilde{R}).$$

On the other hand, a direct calculation of $D_\alpha(R \parallel \tilde{R})$ in terms of the Radon–Nikodym derivatives dP_s/dQ_s shows that

$$D_\alpha(R \parallel \tilde{R}) \leq \text{ess sup}_s D_\alpha(P_s \parallel Q_s),$$

which yields (41).

Applying (41) to P_s, Q_s and using the pointwise bound (40), we obtain

$$\begin{aligned} D_\alpha\left(\Pr(\langle Y_t, u_i \rangle \mid s_i, \theta) \parallel \Pr(\langle Y_t, u_i \rangle \mid s_j, \theta)\right) &= D_\alpha(P \parallel Q) \\ &\leq \text{ess sup}_s D_\alpha(P_s \parallel Q_s) \\ &\leq \frac{\alpha}{2v_{t,i}} h_{t,i}. \end{aligned}$$

Since $\theta, (s_i, s_j), y_{<t}$, and γ were arbitrary, the bound

$$D_\alpha\left(\Pr(\langle Y_t, u_i \rangle \mid s_i, \theta) \parallel \Pr(\langle Y_t, u_i \rangle \mid s_j, \theta)\right) \leq \frac{\alpha h_{t,i}}{2 v_{t,i}}$$

holds uniformly over all admissible choices. \square

L Proof of Theorem 5.6

Fix a slicing profile $\{\mathcal{U}, \omega\}$ with $\mathcal{U} = \{u_\ell\}_{\ell=1}^m \subset \mathbb{S}^{d-1}$ and $\omega \in \Delta(\mathcal{U})$. Let $h = \{h_t\}_{t=1}^T$ be a sequence of valid HUC vectors, with $h_t = (h_{t,1}, \dots, h_{t,m})$ for $t = 1, \dots, T$. That is, for every prior $\theta \in \Theta$, every secret pair $(s_i, s_j) \in Q$ with $P_\theta^S(s_i), P_\theta^S(s_j) > 0$, every history $y_{<t}$ in the support, and every coupling $\gamma \in \Pi(\mu_{s_i}^\theta, \mu_{s_j}^\theta)$, we have $\gamma \times \mathbb{P}_{\eta, \rho}$ -almost surely

$$|\langle f_t(X, y_{<t}; R_t) - f_t(X', y_{<t}; R_t), u_\ell \rangle| \leq h_{t,\ell}, \quad (42)$$

for all $\ell = 1, \dots, m$.

Let the SRPP-SGD mechanism use additive Gaussian noise

$$N_t \sim \mathcal{N}(0, \sigma^2 I_d), \quad t = 1, \dots, T,$$

independent across t and independent of (X, X', R_t) , and write the noisy update at step t as

$$Y_t = f_t(X, y_{<t}; R_t) + N_t.$$

Step 1. Fix $\alpha > 1$, a prior $\theta \in \Theta$, and a secret pair $(s_i, s_j) \in Q$ with positive prior mass. Fix an arbitrary history $y_{<t}$ in the support. For this fixed $y_{<t}$, the HUC condition (42) holds with the same vector h_t . Therefore, Lemma 5.1 applies to the conditional channel

$$(X, X') \mapsto \langle Y_t, u_\ell \rangle \quad \text{given } y_{<t},$$

with covariance $\Sigma_t = \sigma^2 I_d$ and HUC vector h_t .

For each slice $u_\ell \in \mathcal{U}$, Lemma 5.1 together with $v_{t,\ell} := u_\ell^\top \Sigma_t u_\ell = \sigma^2$ gives

$$\begin{aligned} D_\alpha \left(\Pr(\langle Y_t, u_\ell \rangle \mid s_i, \theta, y_{<t}) \parallel \Pr(\langle Y_t, u_\ell \rangle \mid s_j, \theta, y_{<t}) \right) \\ \leq \frac{\alpha}{2} \frac{h_{t,\ell}}{v_{t,\ell}} = \frac{\alpha}{2\sigma^2} h_{t,\ell}. \end{aligned} \quad (43)$$

Define

$$\varepsilon_{t,\ell} := \frac{\alpha}{2\sigma^2} h_{t,\ell}.$$

By (42), the bound (43) holds uniformly over all histories $y_{<t}$, all priors θ , all $(s_i, s_j) \in Q$, and all admissible couplings.

Step 2. Fix a slice index $\ell \in [m]$ and consider the 1-D projected mechanism

$$\mathcal{M}^{(\ell)} : X \mapsto Z_{1:T}^{(\ell)} := (\langle Y_1, u_\ell \rangle, \dots, \langle Y_T, u_\ell \rangle).$$

For each t , denote by $P_{t,y_{<t}}^{(\ell)}$ and $Q_{t,y_{<t}}^{(\ell)}$ the conditional probability measure of $\langle Y_t, u_\ell \rangle$ given $Z_{<t}^{(\ell)} = y_{<t}$ under secrets s_i and s_j , respectively. From the per-step bound (43), we have, for every history $y_{<t}$ in the support,

$$D_\alpha \left(\Pr(\langle Y_t, u_\ell \rangle \mid s_i, \theta, y_{<t}) \parallel \Pr(\langle Y_t, u_\ell \rangle \mid s_j, \theta, y_{<t}) \right) \leq \frac{\alpha}{2\sigma^2} h_{t,\ell}.$$

Equivalently,

$$D_\alpha(P_{t,y_{<t}}^{(\ell)} \parallel Q_{t,y_{<t}}^{(\ell)}) \leq \varepsilon_{t,\ell}, \quad \varepsilon_{t,\ell} := \frac{\alpha}{2\sigma^2} h_{t,\ell}. \quad (44)$$

Let

$$P^{(\ell)} := \Pr(Z_{1:T}^{(\ell)} \mid s_i, \theta), \quad Q^{(\ell)} := \Pr(Z_{1:T}^{(\ell)} \mid s_j, \theta)$$

denote the trajectory probability measures of the projected mechanism along slice u_ℓ .

The family $\{P_{t,y_{<t}}^{(\ell)}, Q_{t,y_{<t}}^{(\ell)}\}_{t,y_{<t}}$ satisfies the assumptions of Lemma L.1 (stated later) with per-step bounds $\varepsilon_t = \varepsilon_{t,\ell}$. Applying Lemma L.1 yields

$$\begin{aligned} D_\alpha \left(\Pr(Z_{1:T}^{(\ell)} \mid s_i, \theta) \parallel \Pr(Z_{1:T}^{(\ell)} \mid s_j, \theta) \right) &= D_\alpha(P^{(\ell)} \parallel Q^{(\ell)}) \\ &\leq \sum_{t=1}^T \varepsilon_{t,\ell} = \frac{\alpha}{2\sigma^2} \sum_{t=1}^T h_{t,\ell}. \end{aligned} \quad (45)$$

Note that (45) is derived for the full projected trajectory $Z_{1:T}^{(\ell)}$. If Algorithm 2 outputs only the final iterate (or any measurable function of the trajectory), the corresponding Rényi divergence can only decrease by data processing, so the same bound (45) applies to the actual output distributions.

Step 3. By the definition of ω -Average Sliced Rényi Divergence (Definition 4.1), applied to the output probability

measure of the mechanism (identified with the full projected trajectories), we have

$$\begin{aligned} \text{ASD}_\alpha^\omega \left(\Pr(M(X) \mid s_i, \theta) \parallel \Pr(M(X) \mid s_j, \theta) \right) \\ = \sum_{\ell=1}^m \omega_\ell D_\alpha \left(\Pr(Z_{1:T}^{(\ell)} \mid s_i, \theta) \parallel \Pr(Z_{1:T}^{(\ell)} \mid s_j, \theta) \right). \end{aligned}$$

Using the per-slice bound (45), we get

$$\begin{aligned} \text{ASD}_\alpha^\omega \left(\Pr(M(X) \mid s_i, \theta) \parallel \Pr(M(X) \mid s_j, \theta) \right) &\leq \sum_{\ell=1}^m \omega_\ell \frac{\alpha}{2\sigma^2} \sum_{t=1}^T h_{t,\ell} \\ &= \frac{\alpha}{2\sigma^2} \sum_{t=1}^T \sum_{\ell=1}^m \omega_\ell h_{t,\ell}. \end{aligned}$$

Therefore, if

$$\sigma^2 \geq \frac{\alpha}{2\varepsilon} \sum_{t=1}^T \sum_{\ell=1}^m \omega_\ell h_{t,\ell},$$

then for every prior θ and every $(s_i, s_j) \in Q$ with positive prior mass, the ω -Ave-SRD between the corresponding output laws is at most ε , i.e., Algorithm 2 is $(\alpha, \varepsilon, \omega)$ -Ave-SRPP.

Step 4. For Joint-SRPP, we use the joint sliced Rényi divergence (Definition 4.3), which for the two output laws can be written as

$$\begin{aligned} \text{JSD}_\alpha^\omega \left(\Pr(M(X) \mid s_i, \theta) \parallel \Pr(M(X) \mid s_j, \theta) \right) \\ = \frac{1}{\alpha-1} \log \mathbb{E}_{U \sim \omega} \left[\exp((\alpha-1) D_\alpha(P_U \parallel Q_U)) \right], \end{aligned}$$

where, for each $u_\ell \in \mathcal{U}$, P_{u_ℓ} and Q_{u_ℓ} denote the laws of $Z_{1:T}^{(\ell)}$ under s_i and s_j , respectively, and P_U, Q_U are the corresponding random choices when $U \sim \omega$.

From (45), for each fixed slice u_ℓ we have

$$D_\alpha(P_{u_\ell} \parallel Q_{u_\ell}) \leq \frac{\alpha}{2\sigma^2} \sum_{t=1}^T h_{t,\ell}.$$

Thus, for the random $U \sim \omega$, it holds almost surely that

$$D_\alpha(P_U \parallel Q_U) \leq \frac{\alpha}{2\sigma^2} \sum_{t=1}^T h_{t,U} \leq \frac{\alpha}{2\sigma^2} \sum_{t=1}^T \max_{\ell} h_{t,\ell}.$$

Plugging this into the definition of Joint-SRD yields

$$\begin{aligned} \text{JSD}_\alpha^\omega \left(\Pr(M(X) \mid s_i, \theta) \parallel \Pr(M(X) \mid s_j, \theta) \right) \\ = \frac{1}{\alpha-1} \log \mathbb{E}_{U \sim \omega} \left[\exp((\alpha-1) D_\alpha(P_U \parallel Q_U)) \right] \\ \leq \frac{1}{\alpha-1} \log \exp \left((\alpha-1) \frac{\alpha}{2\sigma^2} \sum_{t=1}^T \max_{\ell} h_{t,\ell} \right) \\ = \frac{\alpha}{2\sigma^2} \sum_{t=1}^T \max_{\ell} h_{t,\ell}. \end{aligned}$$

Therefore, if

$$\sigma^2 \geq \frac{\alpha}{2\varepsilon} \sum_{t=1}^T \max_{\ell} h_{t,\ell},$$

then for every prior θ and every $(s_i, s_j) \in Q$ the Joint-SRD between the corresponding output laws is at most ε , i.e., Algorithm 2 is $(\alpha, \varepsilon, \omega)$ -Joint-SRPP. \square

Lemma L.1 (Adaptive composition of Rényi divergence). *Let $\alpha > 1$ and let P and Q be probability measures on the product space $\mathcal{Y}_1 \times \dots \times \mathcal{Y}_T$ with coordinate random variables Y_1, \dots, Y_T . For each $t = 1, \dots, T$, let $P_{t|y_{<t}}$ and $Q_{t|y_{<t}}$ denote regular conditional distributions of Y_t given $Y_{<t} = y_{<t}$ under P and Q , respectively, where $y_{<t} = (y_1, \dots, y_{t-1})$. Suppose there exist constants $\varepsilon_t \geq 0$ such that*

$$D_\alpha(P_{t|y_{<t}} \parallel Q_{t|y_{<t}}) \leq \varepsilon_t,$$

for all $t = 1, \dots, T$ and all histories $y_{<t}$ in the support. Then the joint Rényi divergence satisfies

$$D_\alpha(P \parallel Q) \leq \sum_{t=1}^T \varepsilon_t.$$

Proof of Lemma L.1. Let $L := \frac{dP}{dQ}$ be the Radon–Nikodym derivative of P w.r.t. Q , assumed to exist (otherwise $D_\alpha(P \parallel Q) = +\infty$ and the inequality is straightforward). For each t , define the conditional likelihood ratio

$$L_t(y_{\leq t}) := \frac{dP_{t|y_{<t}}}{dQ_{t|y_{<t}}}(y_t), \quad y_{\leq t} = (y_1, \dots, y_t).$$

By the chain rule for densities,

$$L(Y_{1:T}) = \prod_{t=1}^T L_t(Y_{\leq t})$$

Q -almost surely.

By definition of Rényi divergence,

$$D_\alpha(P \parallel Q) = \frac{1}{\alpha-1} \log \mathbb{E}_Q [L(Y_{1:T})^\alpha] = \frac{1}{\alpha-1} \log \mathbb{E}_Q \left[\prod_{t=1}^T L_t(Y_{\leq t})^\alpha \right].$$

For each t , define

$$M_t := \sup_{y_{<t}} \mathbb{E}_Q [L_t(Y_{\leq t})^\alpha \mid Y_{<t} = y_{<t}].$$

Under our assumption,

$$\frac{1}{\alpha-1} \log \mathbb{E}_Q [L_t(Y_{\leq t})^\alpha \mid Y_{<t} = y_{<t}] = D_\alpha(P_{t|y_{<t}} \parallel Q_{t|y_{<t}}) \leq \varepsilon_t.$$

Thus,

$$\mathbb{E}_Q [L_t(Y_{\leq t})^\alpha \mid Y_{<t} = y_{<t}] \leq e^{(\alpha-1)\varepsilon_t},$$

for all $y_{<t}$, and hence

$$M_t \leq e^{(\alpha-1)\varepsilon_t}.$$

We now bound $\mathbb{E}_Q [\prod_{t=1}^T L_t^\alpha]$ iteratively using the tower property:

$$\begin{aligned} \mathbb{E}_Q \left[\prod_{t=1}^T L_t^\alpha \right] &= \mathbb{E}_Q \left[\mathbb{E}_Q [L_T^\alpha \mid Y_{<T}] \prod_{t=1}^{T-1} L_t^\alpha \right] \\ &\leq M_T \mathbb{E}_Q \left[\prod_{t=1}^{T-1} L_t^\alpha \right]. \end{aligned}$$

Repeating this backward for $t = T-1, \dots, 1$ yields

$$\mathbb{E}_Q \left[\prod_{t=1}^T L_t^\alpha \right] \leq \prod_{t=1}^T M_t \leq \prod_{t=1}^T e^{(\alpha-1)\varepsilon_t} = e^{(\alpha-1)\sum_{t=1}^T \varepsilon_t}.$$

Taking $\frac{1}{\alpha-1} \log(\cdot)$ on both sides gives

$$D_\alpha(P \parallel Q) = \frac{1}{\alpha-1} \log \mathbb{E}_Q \left[\prod_{t=1}^T L_t^\alpha \right] \leq \sum_{t=1}^T \varepsilon_t,$$

as claimed. \square

M Proof of Theorem 5.7

Fix a slice profile $\{\mathcal{U}, \omega\}$ with $\mathcal{U} = \{u_\ell\}_{\ell=1}^m \subset \mathbb{S}^{d-1}$ and $\omega \in \Delta(\mathcal{U})$. Let $\alpha > 1$ and fix an arbitrary prior $\theta \in \Theta$ and secret pair $(s_i, s_j) \in Q$.

Let \mathbb{R} denote all subsampling randomness used in SRPP-SGD (minibatch sampling decisions across all iterations), and write $M_{\mathbb{R}}^\theta(s)$ for the distribution of the final output of Algorithm 2 conditional on \mathbb{R} and secret s .

For each iteration t and slice $u_\ell \in \mathcal{U}$, define the (random) directional shift

$$\tilde{\Delta}_{t,\ell}(X, X'; \mathbb{R}) := \langle f_t(X, y_{<t}; R_t(\mathbb{R})) - f_t(X', y_{<t}; R_t(\mathbb{R})), u_\ell \rangle,$$

where $((X, X'), R_t(\mathbb{R}))$ is drawn from the coupling $\gamma \times \mathbb{P}_{\eta, \rho}$ under the fixed subsampling pattern \mathbb{R} .

For each realization $\mathbb{R} = \xi$, let

$$h_{t,\ell}(\xi) = \operatorname{ess\,sup}_{((X, X'), R_t)} |\Delta_{t,\ell}(X, X'; \xi)|^2.$$

Then, for every fixed ξ , the vector $h_t(\xi) = (h_{t,1}(\xi), \dots, h_{t,m}(\xi))$ is a valid HUC vector at iteration t in the sense of Definition 5.1: it uniformly bounds the squared directional shifts along each slice u_ℓ over all priors, secrets, couplings, and histories, with the subsampling pattern held fixed.

Step 1. Fix an arbitrary realization $\mathbb{R} = \xi$. By Lemma 5.1, with isotropic Gaussian noise $N_t \sim \mathcal{N}(0, \sigma^2 I_d)$, so that the projected variance is $v_{t,\ell} = u_\ell^\top \Sigma_t u_\ell = \sigma^2$ for all t, ℓ , the per-iteration, per-slice Rényi cost satisfies

$$\begin{aligned} D_\alpha \left(\Pr(\langle Y_t, u_\ell \rangle \mid s_i, \theta, \mathbb{R} = \xi) \parallel \Pr(\langle Y_t, u_\ell \rangle \mid s_j, \theta, \mathbb{R} = \xi) \right) \\ \leq \frac{\alpha}{2} \frac{h_{t,\ell}(\xi)}{\sigma^2}. \end{aligned}$$

Applying the SRPP accountant of Theorem 5.6 to the *conditional* mechanism \mathcal{M}_ξ^θ (Algorithm 2 with subsampling fixed to ξ), we obtain

$$\text{AveSD}_\alpha^\omega(\mathcal{M}_\xi^\theta(s_i) \parallel \mathcal{M}_\xi^\theta(s_j)) \leq \frac{\alpha}{2\sigma^2} \sum_{t=1}^T \sum_{\ell=1}^m \omega_\ell h_{t,\ell}(\xi), \quad (46)$$

and

$$\text{JSD}_\alpha^\omega(\mathcal{M}_\xi^\theta(s_i) \parallel \mathcal{M}_\xi^\theta(s_j)) \leq \frac{\alpha}{2\sigma^2} \sum_{t=1}^T \max_{\ell \in [m]} h_{t,\ell}(\xi). \quad (47)$$

These inequalities hold for every fixed subsampling pattern ξ , every prior θ , and every secret pair $(s_i, s_j) \in Q$.

Step 2. By Definition 5.3, the given sequence $h_t^{\text{ms}} = \{h_{t,\ell}^{\text{ms}}\}_{\ell=1}^m$ with $h_t^{\text{ms}} = (h_{t,1}^{\text{ms}}, \dots, h_{t,m}^{\text{ms}})$ is a valid ms-HUC vector if, for every $\theta \in \Theta$, $(s_i, s_j) \in Q$, history $y_{<t}$ in the support, and coupling $\gamma \in \Pi(\mu_{s_i}^\theta, \mu_{s_j}^\theta)$, we have, for $\ell = 1, \dots, m$,

$$\mathbb{E}_{\mathbb{R}} \mathbb{E}_{((X, X'), R_t) \sim \gamma \times \mathbb{P}_{\eta, \theta}} [|\Delta_{t,\ell}(X, X'; \mathbb{R})|^2] \leq h_{t,\ell}^{\text{ms}}.$$

In the SRPP-SGD construction of Proposition 5.2, we have

$$h_{t,\ell}(\mathbb{R}) = \left(\frac{2L_{t,\ell}C}{B_t}\right)^2 K_t(\mathbb{R})^2,$$

for a random discrepancy $K_t(\mathbb{R})$, and

$$h_{t,\ell}^{\text{ms}} = \left(\frac{2L_{t,\ell}C}{B_t}\right)^2 \bar{K}_t^2,$$

where \bar{K}_t^2 is any scalar satisfying $\bar{K}_t^2 \geq \mathbb{E}[K_t(\mathbb{R})^2]$.

Therefore

$$\mathbb{E}_{\mathbb{R}}[h_{t,\ell}(\mathbb{R})] = \left(\frac{2L_{t,\ell}C}{B_t}\right)^2 \mathbb{E}_{\mathbb{R}}[K_t(\mathbb{R})^2] \leq \left(\frac{2L_{t,\ell}C}{B_t}\right)^2 \bar{K}_t^2 = h_{t,\ell}^{\text{ms}},$$

and similarly

$$\mathbb{E}_{\mathbb{R}}[\max_{\ell} h_{t,\ell}(\mathbb{R})] \leq \max_{\ell} h_{t,\ell}^{\text{ms}}.$$

Step 3. Taking expectations over subsampling randomness \mathbb{R} in (46) and applying linearity of expectation yields

$$\mathbb{E}_{\mathbb{R}}[\text{AveSD}_\alpha^\omega(\mathcal{M}_{\mathbb{R}}^\theta(s_i) \parallel \mathcal{M}_{\mathbb{R}}^\theta(s_j))] \leq \frac{\alpha}{2\sigma^2} \sum_{t=1}^T \sum_{\ell=1}^m \omega_\ell \mathbb{E}_{\mathbb{R}}[h_{t,\ell}(\mathbb{R})].$$

Using $\mathbb{E}_{\mathbb{R}}[h_{t,\ell}(\mathbb{R})] \leq h_{t,\ell}^{\text{ms}}$, we obtain

$$\mathbb{E}_{\mathbb{R}}[\text{AveSD}_\alpha^\omega(\mathcal{M}_{\mathbb{R}}^\theta(s_i) \parallel \mathcal{M}_{\mathbb{R}}^\theta(s_j))] \leq \frac{\alpha}{2\sigma^2} \sum_{t=1}^T \sum_{\ell=1}^m \omega_\ell h_{t,\ell}^{\text{ms}}.$$

Therefore, if

$$\sigma^2 \geq \frac{\alpha}{2\varepsilon} \sum_{t=1}^T \sum_{\ell=1}^m \omega_\ell h_{t,\ell}^{\text{ms}},$$

then

$$\mathbb{E}_{\mathbb{R}}[\text{AveSD}_\alpha^\omega(\mathcal{M}_{\mathbb{R}}^\theta(s_i) \parallel \mathcal{M}_{\mathbb{R}}^\theta(s_j))] \leq \varepsilon$$

for all $\theta \in \Theta$ and $(s_i, s_j) \in Q$.

By Definition 5.4, this is exactly the $(\alpha, \varepsilon, \omega)$ -ms-Ave-SRPP guarantee in part (i).

Step 4. Similarly, taking expectations in (47) gives

$$\mathbb{E}_{\mathbb{R}}[\text{JSD}_\alpha^\omega(\mathcal{M}_{\mathbb{R}}^\theta(s_i) \parallel \mathcal{M}_{\mathbb{R}}^\theta(s_j))] \leq \frac{\alpha}{2\sigma^2} \sum_{t=1}^T \mathbb{E}_{\mathbb{R}}[\max_{\ell} h_{t,\ell}(\mathbb{R})].$$

In the SRPP-SGD setting of Proposition 5.2, each $h_{t,\ell}(\mathbb{R})$ is of the form $h_{t,\ell}(\mathbb{R}) = a_{t,\ell} K_t(\mathbb{R})^2$ with fixed coefficients $a_{t,\ell} = \left(\frac{2L_{t,\ell}C}{B_t}\right)^2$ that do not depend on \mathbb{R} .

Thus

$$\max_{\ell} h_{t,\ell}(\mathbb{R}) = \left(\max_{\ell} a_{t,\ell}\right) K_t(\mathbb{R})^2,$$

and

$$\begin{aligned} \mathbb{E}_{\mathbb{R}}[\max_{\ell} h_{t,\ell}(\mathbb{R})] &= \left(\max_{\ell} a_{t,\ell}\right) \mathbb{E}_{\mathbb{R}}[K_t(\mathbb{R})^2] \\ &\leq \max_{\ell} a_{t,\ell} \bar{K}_t^2 = \max_{\ell} h_{t,\ell}^{\text{ms}}, \end{aligned}$$

where we used $\bar{K}_t^2 \geq \mathbb{E}[K_t(\mathbb{R})^2]$ and the closed form $h_{t,\ell}^{\text{ms}} = a_{t,\ell} \bar{K}_t^2$ from Proposition 5.2.

Hence

$$\mathbb{E}_{\mathbb{R}}[\text{JSD}_\alpha^\omega(\mathcal{M}_{\mathbb{R}}^\theta(s_i) \parallel \mathcal{M}_{\mathbb{R}}^\theta(s_j))] \leq \frac{\alpha}{2\sigma^2} \sum_{t=1}^T \max_{\ell} h_{t,\ell}^{\text{ms}}.$$

Therefore, if

$$\sigma^2 \geq \frac{\alpha}{2\varepsilon} \sum_{t=1}^T \max_{\ell} h_{t,\ell}^{\text{ms}},$$

then

$$\mathbb{E}_{\mathbb{R}}[\text{JSD}_\alpha^\omega(\mathcal{M}_{\mathbb{R}}^\theta(s_i) \parallel \mathcal{M}_{\mathbb{R}}^\theta(s_j))] \leq \varepsilon$$

for all $\theta \in \Theta$ and $(s_i, s_j) \in Q$, which is exactly the $(\alpha, \varepsilon, \omega)$ -ms-Joint-SRPP guarantee in part (ii) by Definition 5.5. \square

N Proof of Theorem 5.8

Fix a slice profile $\{\mathcal{U}, \omega\}$ and a Pufferfish scenario (S, Q, Θ) . Let $\vec{\mathcal{M}}$ be the composed mechanism in (22):

$$\vec{\mathcal{M}}(X) := (\mathcal{M}_1(X), \dots, \mathcal{M}_J(X)),$$

where X is the underlying common dataset. For every realized dataset x , we assume that the primitive randomness of $\mathcal{M}_1, \dots, \mathcal{M}_J$ is independent across j when the mechanisms are run on x .

Fix $\theta \in \Theta$ and $(s_i, s_j) \in Q$ with $P_\theta^S(s_i), P_\theta^S(s_j) > 0$. Let $\mu_{s_i}^\theta$ and $\mu_{s_j}^\theta$ be the corresponding dataset beliefs. For any fixed

dataset realization x in the support of these beliefs, define the conditional output distribution

$$\begin{aligned} P_j^x &:= \Pr(\mathcal{M}_j(x) \in \cdot \mid s_i, \theta), \\ Q_j^x &:= \Pr(\mathcal{M}_j(x) \in \cdot \mid s_j, \theta), \end{aligned}$$

and

$$\begin{aligned} P^{\text{comp},x} &:= \Pr(\vec{\mathcal{M}}(x) \in \cdot \mid s_i, \theta), \\ Q^{\text{comp},x} &:= \Pr(\vec{\mathcal{M}}(x) \in \cdot \mid s_j, \theta). \end{aligned}$$

By independence of the primitive randomness across j for this fixed x , we have

$$P^{\text{comp},x} = \bigotimes_{j=1}^J P_j^x, \quad \text{and} \quad Q^{\text{comp},x} = \bigotimes_{j=1}^J Q_j^x.$$

For any Rényi order $\alpha > 1$ and product measures $\bigotimes_{j=1}^J P_j$ and $\bigotimes_{j=1}^J Q_j$, the Rényi divergence becomes

$$D_\alpha\left(\bigotimes_{j=1}^J P_j \parallel \bigotimes_{j=1}^J Q_j\right) = \sum_{j=1}^J D_\alpha(P_j \parallel Q_j). \quad (48)$$

Applying this with $P_j = P_j^x$ and $Q_j = Q_j^x$ yields, for every fixed dataset realization x ,

$$D_\alpha(P^{\text{comp},x} \parallel Q^{\text{comp},x}) = \sum_{j=1}^J D_\alpha(P_j^x \parallel Q_j^x).$$

We now prove the composition bound for each SRPP flavor Ξ .

Case 1: $\Xi \in \{\text{Ave}, \text{ms-Ave}\}$. Fix a slice set $\mathcal{U} = \{u_\ell\}_{\ell=1}^m \subset \mathbb{S}^{d-1}$. For each mechanism \mathcal{M}_j , slice u_ℓ , and dataset realization x , define the 1-D projected probability measure

$$\begin{aligned} P_{j,\ell}^x &:= \Pr(\langle \mathcal{M}_j(x), u_\ell \rangle \in \cdot \mid s_i, \theta), \\ Q_{j,\ell}^x &:= \Pr(\langle \mathcal{M}_j(x), u_\ell \rangle \in \cdot \mid s_j, \theta). \end{aligned}$$

Likewise, for the composed mechanism and fixed x ,

$$\begin{aligned} P_\ell^{\text{comp},x} &:= \Pr(\langle \vec{\mathcal{M}}(x), u_\ell \rangle \in \cdot \mid s_i, \theta), \\ Q_\ell^{\text{comp},x} &:= \Pr(\langle \vec{\mathcal{M}}(x), u_\ell \rangle \in \cdot \mid s_j, \theta). \end{aligned}$$

From the independence of the primitive randomness across j (for this fixed x), we have

$$P_\ell^{\text{comp},x} = \bigotimes_{j=1}^J P_{j,\ell}^x \quad \text{and} \quad Q_\ell^{\text{comp},x} = \bigotimes_{j=1}^J Q_{j,\ell}^x.$$

Applying (48) to these 1-D projections gives, for every x and ℓ ,

$$D_\alpha(P_\ell^{\text{comp},x} \parallel Q_\ell^{\text{comp},x}) = \sum_{j=1}^J D_\alpha(P_{j,\ell}^x \parallel Q_{j,\ell}^x). \quad (49)$$

By the definition of $(\alpha, \epsilon_j, \omega)$ -Ave-SRPP, if \mathcal{M}_j is $(\alpha, \epsilon_j, \omega)$ -Ave-SRPP then, for every prior θ , secret pair (s_i, s_j) , and data belief (coupling), the ω -weighted average of the sliced Rényi costs of \mathcal{M}_j is at most ϵ_j . In particular, this bound holds uniformly for every dataset realization x in the support of $\mu_{s_i}^\theta$ and $\mu_{s_j}^\theta$, so we have

$$\sum_{\ell=1}^m \omega_\ell D_\alpha(P_{j,\ell}^x \parallel Q_{j,\ell}^x) \leq \epsilon_j,$$

for all $x, (s_i, s_j), \theta$.

For the composed mechanism and fixed d , the average sliced Rényi divergence is

$$\begin{aligned} \text{AveSD}_\omega^\alpha(P^{\text{comp},x} \parallel Q^{\text{comp},x}) &= \sum_{\ell=1}^m \omega_\ell D_\alpha(P_\ell^{\text{comp},x} \parallel Q_\ell^{\text{comp},x}) \\ &\stackrel{(49)}{=} \sum_{\ell=1}^m \omega_\ell \sum_{j=1}^J D_\alpha(P_{j,\ell}^x \parallel Q_{j,\ell}^x) = \sum_{j=1}^J \sum_{\ell=1}^m \omega_\ell D_\alpha(P_{j,\ell}^x \parallel Q_{j,\ell}^x) \\ &\leq \sum_{j=1}^J \epsilon_j. \end{aligned}$$

Since this bound holds for every dataset realization x and for all $\theta \in \Theta$ and $(s_i, s_j) \in Q$, taking the supremum over all admissible beliefs and couplings shows that the composed mechanism $\vec{\mathcal{M}}$ is $(\alpha, \sum_{j=1}^J \epsilon_j, \omega)$ -Ave-SRPP.

For ms-Ave-SRPP, the same argument applies verbatim after folding the subsampling randomness into the mechanism's output: ms-Ave-SRPP is just Ave-SRPP applied to the channel that includes both SGD updates and subsampling randomness. Thus $\vec{\mathcal{M}}$ is also $(\alpha, \sum_{j=1}^J \epsilon_j, \omega)$ -ms-Ave-SRPP whenever each \mathcal{M}_j is $(\alpha, \epsilon_j, \omega)$ -ms-Ave-SRPP.

Case 2: $\Xi \in \{\text{Joint}, \text{ms-Joint}\}$. By Definition 4.3 and the discussion in Appendix B, Joint-SRPP can be interpreted as standard Rényi Pufferfish Privacy applied to the *sliced channel*

$$\text{Slice} \circ \mathcal{M} : X \mapsto (U, Z) \quad \text{with} \quad U \sim \omega, Z = \langle \mathcal{M}(X), U \rangle.$$

More precisely, for any mechanism \mathcal{M} we have

$$\begin{aligned} \text{JSD}_\alpha^\omega(\Pr(\mathcal{M}(X) \mid s_i, \theta) \parallel \Pr(\mathcal{M}(X) \mid s_j, \theta)) \\ = D_\alpha\left(\Pr(\text{Slice} \circ \mathcal{M}(X) \mid s_i, \theta) \parallel \Pr(\text{Slice} \circ \mathcal{M}(X) \mid s_j, \theta)\right). \end{aligned}$$

Thus, if \mathcal{M}_j is $(\alpha, \epsilon_j, \omega)$ -Joint-SRPP, then the sliced channel $\text{Slice} \circ \mathcal{M}_j$ is (α, ϵ_j) -RPP in the underlying Pufferfish scenario.

Consider the sliced channels

$$\mathcal{N}_j := \text{Slice} \circ \mathcal{M}_j, \quad j = 1, \dots, J,$$

and their composition

$$\begin{aligned} \vec{\mathcal{N}}(X) &:= (\mathcal{N}_1(X), \dots, \mathcal{N}_J(X)) \\ &= (\text{Slice} \circ \mathcal{M}_1(X), \dots, \text{Slice} \circ \mathcal{M}_J(X)). \end{aligned}$$

By independence of the primitive randomness across j , the same process of (48) implies that standard 1-D RPP enjoys additive composition: if each \mathcal{N}_j is (α, ϵ_j) -RPP, then $\vec{\mathcal{N}}$ is $(\alpha, \sum_{j=1}^J \epsilon_j)$ -RPP. Equivalently, for every θ and (s_i, s_j) ,

$$D_\alpha\left(\Pr(\vec{\mathcal{N}}(X) \mid s_i, \theta) \parallel \Pr(\vec{\mathcal{N}}(X) \mid s_j, \theta)\right) \leq \sum_{j=1}^J \epsilon_j.$$

Finally, observe that applying the sliced channel `Slice` to the composed mechanism $\vec{\mathcal{M}}$ produces exactly $\vec{\mathcal{N}}$ as a post-processing:

$$\vec{\mathcal{N}} = \text{Slice} \circ \vec{\mathcal{M}}.$$

Since Rényi divergence (and therefore 1-D RPP) is non-increasing under post-processing, the above bound on $\vec{\mathcal{N}}$ implies the same bound for the Joint-SRD of $\vec{\mathcal{M}}$, i.e.

$$\text{JSD}_\alpha^\omega(\Pr(\vec{\mathcal{M}}(x) \mid s_i, \theta) \parallel \Pr(\vec{\mathcal{M}}(x) \mid s_j, \theta)) \leq \sum_{j=1}^J \epsilon_j.$$

Thus, by taking the supremum over all θ and (s_i, s_j) , we can show that $\vec{\mathcal{M}}$ is $(\alpha, \sum_{j=1}^J \epsilon_j, \omega)$ -Joint-SRPP. As in the average case, ms-Joint-SRPP is defined by applying Joint-SRPP to the channel that includes subsampling randomness in its output. Hence the same composition argument applies directly, giving $(\alpha, \sum_{j=1}^J \epsilon_j, \omega)$ -ms-Joint-SRPP whenever each \mathcal{M}_j is $(\alpha, \epsilon_j, \omega)$ -ms-Joint-SRPP.

Combining Case 1 and Case 2, we conclude that for any $\Xi \in \{\text{Ave}, \text{Joint}, \text{ms-Ave}, \text{ms-Joint}\}$, if each \mathcal{M}_j is $(\alpha, \epsilon_j, \omega)$ - Ξ -SRPP, then the composed mechanism $\vec{\mathcal{M}}$ is $(\alpha, \sum_{j=1}^J \epsilon_j, \omega)$ - Ξ -SRPP. \square

O Experiment Details

In this appendix, we provide additional details for the experiments in Section 6 and present further empirical results.

O.1 Experimental Setup: Gaussian Sliced Wasserstein Mechanisms for Static Privatization

This section provides additional details on our experimental methodology beyond what is presented in Section 6 of the main text.

Dataset configurations and prior distributions. As described in the main text, we evaluate our sliced SRPP mechanisms on three standard tabular benchmarks: Adult Census (30,162 records), Cleveland Heart Disease (303 records), and Student Performance (395 records). Each dataset is studied under two prior configurations to examine the impact of class imbalance on both privacy protection and utility.

For *Adult*, the imbalanced configuration uses the natural race distribution from the full dataset, where the majority class (White) accounts for approximately 86% of records, yielding a prior-only baseline accuracy of $\text{Acc}_{\text{maj}}^{0.86} = 0.86$ for attribute inference attacks. The balanced configuration constructs synthetic groups via deterministic hash-based assignment, partitioning records into five approximately equal groups with uniform prior $\pi(s) \approx 0.20$ for each synthetic secret value $s \in \{G_1, \dots, G_5\}$, giving $\text{Acc}_{\text{maj}}^{0.20} = 0.20$.

For *Cleveland*, the imbalanced configuration uses the full dataset with its natural sex distribution (majority class probability ≈ 0.70), while the balanced configuration performs stratified subsampling to obtain equal numbers of male and female records, yielding a uniform prior with $\text{Acc}_{\text{maj}}^{0.50} = 0.50$.

For *Student Performance*, we similarly consider both the full dataset with its empirical sex distribution ($\text{Acc}_{\text{maj}}^{0.60} \approx 0.60$) and a balanced subsample with equal representation of each sex ($\text{Acc}_{\text{maj}}^{0.50} = 0.50$).

Detailed descriptions of each dataset configuration, including feature construction and sampling procedures, are provided in the following subsections.

Query construction. We consider two families of queries, both of which aggregate information at the group level rather than releasing individual records.

Summary statistics queries. For each secret value $s \in \mathcal{S}$, we compute a d -dimensional aggregate statistic over all records with $S = s$. For *Adult* ($d = 9$), the query includes: means and standard deviations of age, education level, and hours worked per week, together with the fraction of records with positive capital gain, positive capital loss, and income exceeding \$50K. For *Cleveland* ($d = 9$), we compute means and standard deviations of age, resting blood pressure, and cholesterol level, along with rates of high cholesterol (≥ 240 mg/dL), high blood pressure (≥ 140 mmHg), and presence of heart disease. For *Student* ($d = 9$), we use means and standard deviations of grades G1, G2, and G3, together with rates of high study time (≥ 3 hours/week), any past failures, and high absences (> 10 days).

Machine learning model queries. For the *Adult* dataset, we also treat trained model parameters as query outputs. For each race group $s \in \mathcal{S}$, we train a binary classifier to predict high income ($> \$50K$) using a 9-dimensional feature vector constructed from demographic and employment attributes. The query output X consists of model parameters: for linear SVM and logistic regression, we extract the $d = 10$ coefficients (9 feature weights plus intercept); for random forest and gradient boosting, we extract the $d = 9$ feature importance scores. Each model is trained independently per secret group, so the query reflects group-specific predictive patterns.

Privacy mechanism and calibration. All experiments use isotropic Gaussian noise mechanisms of the form

$$Y = X + Z, \quad Z \sim \mathcal{N}(0, \sigma^2 I_d),$$

where the noise scale σ is calibrated via our sliced SRPP composition bounds.

For slicing, we generate $m = 200$ directions $\{u_\ell\}_{\ell=1}^m$ sampled uniformly from the unit sphere \mathbb{S}^{d-1} with equal weights $\omega_\ell = 1/m$. Along each direction u_ℓ , we compute the one-dimensional Wasserstein- ∞ sensitivity

$$\Delta_\infty^{u_\ell} = \max_{(s_i, s_j) \in Q} W_\infty(P_{u_\ell^\top X|S=s_i}^\theta, P_{u_\ell^\top X|S=s_j}^\theta),$$

where $P_{u_\ell^\top X|S=s}^\theta$ is the empirical distribution of the projected query values for secret s under world θ . These per-slice sensitivities are then aggregated according to the Ave-SRPP and Joint-SRPP definitions to determine the required noise level for target privacy parameters (α, ϵ) .

We fix Rényi order $\alpha = 4$ throughout and sweep the privacy budget ϵ over the range $[0.05, 60]$ to study the privacy-utility tradeoff. Each configuration is evaluated over $N_{\text{trials}} = 3$ independent trials with different random seeds to account for Monte Carlo variability in the slicing directions and noise realization.

Utility and privacy evaluation. For utility, we report mean squared error (MSE), mean absolute error (MAE), average ℓ_2 distance per record, relative Frobenius error, and signal-to-noise ratio (SNR in dB). The primary utility metric is MSE:

$$\text{MSE} = \frac{1}{n} \sum_{i=1}^n \|X_i - Y_i\|_2^2.$$

For empirical privacy auditing, we implement a prior-aware Gaussian maximum a posteriori (MAP) attack. Given a privatized output y_i , the attacker estimates the secret as

$$\hat{s}(y_i) = \arg \max_{s \in \mathcal{S}} \left\{ \log \pi(s) + \log \phi(y_i; \mu_s, \sigma^2 I_d) \right\},$$

where $\pi(s)$ is the prior distribution over secrets (either the empirical distribution from the dataset or the uniform prior for balanced configurations), $\mu_s = \mathbb{E}[X | S = s]$ is the mean query output for secret s computed from the unprivatized data, and $\phi(\cdot; \mu, \Sigma)$ denotes the Gaussian density with mean μ and covariance $\Sigma = \sigma^2 I_d$.

We report two metrics: (i) overall attack accuracy, and (ii) advantage over the prior-only baseline, defined as $\text{Adv} = \text{Acc} - \text{Acc}_{\text{maj}}$. For imbalanced Adult, the baseline is $\text{Acc}_{\text{maj}}^{0.86} = 0.86$; for balanced Adult, Cleveland, and Student (balanced), the baseline is $\text{Acc}_{\text{maj}}^{0.20} = 0.20$, $\text{Acc}_{\text{maj}}^{0.50} = 0.50$, and $\text{Acc}_{\text{maj}}^{0.50} = 0.50$, respectively; for imbalanced Cleveland and Student, the baselines are $\text{Acc}_{\text{maj}}^{0.70} = 0.70$ and $\text{Acc}_{\text{maj}}^{0.60} = 0.60$.

An advantage close to zero indicates that the privacy mechanism successfully prevents the attacker from learning substantially more than what the prior distribution already reveals.

The following subsections provide detailed specifications of each dataset configuration.

O.1.1 Adult Census (race as secret)

We use the *Adult Census Income* dataset (30,162 records after preprocessing) in an attribute-privacy setting where the sensitive attribute is *race*. Let

$$\mathcal{S} \in \mathcal{S}$$

$$= \{\text{White, Black, Asian-Pac-Islander, Amer-Indian-Eskimo, Other}\},$$

with $k = |\mathcal{S}| = 5$, and let $X \in \mathbb{R}^d$ denote the per-record query vector constructed from demographic and socioeconomic features (see below for the specific query families). The Pufferfish scenario specifies the discriminatory set

$$\mathcal{Q} = \{(s_i, s_j) : s_i, s_j \in \mathcal{S}, s_i \neq s_j\},$$

so that every ordered pair of distinct secret values is protected. We consider two configurations of the dataset that differ only in the prior over \mathcal{S} .

Adult-0.86 prior (imbalanced). We use the full processed dataset with its empirical race distribution. Writing

$$\pi_{0.86}(s) = \frac{1}{n} \sum_{i=1}^n \mathbf{1}\{S_i = s\}, \quad s \in \mathcal{S},$$

for the empirical prior over \mathcal{S} , the corresponding *majority-class baseline* for any attribute-inference attack is

$$\text{Acc}_{\text{maj}}^{0.86} = \max_{s \in \mathcal{S}} \pi_{0.86}(s) \approx 0.86.$$

The associated Pufferfish world $\theta_D^{0.86}$ is given by the empirical joint distribution of (X, S) over all records in the full dataset.

Adult-0.20 prior (balanced). To study a uniform prior, we construct a balanced configuration by creating synthetic balanced groups via hash-based assignment. We partition the full dataset into $k = 5$ groups of approximately equal size using a deterministic hash function applied to each record's feature vector, yielding a subsample with an approximately uniform prior

$$\pi_{0.20}(s) = \frac{1}{n'} \sum_{i=1}^{n'} \mathbf{1}\{S_i = s\} \approx 0.20, \quad s \in \mathcal{S}.$$

In this configuration, the majority-class baseline is

$$\text{Acc}_{\text{maj}}^{0.20} = \max_{s \in \mathcal{S}} \pi_{0.20}(s) \approx 0.20.$$

The corresponding Pufferfish world $\theta_D^{0.20}$ is the empirical joint distribution of (X, S) restricted to this balanced subsample.

In both configurations, the Pufferfish family is instantiated by the empirical conditionals $\{P_{X|S=s}^\theta\}_{s \in S}$ under the chosen world $\theta \in \{\theta_D^{0.86}, \theta_D^{0.20}\}$, together with the discriminatory set Q defined above. Our sliced SRPP mechanisms are calibrated to protect all pairs in Q for the specified Rényi order and privacy budget.

O.1.2 Cleveland Heart Disease (sex as secret)

We use the *processed Cleveland Heart Disease* dataset (303 records) in an attribute-privacy setting where the sensitive attribute is *sex*. Let

$$S \in \mathcal{S} = \{\text{female}, \text{male}\}, \quad k = |\mathcal{S}| = 2,$$

and let $X \in \mathbb{R}^d$ denote the per-record query vector constructed from clinical features (see below for the specific query families). The Pufferfish scenario specifies the discriminatory set

$$Q = \{(s_i, s_j) : s_i, s_j \in \mathcal{S}, s_i \neq s_j\} = \{(\text{female}, \text{male}), (\text{male}, \text{female})\},$$

so that every ordered pair of distinct secret values is protected. We consider two configurations of the dataset that differ only in the prior over S .

Cleveland-0.7 prior. We use the full processed dataset with its empirical sex distribution. Writing

$$\pi_{0.7}(s) = \frac{1}{n} \sum_{i=1}^n \mathbf{1}\{S_i = s\}, \quad s \in \mathcal{S},$$

for the empirical prior over S , the corresponding *majority-class baseline* for any attribute-inference attack is

$$\text{Acc}_{\text{maj}}^{0.7} = \max_{s \in \mathcal{S}} \pi_{0.7}(s) \approx 0.7.$$

The associated Pufferfish world $\theta_D^{0.7}$ is given by the empirical joint distribution of (X, S) over all records in the full dataset.

Cleveland-0.5 prior. To study a uniform prior, we construct a balanced configuration by stratified subsampling on sex. Let n_f and n_m denote the numbers of female and male records in the full dataset. We draw $n' = \min(n_f, n_m)$ records uniformly at random without replacement from each sex subset, yielding a subsample of size $2n'$ with an approximately uniform prior

$$\pi_{0.5}(s) = \frac{1}{2n'} \sum_{i=1}^{2n'} \mathbf{1}\{S_i = s\} \approx 0.5, \quad s \in \mathcal{S}.$$

In this configuration, the majority-class baseline is

$$\text{Acc}_{\text{maj}}^{0.5} = \max_{s \in \mathcal{S}} \pi_{0.5}(s) \approx 0.5.$$

The corresponding Pufferfish world $\theta_D^{0.5}$ is the empirical joint distribution of (X, S) restricted to this balanced subsample.

In both configurations, the Pufferfish family is instantiated by the empirical conditionals $\{P_{X|S=s}^\theta\}_{s \in \mathcal{S}}$ under the chosen world $\theta \in \{\theta_D^{0.7}, \theta_D^{0.5}\}$, together with the discriminatory set Q defined above. Our sliced SRPP mechanisms are calibrated to protect all pairs in Q for the specified Rényi order and privacy budget.

O.1.3 Student Performance (grade group as secret)

We use the *Student Performance* dataset [27] (395 records) in an attribute-privacy setting where the sensitive attribute is a discretized *grade group* derived from the final grade $G3 \in \{0, \dots, 20\}$. We partition students into $k = 5$ grade groups using quantile-based binning:

$$S \in \mathcal{S} = \{G1, G2, G3, G4, G5\}, \quad k = |\mathcal{S}| = 5,$$

where each group corresponds to a quintile of the final grade distribution (G1 = lowest quintile, G5 = highest quintile). Let $X \in \mathbb{R}^d$ denote the per-record query vector constructed from grade and study-related features. The Pufferfish scenario specifies the discriminatory set

$$Q = \{(s_i, s_j) : s_i, s_j \in \mathcal{S}, s_i \neq s_j\},$$

so that every ordered pair of distinct grade groups is protected. We consider two configurations of the dataset that differ in the prior over S .

Student (full dataset). We use all 395 records with grade groups assigned via 5-quantile binning. Since quantile-based binning attempts to create approximately equal-sized groups by construction, the empirical prior is

$$\pi(s) = \frac{1}{n} \sum_{i=1}^n \mathbf{1}\{S_i = s\}, \quad s \in \mathcal{S},$$

with majority-class baseline

$$\text{Acc}_{\text{maj}} = \max_{s \in \mathcal{S}} \pi(s).$$

Due to tied final grade values preventing perfect equal division, the empirical distribution may deviate slightly from uniform. The Pufferfish world θ_D^{full} is the empirical joint distribution of (X, S) over the full dataset.

Student (balanced subsample). To ensure an exactly uniform prior, we perform stratified subsampling: let n_s denote the number of records in grade group s in the full dataset, and set $n' = \min_{s \in \mathcal{S}} n_s$. We draw n' records uniformly at random without replacement from each grade group, yielding a subsample of size $5n'$ with exactly uniform prior

$$\pi^{\text{bal}}(s) = \frac{1}{5n'} \sum_{i=1}^{5n'} \mathbf{1}\{S_i = s\} = 0.2, \quad \forall s \in \mathcal{S}.$$

The corresponding majority-class baseline is

$$\text{Acc}_{\text{maj}}^{0.2} = \max_{s \in S} \pi^{\text{bal}}(s) = 0.2.$$

The Pufferfish world θ_D^{bal} is the empirical joint distribution of (X, S) restricted to this balanced subsample.

In both configurations, the Pufferfish family is instantiated by the empirical conditionals $\{P_{X|S=s}^\theta\}_{s \in S}$ under the chosen world $\theta \in \{\theta_D^{\text{full}}, \theta_D^{\text{bal}}\}$, together with the discriminatory set Q defined above. Our sliced SRPP mechanisms are calibrated to protect all pairs in Q for the specified Rényi order and privacy budget.

O.1.4 Additional Results.

Figure 4 presents analogous privacy-utility tradeoff curves for the Cleveland Heart Disease and Student Performance datasets, evaluating the same four query types (logistic regression, random forest, SVM, and summary statistics) under both balanced and imbalanced prior configurations.

The results exhibit qualitatively similar behavior to the Adult dataset experiments shown in Section 6. Across all configurations, Ave-SRPP and Joint-SRPP demonstrate the expected monotonic tradeoff: as the privacy budget ϵ increases, MSE decreases while attack accuracy rises from the prior baseline toward perfect inference. At small ϵ , both mechanisms successfully limit attack accuracy to near the prior baselines (Cleveland: 0.7 and 0.5; Student: 0.6 and 0.2), confirming effective privacy protection. At any fixed ϵ , Joint-SRPP remains more conservative than Ave-SRPP, inducing higher MSE but lower attack accuracy, with the gap most pronounced in the moderate privacy regime. These additional experiments validate that the comparative performance of Ave-SRPP and Joint-SRPP generalizes across datasets of varying size (Cleveland: 303 records, Student: 395 records versus Adult: 30,162 records), different numbers of secret classes ($k = 2$ for Cleveland and Student-sex versus $k = 5$ for Adult and Student-grade).

O.2 SRPP- ms-SRPP-SGD with Gradient Clipping

For our CIFAR-10 experiments (Figures 3i-3l) in Section 6, we use the ResNet22, adapted for compatibility with Opacus [34] by following the architecture of [32],

The network is a 22-layer residual network with three stages of channel sizes (16, 32, 64) and (3, 4, 3) residual blocks per stage. The first layer is a 3×3 convolution (16 channels, stride 1, padding 1) followed by group normalization and ELU. Stages 2–3 downsample via stride 2 in their first blocks; shortcuts use spatial subsampling with channel zero-padding.

Each residual block has the form

$$\begin{aligned} x &\mapsto \text{GN}_1(\text{ELU}(\text{Conv}_1(x))) \\ &\mapsto \text{GN}_2(\text{Conv}_2(\cdot)) + \text{shortcut}(x) \\ &\mapsto \text{GN}_3(\text{ELU}(\cdot)), \end{aligned}$$

where both convolutions are 3×3 with padding 1; Conv_1 uses stride 2 for downsampling blocks and stride 1 otherwise, while Conv_2 always uses stride 1. Group normalization layers $\text{GN}_1, \text{GN}_2, \text{GN}_3$ use at most four groups without affine parameters.

After the final stage, we apply 3×3 adaptive average pooling and flatten to $z \in \mathbb{R}^{576}$. Before classification, we apply per-example standardization $\tilde{z} = (z - \mu(z)) / (\sigma(z) + 10^{-6})$ where $\mu(z)$ and $\sigma(z)$ are the sample mean and standard deviation, then compute logits via $\ell = W\tilde{z} + b$ with $W \in \mathbb{R}^{10 \times 576}$ and $b \in \mathbb{R}^{10}$. Weights use Kaiming-normal initialization. The model contains approximately 270,000 parameters. This architecture is fully compatible with per-example gradient computation in Opacus; in particular, we replace non-picklable lambda-based shortcut layers with explicit `PaddingShortcut` modules.

Standard SGD With this ResNet22 model, we consider a *global Lipschitz constant* as a special case of Assumption 5.2: the update map $T_t(z; y_{<t}) = \xi_{t-1} - \eta_t(\mu v_{t-1} + z)$ for SGD with momentum satisfies

$$|u_i^\top (T_t(z; y_{<t}) - T_t(z'; y_{<t}))| = \eta_t |u_i^\top (z - z')|$$

for all slices $u_i \in \mathcal{U}$ and all histories $y_{<t}$, yielding the *uniform slice-wise Lipschitz constant* $L_{t,i} = \eta_t$ for all $i \in [m]$. This simplifies the HUC from Proposition 5.1 to

$$h_{t,i} = \left(\frac{2K_t \eta_t C}{B_t} \right)^2, \quad \forall i \in [m],$$

which depends only on the learning rate η_t , clipping threshold C , batch size B_t , and discrepancy cap K_t , but is *independent of the slice direction*. As a result, Ave-SRPP and Joint-SRPP require the same noise calibration in this uniform case, though their privacy quantification schemes remain different.

O.3 Experiment Setup

Now, we provide detailed specifications for our SRPP-SGD and ms-SRPP-SGD experiments (Figures 3i-3l) in Section 6 of the main text.

Pufferfish two-world construction. We construct a Pufferfish privacy scenario on CIFAR-10 by creating two aligned worlds that differ minimally in the prevalence of a designated secret class. Specifically, we select `cat` as the secret class and define two target prevalences: $p_{\text{low}} = 0.10000$ and $p_{\text{high}} = 0.10004$.

The world construction proceeds in two steps to ensure minimal edit distance:

1. *Base labels* \rightarrow *world* s_0 : Starting from CIFAR-10’s original training labels (50,000 examples), we minimally relabel examples to achieve exactly $n_0 = \lfloor p_{\text{low}} \cdot N \rfloor$ cat instances. If the original dataset contains fewer than n_0 cats, we randomly select non-cat examples and relabel them as cats; if it contains more, we randomly select cat examples and relabel them to other (non-cat) classes.
2. *World* $s_0 \rightarrow$ *world* s_1 : From s_0 , we perform minimal edits to reach exactly $n_1 = \lfloor p_{\text{high}} \cdot N \rfloor$ cat instances, producing world s_1 . The edit operations are analogous to step 1.

This construction yields two label vectors y_0 and y_1 (both of length $N = 50,000$) that differ on exactly $\Delta = |n_1 - n_0| = 20$ examples, while the image data remains identical across both worlds. The mismatch rate between worlds is $p_{\text{realized}} = \Delta/N = 0.0004$.

For training, we fix a single *realized world*—either s_0 or s_1 —and overwrite the CIFAR-10 training labels with the corresponding realized label vector. All subsequent training (private and non-private) operates exclusively on this realized world, ensuring that the privacy guarantee protects against an adversary who might observe the other world.

Privacy accounting: SRPP-SGD, ms-SRPP-SGD, and group-DP-SGD. We compare three privacy accounting methods.

(1) *SRPP-SGD (deterministic worst-case cap)*: For each iteration t , we bound the number of differing examples in a batch by the deterministic cap $K_{\text{cap}} = \min(L, \Delta) = 20$. Under isotropic Gaussian noise with single-block clipping, the per-step HUC is

$$h_t^* = \left(\frac{2\eta_t C K_{\text{cap}}}{L} \right)^2 = \left(\frac{2\eta_t \cdot 4.0 \cdot 20}{512} \right)^2.$$

The total HUC over all T steps is $H_{\text{total}} = \sum_{t=1}^T h_t^*$, and the noise scale is calibrated via:

$$\sigma^2(\epsilon) = \frac{\alpha}{2\epsilon} \cdot H_{\text{total}},$$

where $\alpha = 16$ is the Rényi order. The Opacus noise multiplier is $\sigma(\epsilon) \cdot L/C$.

(2) *ms-SRPP-SGD (expected K^2 via hypergeometric model)*: We model the number of differing examples K_t in each batch as a random variable following a hypergeometric distribution: $K_t \sim \text{Hypergeometric}(N, \Delta, L)$ under fixed-size sampling without replacement. For this distribution,

$$\mathbb{E}[K_t] = L \cdot \frac{\Delta}{N}, \quad \text{Var}[K_t] = L \cdot \frac{\Delta}{N} \cdot \left(1 - \frac{\Delta}{N}\right) \cdot \frac{N-L}{N-1},$$

and thus $\mathbb{E}[K_t^2] = \text{Var}[K_t] + \mathbb{E}[K_t]^2$. We define

$$\gamma^2 = a^2 \cdot \frac{\mathbb{E}[K_t^2]}{L^2},$$

where $a = 1$ for add-remove adjacency (our default) or $a = 2$ for replace adjacency. The total HUC is then

$$H_{\text{total}} = 4C^2\gamma^2 \sum_{t=1}^T \eta_t^2,$$

and the noise scale is calibrated identically to SRPP-SGD via $\sigma^2(\epsilon) = (\alpha/2\epsilon) \cdot H_{\text{total}}$.

(3) *group-DP-SGD (baseline)*: As a baseline, we also implement group-DP-SGD using the standard DP-SGD accountant [1] with group size $G = \lceil \mathbb{E}_\eta[K_t^2]^{1/2} \rceil$ (derived from the hypergeometric model). The DP-SGD accountant computes a per-step privacy loss, which we then convert to group DP by scaling with the group size. Appendix C provides detailed discussions of the relationship between SRPP/ms-SRPP-SGD and group DP-SGD.

In the experiments for Figures 3i and 3j, we sweep the privacy budget ϵ over the range $\{80, 70, 65, 60, 55, 50, 45, 40, 35, 30, 25, 20, 18, 14, 12, 10, 8, 4, 2, 1, 0.5\}$ and report test accuracy at each ϵ . We evaluate two sampling rates corresponding to batch sizes $L = 512$ (sampling rate $q \approx 0.01$) and $L = 1024$ (sampling rate $q \approx 0.02$) on the full 50,000-example training set. Training uses 40 epochs for $L = 512$ and 40 epochs for $L = 1024$, with clipping norm $C = 4.0$ (for $L = 512$) or $C = 5.0$ (for $L = 1024$), learning rate $\eta_0 = 0.2$ (for $L = 512$) or $\eta_0 \approx 0.14$ (for $L = 1024$) with cosine decay and 5% warmup, momentum 0.9, and weight decay 5×10^{-4} . All privacy accounting uses Rényi order $\alpha = 16$ and add-remove adjacency.

Evaluation metrics. For each privacy budget ϵ , we train the model to convergence (50 epochs) and report:

- *Test accuracy*: Classification accuracy on the CIFAR-10 test set (10,000 examples).
- *Training accuracy*: Classification accuracy on the training set (for diagnostic purposes).
- *Reference ϵ* : The privacy budget computed by Opacus’s built-in accountant (at $\delta = 10^{-5}$) for comparison.

Overfitted regime and membership inference attacks.

To perform empirical privacy auditing, we conduct additional experiments in an overfitted regime where membership attacks are most effective. We randomly subsample 1,000 examples from the CIFAR-10 training set and train models for 200 epochs with reduced regularization (weight decay set to zero) to induce overfitting. We use batch size $L = 256$, clipping norm $C = 5.0$, learning rate $\eta_0 = 0.1$ with cosine decay, and evaluate privacy budgets $\epsilon \in \{2, 8, 20, 50, 70, 100, 200, 300, 500\}$ plus a non-private baseline.

On these overfitted models, we apply the loss-threshold membership inference attack of [33]. For each example x with true label y , we compute the cross-entropy loss $\ell(x) = -\log p_\theta(y | x)$ and use the negative loss as a membership

score: lower loss suggests the example is more likely a training member. We compute the ROC AUC for distinguishing the 1,000 training members from an equal-sized set of non-members sampled from the remaining CIFAR-10 training data. ROC AUC of 0.5 indicates random guessing (perfect privacy), while higher values indicate successful membership inference. We report ROC AUC as a function of ϵ to demonstrate how privacy protection degrades membership leakage.

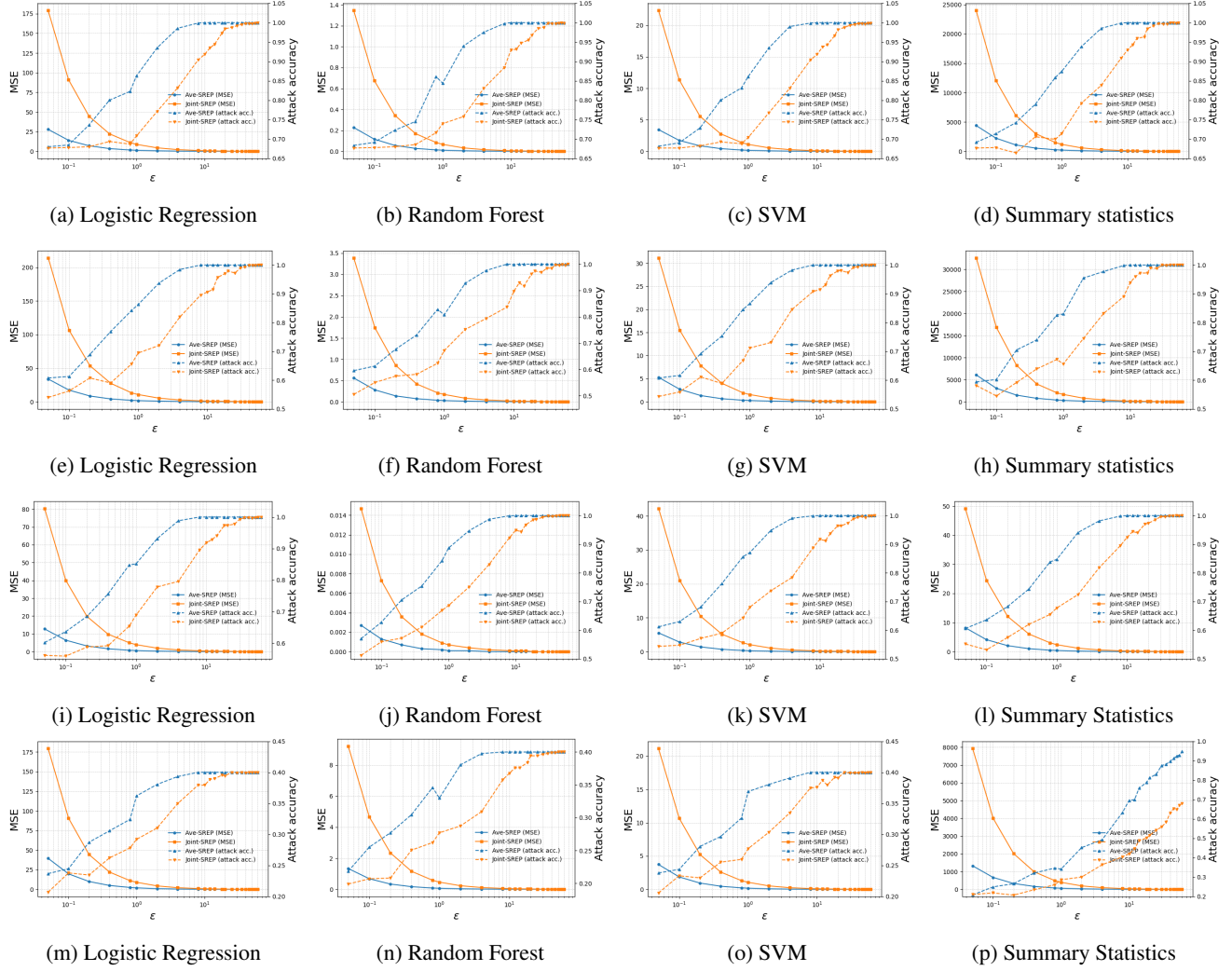


Figure 4: **Privacy-utility tradeoffs on Cleveland Heart Disease and Student Performance datasets.** (a)–(d): Cleveland dataset with imbalanced prior (majority-class baseline $\text{Acc}_{\text{maj}}^{0.7} = 0.7$). (e)–(h): Cleveland dataset with balanced prior ($\text{Acc}_{\text{maj}}^{0.5} = 0.5$). (i)–(l): Student Performance dataset with imbalanced prior (sex as secret, $\text{Acc}_{\text{maj}}^{0.6} = 0.6$). (m)–(p): Student Performance dataset with balanced prior (grade group as secret, $\text{Acc}_{\text{maj}}^{0.2} = 0.2$). Each configuration evaluates Ave-SRPP and Joint-SRPP mechanisms across privacy budgets $\epsilon \in \{0.05, 0.1, 0.2, 0.4, 0.8, 1.0, 2.0, 4.0, 8.0, 10.0, 12.0, 14.0, 18.0, 20.0, 25.0, 30.0, 35.0, 40.0, 45.0, 50.0, 55.0, 60.0\}$ with Rényi order $\alpha = 4$. Metrics shown: mean squared error (MSE), attack accuracy, and attack advantage over the priors.